SISSA
Scuola
Internazionale
Superiore di
Studi Avanzati

Physics Area - PhD course in
Theory and Numerical Simulation of Condensed Matter

On Thermodynamics of Driven Quantum Systems: Novel Results and Perspectives

Candidate:
Daniele Nello

Advisor:
Alessandro Silva

Academic Year 2023-2024

"Only for you, children of doctrine and learning, have we written this work. Examine this book, ponder the meaning we have dispersed in various places and gathered again; what we have concealed in one place, we have disclosed in another, that it may be understood by your wisdom."

— **Heinrich Cornelius Agrippa von Nettesheim**, *De occulta philosophia*

"Qual è 'l geomètra che tutto s'affige
per misurar lo cerchio, e non ritrova,
pensando, quel principio ond'elli indige,
tal era io a quella vista nova:
veder voleva come si convenne
l'imago al cerchio e come vi s'indova;
ma non eran da ciò le proprie penne:
se non che la mia mente fu percossa
da un fulgore in che sua voglia venne."

-Dante Alighieri, *Divina Commedia, Paradiso, Canto XXXIII*

Acknowledgements

To my parents

First of all, I would like to thank my supervisor, Alessandro, for his useful teaching and advice, as well as for his feedback on this Thesis. Likewise, I would like to thank all my collaborators, colleagues, and researchers with whom I shared my thoughts and my research.

My gratitude goes to all my closest friends I met here in Trieste: Bengi, Gloria, Luca, Fabio, Simona, Sara, Drugo, Alessia, Ricky, Ele and Daniele. It is thanks to you that I (hopefully) maintained my mental sanity. I would like to thank the "104" group for the wonderful memories we have created together: the trips, the parties and all that. I also would like to mention "il Villaggio" group for the funny games nights under the light of the moon.

I want to acknowledge my parents for their continuous support during all these years, especially during the Covid-19 pandemic.

I would like to thank my long-standing office mates for the friendly environment, the chats and the coffees. In particular, Alessandro, Giacomo, Carlo, and the most recent acquisition, Giovanni.

I would also like to thank the group "i Faggi" for the moments of conviviality we have shared.

Finally, let me mention my longstanding friends from the school era, particularly Eugenio and Novella.

This page couldn't contain everyone who had a part in this chapter of my life. If you are among those, *consider yourself as thanked.*

Abstract

Driven quantum systems are systems in which a set of parameters obeys a time-dependent protocol, both periodic and non-periodic. The study of these systems bridges theoretical advances with experimental realizations in a variety of platforms—these range from quantum dot arrays to molecular junctions to trapped ions. The theoretical study is challenging due to the inherent non-equilibrium nature of the problem.

These systems offer an interesting playground for quantum thermodynamics. They can be studied as quantum machines, such as refrigerators, heat pumps or engines. This poses the challenge of redefining the laws of thermodynamics in the quantum realm. This effort implies taking into account the presence of coherence, entanglement and strong correlations with the environment.

In this conceptual framework, we attempt to shed new light on specific setups with applications in quantum metrology. In the first part of the Thesis, we present novel results on the thermodynamics and transport properties of quantum dots. After thoroughly introducing the main methods, namely non-equilibrium Green's functions and scattering matrix techniques, we apply these tools to adiabatic charge pumping. In this context, quantum dots, subjected to external periodic driving, act as nano-mechanical engines, transferring charge from a source to a drain. We investigate the conditions under which the pumped charge becomes quantized and how thermodynamic quantities behave in this regime.

Next, we will focus on the charge shuttle mechanism in movable quantum dots as an example of a quantum clock. This physical model describes transport through a molecular state bound to two leads by van der Waals forces, with an electric field pushing the molecule from the source to the drain. The periodic oscillations arising from the system's dissipative limit cycle solution provide the basis for time measurement. We examine quantum noise primarily associated with the tunnelling process.

In the second part, we propose a quantum clock that utilizes the free energy resources generated by coupling to a quantum battery, consisting of an integrable spin chain driven out of equilibrium by a quench in a chosen parameter. The operating conditions of the clock in the manifold of parameters are examined, leading to the requirement of the crossing of the critical point in the battery. The lifetime of the battery's resources is found to be extensive in its size, even when choosing a global coupling observable in the battery.

List of publications

This Thesis is entirely based on the following publications, constituting the bulk of the work of the PhD:

- **D.Nello**, A. Silva "*Thermodynamics of adiabatic quantum pumping in quantum dots*" (2024), published in "Scipost Physics Core", doi:"10.21468/SciPostPhysCore.7.4.067" , url: "https://scipost.org/SciPostPhysCore.7.4.067"
- **D.Nello**, A. Silva "*Electronic shuttling in quantum dots for quantum timekeeping*" (2024), in preparation
- **D.Nello**, A. Silva "*Quantum clocks powered by quantum batteries*" (2024), in preparation

List of Recurrent Symbols

E	internal energy
S	entropy
N	number of particles
F	free energy
$\dot{E}$	energy rate of variation
$\dot{W}$	work rate
$\dot{\mathcal{Q}}$	heat rate
$\dot{N}$	rate of variation of the number of particles
$\dot{\Sigma}$	rate of entropy production
$\dot{N}_\alpha$	variation of the number of particles in thermal bath α
$\dot{\mathcal{Q}}_\alpha$	heat flow to bath α
T_α	temperature of bath α
μ_α	chemical potential of bath α
Q_α	charge transport from bath α
I_α	current from bath α
$\delta Q_{\alpha\beta}$	charge noise
F	force
ν	precision
N	accuracy
T_0	driving period
Ω	driving frequency
$G^<$	quantum dot's lesser Green's function
$G^>$	dot's greater Green's function
G^R	dot's retarded Green's function
G^A	dot's advanced Green's function
$\Sigma^{\lessgtr,R,A}$	self energy associated to the dot's Dyson equation
$\Sigma^{\lessgtr,R,A}_{\substack{k\alpha \\ k'\alpha'}}$	self energy associated to the lead's Dyson equation
$G^{\lessgtr,R,A}_{d,k\alpha}$	mixed dot-lead Green's function
$G^{\lessgtr,R,A}_{k\alpha}$	lead's dressed Green's function
$g^{\lessgtr,R,A}_{\substack{k\alpha \\ k'\alpha'}}$	free bath α Green's function
Γ_α	coupling strength between the dot and lead α
A	density of states of the dot
f	Fermi-Dirac distribution
k_B	Boltzmann's constant

Contents

Chapter 1

Introduction: Thermodynamics of driven quantum systems

- Where we give a general introduction to driven quantum systems, with introductory examples.

> *"That was when I saw the Pendulum.*
> *The sphere, hanging from a long wire set into the ceiling of the choir, swayed back and forth with isochronal majesty.*
> *I knew- but everyone could have sensed it in the magic of that serene breathing- that the period was governed by the square root of the wire and by π, that number which, however irrational to sublunar minds, through a higher rationality binds the circumference and diameter of all possible circles. The time it took the sphere to swing from end to end was determined by an arcane conspiracy between the most timeless of measures: the singularity of the point of suspension, the duality of the plane's dimensions, the triadic beginning of π, the quadratic nature of the root, and the unnumbered perfection of the circle itself.*
> *I also knew that a magnetic device centred in the floor beneath issued a command to a cylinder hidden in the heart of the sphere, thus assuring continual motion. This device, far from interfering with the laws of the Pendulum, in fact permitted its manifestation, for in a vacuum any object hanging from a weightless and unstretchable wire free of air resistance and friction will oscillate for eternity. "*
>
> — **Umberto Eco**, *Foucault's Pendulum*

Thermodynamics is an old theory dating back to the Industrial Revolution. Its aim was to understand the functioning of thermal machines. This effort culminated in the conceivement of the three laws. Then, mainly thanks to the combined effort of Boltzmann

and Ehrenfest, statistical mechanics was born, providing a microscopic description that gives substance to the laws of thermodynamics.

The discovery of quantum theory has been, in some way, connected to thermodynamics and statistical mechanics. In fact, the fundamental problem of black-body radiation has been studied in the seminal study of Planck, leading to the serendipitous birth of quantum mechanics. However, quantum mechanics predicts reversible dynamics at the fundamental level, while the second law of thermodynamics entails an emergent irreversibility. This is an interesting and still open question posed by the interplay of the two.

The study of mesoscale phenomena, such as protein folding, polymers, and molecular motors justified the redefinition of the foundations of thermodynamics in the field of stochastic thermodynamics [82], still much active. In this kind of system, the entity of the fluctuations is relevant and should be incorporated in the analysis. The key results of this field are fluctuation theorems [84] and Jarzynski's equality [50].

In recent years, in association with the growing field of quantum information, tremendous progress has been achieved in gaining an unprecedented degree of control over nanoscale systems. Many of these devices are driven quantum systems. A driven system is a physical system in which a subsystem of the associated parameters follows a time-dependent protocol (both periodic and non-periodic). These systems require a non-equilibrium description, going beyond the standard equilibrium theory. The description is relevant for a number of different experimental platforms, which have seen impressive progress in recent years. In particular, we're talking about cold-atomic gases [85], Rydberg atoms [11], trapped ions [53], systems with a light-matter interaction [56], and quantum dots [3] just to cite a few of them.

These experimental advances motivate a fundamental redefinition of thermodynamics [55, 40, 41], which must be reconciled with a quantum description of the associated dynamics. This has led to quantum thermodynamics, whose basic tenets we will discuss in Section 1.1.

The purpose of the present Thesis is to shed light on driven quantum systems from the point of view of quantum thermodynamics. In particular, we will specialize in key applications from quantum metrology, which will be presented in Sections 1.2 and 1.3, in particular quantum clocks and adiabatic charge pumping.

1.1 The laws of thermodynamics in the quantum realm

Let us start with the general description of a system S interacting with an environment E. Since we are dealing with driven systems, say we have a set of N parameters of the Hamiltonian obeying a time-dependent protocol $\vec{\lambda}(t) = \{\lambda_i(t)\}_{i=1}^{N}$.

The definition of the key thermodynamics quantities has to be constructed from these elements. In doing so, we follow the guide of Ref. [37]. Note that there is still a lively debate in this context in the scientific community.

In the usual interaction representation, the total work done on a protocol defined on time $[0, \tau]$ is

$$\Delta W(\tau) = Tr[\rho(\tau)H(\tau)] - Tr[\rho(0)H(0)]. \tag{1.1}$$

In the context of open, driven systems the definitions of heat and work are highly dependent on the information-theoretic choice of system and environment, depending on the parameters one has in control. In particular, beyond the weak coupling approximation, the role of the coupling term will be discussed at length in the following Sections. By defining internal energy as the (time-dependent) expectation value of the system Hamiltonian

$$E(t) = Tr[\rho_S(t)H_S(t)]. \tag{1.2}$$

over the system density matrix $\rho_S(t)$, one can arrive at a differential expression of work and heat. One defines the work as

$$\dot{W}(t) = \sum_i Tr\left[\rho_S(t)\frac{\partial H_S(t)}{\partial \lambda_i}\right]\dot{\lambda}_i \tag{1.3}$$

One introduces $\dot{U}(t)$ satisfying

$$\dot{E}(t) = \frac{d}{dt}Tr[\rho_S(t)H_S(t)] = \dot{U}(t) + \dot{W}(t). \tag{1.4}$$

Beware that these expressions can be ill-defined, whenever the chosen protocol has a discontinuity in a certain point. The term $\dot{U}(t)$ corresponds to

$$\dot{U}(t) = \dot{\mathcal{Q}}(t) + \dot{U}_{chem}(t), \tag{1.5}$$

where the first term is the heat flow and the second represents the chemical work due to the particle flow. For example, if the environment is constituted by a collection of reservoirs with associated chemical potentials μ_α, then this term is

$$\dot{U}_{chem}(t) = \sum_\alpha \mu_\alpha \dot{N}_\alpha(t), \tag{1.6}$$

where $\dot{N}_\alpha(t)$ represents the individual flux associated with reservoir α.

The first law of thermodynamics bears a statement about the *conservation of energy*. We can write it in the form [37]

$$\dot{E}(t) = \dot{W}(t) + \dot{\mathcal{Q}}(t) + \dot{U}_{chem}(t), \tag{1.7}$$

The second law, in contrast, identifies an inherent irreversibility of thermodynamic processes associated with the presence of an arrow of time. The two classical formulations are due to Clausius (1854): "Heat can never pass from a colder to a warmer body without some other change, connected therewith, occurring at the same time." and by Lord Kelvin (1851)

"It is impossible for a self-acting machine, unaided by any external agency, to convey heat from one body to another at a higher temperature. It is impossible, by means of inanimate material agency, to derive mechanical effect from any portion of matter by cooling it below the temperature of the coldest of the surrounding objects.". It can be shown that the two statements are indeed equivalent. This principle identifies a key quantity, dubbed entropy production, being non-negative and zero only when we are in the presence of a reversible process

$$\dot{\Sigma} \geq 0. \tag{1.8}$$

But, how is this quantity defined? The entropy flow to reservoir α is defined as

$$\Phi_\alpha = \frac{\dot{\mathcal{Q}}_\alpha}{T_\alpha} \tag{1.9}$$

where T_α is the associated temperature and $\dot{\mathcal{Q}}_\alpha$ is the heat flow to the individual reservoir. According to Clausius's principle, the corresponding change in the system's entropy is bounded by this quantity

$$\dot{S} \geq \sum_\alpha \frac{\dot{\mathcal{Q}}_\alpha}{T_\alpha}. \tag{1.10}$$

and we define entropy production as

$$\dot{\Sigma} = \dot{S} - \sum_\alpha \frac{\dot{\mathcal{Q}}_\alpha}{T_\alpha} \tag{1.11}$$

and we see this quantity respects the non-negativity desideratum. In the quantum formulation, the entropy of the system is represented by the von Neumann entropy of the density matrix

$$S(\rho) = Tr[\rho \ln \rho]. \tag{1.12}$$

In the case of the temperature being unique and fixed to the value T, one can give another formulation of entropy production by substituting the first law, as

$$\dot{\Sigma} = \beta(\dot{W} - \Delta F) \tag{1.13}$$

where the latter term is the change in free energy in the system. This relation identifies entropy production with the irreversible part of the work.

The third law of thermodynamics is the unattainability principle derived by Nernst "It is impossible for any process, no matter how idealized, to reduce the entropy of a system to its absolute-zero value in a finite number of operations.", related to the entropy of the physical ground state being constant. A quantum version of the third law of thermodynamics, from the original formulation of Nernst, has been recently proposed, stating that reaching the ground state requires infinite resources in terms of either time, energy or complexity [89].

Now, let's shift to a more resource-theoretic framework by defining the concepts of ergotropy and *passive* states [5]. Ergotropy quantifies the amount of energy extractable via unitary operations U on a given state ρ. It is defined as

$$\mathcal{E}[\rho] = Tr[H_S\rho] - \min_{U\in SU(d)}\{Tr[H_S U\rho U^\dagger]\}. \tag{1.14}$$

The minimization happens in the set of unitary operations drawn from the special unitary group $SU(d)$ [19]. When no work can be extracted from a given state, this state is called "passive". A state is passive if and only if it is diagonal in the basis of the Hamiltonian H_S and its density matrix eigenvalues are non-increasing with the energy

$$\sigma = \sum_{k=1}^{d} s_k|k\rangle\langle k|, \qquad s_{k+1} \leq s_k, \tag{1.15}$$

where $|k\rangle$ corresponds to the energy eigenstates sorted in ascending order. Upon reminding the definition of thermal state in quantum mechanics

$$\rho_{th} = \frac{e^{-\beta H}}{Z}, Z = Tr[e^{-\beta H}], \tag{1.16}$$

it is evident that all thermal states are passive. As a consequence, we define as "non-passive" any state from which a finite amount of work is extractable. Interestingly, for any non-passive state, there exists a unique passive state σ, under the condition of H_S having a non-degenerate spectrum, obtained via a unitary operation having the function of ordering the eigenvalues in non-increasing order

$$\sigma = U_\rho \rho U_\rho^\dagger = \sum_{k=1}^{d} r'_k|k\rangle\langle k|. \tag{1.17}$$

1.2 Introduction to Adiabatic Charge Pumping

An interesting phenomenon in the context of driven systems is adiabatic charge pumping. The idea, first introduced by Thouless in 1983, that applying a quasi-static operation on a system could lead to the transport of electrons [21, 23] in the context of isolated quantum systems. Adiabatic quantum pumping has been studied in the different context of open quantum systems, in interaction with multiple reservoirs. These systems exhibit coherent transport. What is most important is that tuning the system's parameters makes it possible to achieve a finite transport without any bias between the reservoirs. This is achievable experimentally by the current state-of-the-art setups [88]. Most notably, in the context of adiabatic non-interacting quantum pumps, in his seminal paper of 1998 [70], Brouwer was able to describe the charge pumped in a cycle pumping through an open, yet non-interacting

system, as a geometrical quantity written in terms of the instantaneous scattering matrix of the system (without reference to a specific time dependence). Generalizations of this phenomenon to interacting systems have been attempted [87, 33, 81]. What makes it interesting for specific applications, such as in metrology, is the possibility of achieving a transport of a quantized charge (with zero associated charge noise [24]).

1.3 Introduction to clocks

What is a clock? According to the standard dictionary definition "A clock is a device to measure time". But what is time? From the physical point of view, time is defined by its measurement. We can see that there is an evident circularity in these definitions. As pointed out by [36] in his classic review, the apparent regularity in the motion of our elegant pendulum clock, or the wall clock in our home hides a more profound scientific truth: all of these devices require an external source of low-entropy energy to power them. This hints at the essential irreversibility in the nature of clocks, being dissipative systems.

Moreover, there is a certain degree of stochasticity hidden in their motion. Even the pendulum has its thermal noise present due to the fluctuation-dissipation theorem. However being negligible, this effect is nevertheless present. As a consequence of this fact, the question of characterizing the sources of noise in these devices is indeed relevant. The question of how these two are related has been posed in the scientific literature, relating to the concept of the entropic cost of the measurement of time. The direct relation between the performance, in particular the accuracy, and the entropy production implies that to improve the clock's performance it is necessary to spend more and more resources. As we will see, the two quantities are constrained by the thermodynamic uncertainty relations.

In terms of performance, the best technology available nowadays is offered by atomic clocks, reaching an uncertainty below the level of 10^{-18} [2]. However, numerous nanoscale platforms have been tested for timekeeping and it would be pointless to offer an endless list in this context. Some notable examples can be found in the recent review by Milburn [36].
In the following, we will describe the most relevant estimators of a clock's performance and present a basic, however interesting, example, namely the classical pendulum clock.

1.4 A summary of the estimators of the clock's performance

In general, to quantify how good a clock is, one has to compare the entity of its fluctuations vis-à-vis the average period. Equivalently, one can take the time of arrival to n ticks T_n and the number of ticks at time t n_t. Choosing the latter, one can concoct the following estimator of performance [86]

$$R_1 = \frac{\nu}{N} = \frac{\langle n_t \rangle}{\langle n_t^2 \rangle - \langle n_t \rangle^2}. \tag{1.18}$$

In the case of an elementary reset clock, where μ, σ^2 are the mean and the variance of the distribution of the waiting time between the ticks, this measure is analogous to this estimator

$$R_2 = \frac{\sigma^2}{\mu^2}. \tag{1.19}$$

And, in particular, the precision is

$$\nu = \frac{1}{\mu} \tag{1.20}$$

and the accuracy reads

$$N = \frac{\sigma^2}{\mu^3} \tag{1.21}$$

As we will see, another key measure of the clock's performance is Allan's variance (Section 3.6.2), associated with the stability of the clock's frequency.

1.5 Thermodynamic Uncertainty Relations and Clocks

The Thermodynamic Uncertainty Relations describes a trade-off between the overall cost for driving a system and the precision observed in any output current [37]. Let's consider a Markovian state producing a steady-state generic current $Y(t)$ [49] and the consequent entropy production rate $\dot{\Sigma}$, then the associated TUR states

$$\frac{Var[Y(t)]}{\langle Y(t)\rangle^2} \geq \frac{2}{\dot{\Sigma}t} \tag{1.22}$$

where $Var[Y(t)] = \langle Y^2(t)\rangle - \langle Y(t)\rangle^2$. Extensions of the original TUR invoke functionals of the entropy production rate in the r.h.s. $F(\dot{\Sigma})$. In terms of the clock's performance, this relation implies a bound on the resolution

$$N \leq \frac{\Delta S}{2t_{tick}}. \tag{1.23}$$

The validity of the TURs has been shown in the context of discrete systems. However, numerous violations have been observed in continuous systems, both classical and quantum [74] and as a result of the presence of coherence in the systems [62, 52].

1.6 Example: The classical pendulum

Let's examine the simplest and most common example of a clock, the pendulum clock many people have at home. A pendulum, for small oscillations in the absence of dissipation, oscillates at a constant frequency determined by the constant gravitational acceleration and by its length $\omega = \sqrt{\frac{g}{L}}$. However, when dissipation is present, in the form of air resistance

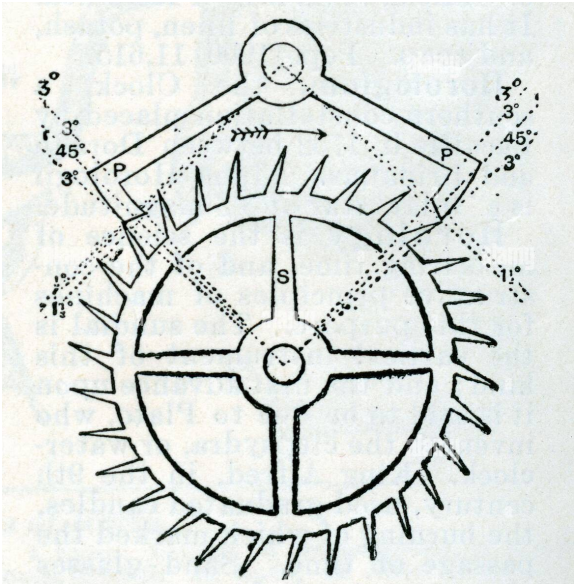

Figure 1.1: The Graham escapement mechanism: a falling mass (not shown) provides constant torque to the wheel. The momentum of the pendulum shifts the anchor, unlocking it repeatedly from the left and right-hand positions. Each time the anchor is locked to the wheel, it imparts a small torque to the pendulum.

or friction between the rod and the support, one would observe damped oscillations and eventually the motion stops. This can be prevented by connecting it to an escapement so that the pendulum becomes *driven* [36]. The purpose of this escapement is to counteract the effects of dissipation and provide energy for the stability of the periodic oscillations. This constitutes an instance of a dissipative limit cycle, a sustained periodic solution in driven non-linear systems. As we will see, the fluctuation-dissipation theorem constrains the noise of this system, which is stochastic in nature, despite its appearance.

In the following, we will examine the Graham escapement mechanism, as in [36], imparting a small kick every time the pendulum frees the anchor from its position, as in Fig. (1.1). One can model this system using a stochastic differential equation in the phase space

$$\begin{cases} \dot{\theta} = \frac{p}{m\omega L} \\ \dot{p} = -mg\theta - \gamma p + K(\theta, p) + \xi(t), \end{cases} \tag{1.24}$$

where θ is the angular coordinate, p the momentum, m is the mass and γ is the friction coefficient. Furthermore, $K(\theta, p)$ describes the effect of the impulsive driving. The white

noise coefficient $\xi(t)$ satisfies the relation

$$\overline{\xi(t)\xi(t')} = D\delta(t-t'). \tag{1.25}$$

In turn, the diffusion coefficient is constrained by the fluctuation-dissipation theorem to be

$$D = 2m\gamma k_B T. \tag{1.26}$$

Moving to dimensionless variables $x = \theta$ and $y = \frac{p}{m\omega L}$ the differential equation reads

$$\begin{cases} \dot{x} = y \\ \dot{y} = -x - \Gamma y + K(x,y) + \eta(t), \end{cases} \tag{1.27}$$

where one defines the new constant $\Gamma = \frac{\gamma}{m\omega^2 L}$ and noise coefficient $\eta(t) = \frac{\xi(t)}{m\omega^2 L}$. The kick function is

$$K(x,y) = -\mu\Theta(\sin\psi_0 x - \cos\psi_0 y), \tag{1.28}$$

μ and ψ_0 being two arbitrary constants fixed by the design of the escapement.

To extract the presence of the limit cycle, it is convenient to change variables to polar coordinates, defining new variables as

$$\begin{cases} x = r\cos\psi \\ y = r\sin\psi. \end{cases} \tag{1.29}$$

In terms of these variables, the phase-averaged differential equation for the r variable reads

$$\dot{r} = -\frac{\Gamma r}{2} + \frac{2\mu}{\pi}\cos\psi_0, \tag{1.30}$$

from which one can find the value of the limit cycle radius, correspondent to the fixed point of this differential equation

$$r^* = \frac{4\mu}{\pi\Gamma}\cos\psi_0. \tag{1.31}$$

The equation for the phase variable reads

$$\dot{\psi} = -1 + \frac{2\mu}{r\pi}\sin\psi_0. \tag{1.32}$$

The energy of the oscillator can be associated to

$$E = \frac{1}{2}(x^2 + y^2), \tag{1.33}$$

and the time-averaged differential equation obeyed by this quantity is

$$\dot{E} = -\Gamma E + \frac{2\sqrt{2E}\mu}{\pi}\cos\psi_0. \tag{1.34}$$

In this equation, the first term represents the energy lost due to friction, while the second is the energy gain due to the action of the escapement, so the limit cycle forms when the two terms are balanced. In the steady state, the average energy is

$$\bar{E} = \frac{8\mu^2}{\Gamma^2\pi^2}\cos^2\psi_0, \tag{1.35}$$

when noise is neglected. When including the noise, the system of differential equations for r and ψ reads

$$\begin{cases} dr = \left[-\frac{\Gamma r}{2} + \frac{2\mu}{\pi}\cos\psi_0 + \frac{D'}{4r} \right] dt + \sqrt{\frac{D'}{2}} dW_1(t) \\ \dot{\psi} = \left[-1 + \frac{2\mu}{r\pi}\sin\psi_0 \right] dt + \frac{\sqrt{D'/2}}{r} dW_2(t), \end{cases} \tag{1.36}$$

where we have two independent Wiener increments $dW_1(t)$ and $dW_2(t)$ and the rescaled diffusion coefficient reads

$$D' = \frac{D\omega}{m^2 g^2}. \tag{1.37}$$

As a consequence of the noise, the radial fixed point is displaced to greater values

$$r^* = \frac{4\mu}{\pi\Gamma}\cos\psi_0 + \sqrt{\frac{4\mu^2}{\pi^2\Gamma^2}\cos^2\psi_0 + D'/4}. \tag{1.38}$$

Indeed, as it is clear from the differential equation of the variable ψ, the phase diffusion noise is inversely proportional to the size of the limit cycle. This quantity is related to the dispersion of the period.

In the deterministic case, the average heat dissipated [36] is

$$\bar{Q} = \left(\frac{2\mu r^* \cos\psi_0}{\pi\Gamma} \right) T. \tag{1.39}$$

This quantity is directly proportional to the radial fixed point. The key take-home message is that thermodynamics limits the clock's performance even in this very simple case. In particular, the dispersion of the period is inversely related to the dissipated heat.

1.7 Thesis outline

The structure of the Thesis is organized in the following way.

In Chapter 2, we will present a general thermodynamic analysis of the resonant level model, accounting for the periodic driving of its parameters, and its transport properties. We will employ diagrammatic methods, based on the Keldysh non-equilibrium Green's functions and scattering matrix techniques for this purpose. They are properly introduced in the Appendix. We use these results to study the phenomenon of adiabatic pumping,

previously introduced, in the context of quantum dots interacting with multiple leads. We will study the set of periodic processes yielding a quantized transport, describing the behaviour of the most relevant thermodynamic quantities.

Chapter 3 will be devoted to a categorization of the properties of the charge shuttle as a device for time metrology. In there, we will explore the phase portrait of this dynamical system, in particular assessing the presence of dissipative limit cycles beyond the weak coupling approximation. We will include the noise in my picture, thereby enabling a thorough assessment of the trade-off relation between the performance in terms of timekeeping and entropy production. A further indicator of the clock's performance will be analyzed, viz. the Allan variance.

In Chapter 4 we introduce a new proposal of a quantum clock relying on the free energy resources of the stationary state of an integrable spin chain, acting as a quantum battery. The spin chain is driven away from equilibrium by means of a global quench. Here again, the performance/dissipation trade-off will be analyzed. More importantly, the conditions guaranteeing the clock's functioning will be thoroughly examined, with relevant examples for their experimental simulation. For these examples, the lifespan of the battery will be computed in relation to its size.

Finally, in Chapter 5 we will conclude by summarizing this Thesis's main results and give an outlook of the questions open for future research.

Part I

Part I: Transport and Thermodynamics in Quantum dots

Chapter 2

Quantum Thermodynamics of Adiabatic Quantum Pumping

- Where we give a thermodynamic description of adiabatic quantum pumping in quantum dots.

> *"If your theory goes against the second law of thermodynamics, I give you no hope; there is nothing for it but to collapse in deepest humiliation"*
>
> — **Arthur Eddington**

2.1 Introduction

As we have seen in Chapter 1, adiabatic quantum pumps are notable examples of quantum machines. In some special settings, they can achieve finite transport between different reservoirs. Looking at it as an engine, the operation of a quantum pump should be characterized by standard thermodynamic quantities: the work done, the entropy produced and the heat exchanged. A fresh thermodynamic view of quantum pumping opens up the possibility of addressing qualitatively different questions. For example, is there a minimal work done associated with charge quantization? Or can one find a connection between entropy production and current noise? These issues relating transport to the thermodynamic properties of a pumping cycle can be addressed only by developing a description of transport and thermodynamics within the same formalism (cf. with [35] for classical pumps). Here, we focus on this task by addressing adiabatic pumping through the simplest, yet nontrivial system that displays all significant ingredients one is looking for (charge quantization, noise): a resonant level coupled to two leads.

2.2 The model

In this Chapter, we consider adiabatic pumping through a time-dependent resonant level model consisting of a single energy level coupled to two metallic leads. The leads act as fermionic reservoirs and are kept fixed at temperature T and chemical potentials μ_L and μ_R. This model describes transport through nanostructures, such as molecular junctions or quantum point contacts (QPCs). When its parameters, namely the level of the dot and its hybridization strength with the reservoirs are tuned by an external agent, such as a gate voltage, then it can act as a molecular-level nano-engine [14].

The Hamiltonian of the system consists of three different terms

$$H = H_D + H_V + H_B, \tag{2.1}$$

where H_D is the Hamiltonian associated with the dot

$$H_D = \epsilon_d(t) d^\dagger d, \tag{2.2}$$

H_B is associated with the leads

$$H_B = \sum_{k\alpha} \epsilon_{k\alpha} c^\dagger_{k\alpha} c_{k\alpha}, \tag{2.3}$$

and H_V to the leads-dot coupling

$$H_V = \sum_\alpha H_V^\alpha = \sum_\alpha V_\alpha(t) \sum_k (d^\dagger c_{k\alpha} + h.c.). \tag{2.4}$$

Here d is the annihilation operator of the dot level, whilst $c_{k\alpha}$ is associated with an electron with momentum k in the $\alpha = L, R$ lead (in this case there is only one channel associated to each lead), and V_α is the coupling between the dot and lead α. In the context of our analysis, we will assume the leads to have a constant density of states and an infinite bandwidth (wideband limit), implying that the decay rate

$$\Gamma_\alpha = 2\pi |V_\alpha|^2 \sum_k \delta(\epsilon - \epsilon_{k\alpha}) \tag{2.5}$$

does not depend on energy. In this case, as we will explain, the expression for the spectral function of the dot (in Fig.(2.1)) is

$$A(\epsilon) = \frac{\Gamma}{(\epsilon - \epsilon_d)^2 + (\frac{\Gamma}{2})^2}, \tag{2.6}$$

where $\Gamma = \Gamma_L + \Gamma_R$ is the total decay rate.

Quantum pumping requires at least two of the system parameters to be varied periodically in time along a certain cycle [70]. We will therefore take both the energy dot level $\epsilon_d(t)$ and the level-dot couplings $V_\alpha(t)$ to be time-dependent and driven by an external agent.

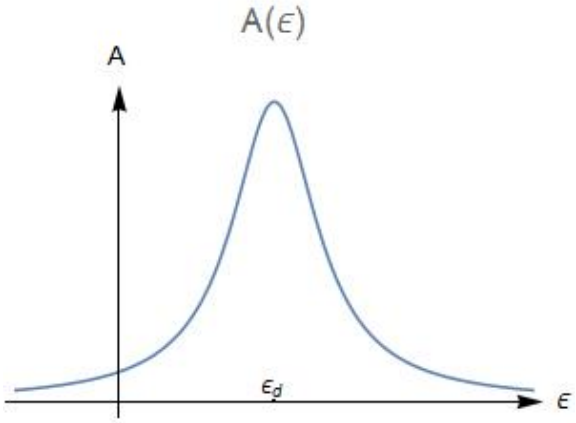

Figure 2.1: This is the density of states of a single-level quantum dot. Note that it is a Lorentzian centred on its energy level ϵ_d and its width is proportional to the total decay rate from the dot to the leads.

2.3 The gradient expansion of the Green's functions

All the physical quantities we will be computing are expressed in terms of Green's functions, which, in turn, can be expressed through a perturbative expansion. Below, we will consider the adiabatic limit, where the driving period satisfies $T_0 \gg \frac{1}{\Gamma}$. We use as small parameters $\dot{\epsilon}_d/\Gamma^2$ and $\dot{\Gamma}_\alpha/\Gamma^2$ The first ingredient one needs to have ready to get a universal description of pumping is an adiabatic expansion of the Green's functions. They are connected to the observables one finds in the thermodynamic and transport quantities we will evaluate in the subsequent Sections.
Let us start with the diagrammatic expansion of the dot Green's function (relative to the physical model introduced in the previous Section) on the Keldysh contour (see Section A.1), following the approach of Ref. [13]. It can be represented graphically as depicted in Fig. (2.2). Its equivalent expression in integral form is

$$G^C(t,t') = G_0^C(t,t') + \int_{C_K} d\tau_1 d\tau_2 G_0^C(t,\tau_1)\Sigma^C(\tau_1,\tau_2)G^C(\tau_2,t'), \tag{2.7}$$

where G^C are the contour-ordered green functions (see Appendix A.1) and the self-energy term reads

$$\Sigma^C(\tau_1,\tau_2) = \sum_{k\alpha} |V_\alpha|^2 g^c_{k\alpha}(\tau_1,\tau_2). \tag{2.8}$$

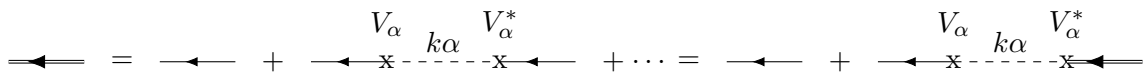

Figure 2.2: This is a visual representation of the diagrammatic expansion of the Green's function on the Keldysh contour. Here the single line represents the bare Green's function of the dot G_C^0, the double line represents the full Green function G^C, while the dashed line the bath's Green function $g_{k\alpha}^C$

Using analytic continuation techniques (see Appendix A.2) one may use Eq. 2.7 to obtain Green's functions defined in real times.

One may now use the separation of time scales to write a gradient expansion of the equation of motion for the Green's function. Switching to the Wigner transform, defined as

$$G(\epsilon, t) = \int d\tau G(t_1, t_2) e^{i\epsilon\tau}, \tag{2.9}$$

where $t = \frac{t_1+t_2}{2}$ and $\tau = t_1 - t_2$, one has to recall that for a convolution, the Wigner transform (Section A.3) is

$$\int dt' C(t_1, t') D(t', t_2) = \int \frac{d\epsilon}{2\pi} e^{-i\epsilon\tau} C(\epsilon, t) * D(\epsilon, t), \tag{2.10}$$

where $C(\epsilon, t) * D(\epsilon, t) = C(\epsilon, t)[\frac{i}{2}(\overleftarrow{\partial_\epsilon}\overrightarrow{\partial_t} - \overleftarrow{\partial_t}\overrightarrow{\partial_\epsilon})]D(\epsilon, t)$.

Applying this expansion to the example of the retarded Green's function of the dot, whose definition is

$$G^R(t, t') = -i\theta(t_1 - t_1')(\langle\{d(t)d^\dagger(t')\}\rangle), \tag{2.11}$$

where the graph parenthesis represents an anti-commutator, one starts from the associated equation of motion

$$\delta(t - t') = \int dt_1 G^R(t, t_1)[i\partial_{t_1}\delta(t_1 - t') - \epsilon_d(t_1)\delta(t_1 - t') - \Sigma^R(t_1 - t')], \tag{2.12}$$

with the retarded self-energy $\Sigma^R(t, t') = \sum_{k\alpha} |V_\alpha(t)|^2 g_{k\alpha}^R(t, t')$ and obtains up to the first order

$$1 = G^R(\epsilon, t)\left[\epsilon - \epsilon_d(t) + \frac{i}{2}\Gamma(t)\right] + \frac{i}{2}\left[\partial_\epsilon G^R(\epsilon, t)(-\dot{\epsilon_d}(t) + \frac{i}{2}\dot{\Gamma}(t)) - \partial_t G^R(\epsilon, t)\right]. \tag{2.13}$$

Therefore, up to the first order in the velocities, for the retarded and advanced Green functions one has

$$G^R(\epsilon, t) = (\epsilon - \epsilon_d(t) + i\frac{\Gamma(t)}{2})^{-1} \tag{2.14}$$

and

$$G^A(\epsilon, t) = (\epsilon - \epsilon_d(t) - i\frac{\Gamma(t)}{2})^{-1}. \tag{2.15}$$

To derive the lesser component of the Green function

$$G^{<}(t,t') = i\langle d^{\dagger}(t')d^{\dagger}(t)\rangle), \tag{2.16}$$

one starts from Eq. A.3 which gives

$$G^{<}(t,t') = G^{0<}(t,t') + \int dt_1 dt_2 G^{0R}(t,t_1)\Sigma^{R}(t_1,t_2)G^{<}(t_2,t') \tag{2.17}$$
$$+ \int dt_1 dt_2 G^{0R}(t,t_1)\Sigma^{<}(t_1,t_2)G^{A}(t_2,t') + \int dt_1 dt_2 G^{0<}(t,t_1)\Sigma^{A}(t_1,t_2)G^{A}(t_2,t').$$

Then, one applies $(i\partial_t - \epsilon_d)$ at both sides of the equation, satisfying

$$(i\partial_t - \epsilon_d)G^{0R}(t,t') = \delta(t-t') \tag{2.18}$$

and

$$(i\partial_t - \epsilon_d)G^{0<}(t,t') = 0. \tag{2.19}$$

What one gets is

$$\int dt_1[\delta(t-t_1)(i\partial_t - \epsilon_d(t)) - \Sigma^{R}(t,t_1)]G^{<}(t_1,t') = \int dt_2 \Sigma^{<}(t,t_2)G^{A}(t_2,t'). \tag{2.20}$$

Inserting the relation

$$[G^{R}]^{-1}(t,t') = (i\partial_t - \epsilon_d(t))\delta(t-t') - \Sigma^{R}(t,t'), \tag{2.21}$$

one has the equality

$$G^{<} = \int dt_1 dt_2 G^{R}(t,t_1)\Sigma^{<}(t_1,t_2)G^{A}(t_2,t'). \tag{2.22}$$

One recognizes in the latter an example of double convolution, whose associated gradient expansion of the Wigner transform is

$$G^{<} = G^{R} * \Sigma^{<} * G^{A}. \tag{2.23}$$

The zero order reads

$$G^{<(0)} = G^{R}\Sigma^{<}G^{A} = iAf, \tag{2.24}$$

where we have introduced the superscript (i), denoting the order of the expansion. We remind that $A(\epsilon)$ is the density of states (Eq. (2.6)) and f is the Fermi distribution $f(\epsilon) = 1/(1 + Exp[\beta(\epsilon - \mu)])$ Regarding the first order, the part dependent on $\dot{\epsilon_d}$ yields a contribution $-i\frac{\dot{\epsilon_d}}{2}\partial_\epsilon f A^2$. Now, extending the results of Ref. [13], we calculate the different contributions to the part which is dependent on $\dot{\Gamma}$

$$\begin{aligned} 1) \qquad & \frac{i}{2}\Big(\partial_\epsilon G^{R}\partial_t\Sigma^{<}G^{A} - G^{R}\partial_t\Sigma^{<}\partial_\epsilon G^{A}\Big) = \frac{i}{2}(i\dot{\Gamma}f)(\partial_\epsilon G^{R}G^{A} - G^{R}\partial_\epsilon G^{A}) \\ & = -\frac{i}{2}\dot{\Gamma}f\frac{A^2}{\Gamma} \end{aligned} \tag{2.25}$$

$$\begin{aligned} 2) \qquad & \frac{i}{2}\Big(- \partial_t G^R \partial_\epsilon \Sigma^< G^A + G^R \partial_\epsilon \Sigma^< \partial_t G^A \Big) \\ & = \frac{i}{2}\dot{\Gamma}(i\Gamma\partial_\epsilon f)\frac{i}{2}([G^R]^2 G^A + G^R[G^A]^2) = -\frac{i}{2}\dot{\Gamma}\partial_\epsilon f \frac{A^2}{\Gamma}(\epsilon - \epsilon_d(t)) \end{aligned} \tag{2.26}$$

$$\begin{aligned} 3) \qquad & \frac{i}{2}\Big(\partial_\epsilon G^R \Sigma^< \partial_t G^A - \partial_t G^R \Sigma^< \partial_\epsilon G^A\Big) \\ & = \frac{i}{2}\dot{\Gamma}(i\Gamma f)\frac{i}{2}\Big(\partial_\epsilon G^R [G^A]^2 + [G^R]^2 \partial_\epsilon G^A\Big) = \frac{i}{2}\dot{\Gamma} f \frac{A^2}{\Gamma} \end{aligned} \tag{2.27}$$

where we have used the following relations: $\partial_\epsilon G^R G^A - G^R \partial_\epsilon G^A = i\frac{A^2}{\Gamma}$, $\partial_t G^{R/A} = -\dot{\epsilon_d}\partial_\epsilon G^{R/A} + \dot{\Gamma}(\mp\frac{i}{2})[G^{R/A}]^2$, $Re(G^R) = \frac{\epsilon-\epsilon_d}{\Gamma}A$ and $[G^R]^2[G^A]^2 = (\frac{A}{\Gamma})^2$.
Overall, we obtain

$$G^<(\epsilon, t) = iAf - i\frac{\dot{\epsilon_d}}{2}\partial_\epsilon f A^2 - i\frac{\dot{\Gamma}}{2}\partial_\epsilon f \frac{A^2}{\Gamma}(\epsilon - \epsilon_d) \tag{2.28}$$

Bearing in mind the form of Eq. 2.24, we can identify a non-equilibrium distribution function

$$\phi = f - \frac{\dot{\epsilon_d}}{2}\partial_\epsilon f A - \frac{\dot{\Gamma}}{2}\partial_\epsilon f \frac{A}{\Gamma}(\epsilon - \epsilon_d). \tag{2.29}$$

2.4 The pumped charge and its noise

The purpose of the present Section is to connect transport quantities to thermodynamic ones. The study of transport through quantum pumps has been the subject of many studies [70, 66, 67, 64, 65, 68, 7, 57]. In particular, the two quantities of interest in transport are the charge pumped in a cycle and its noise. Defining the stroboscopic times in terms of the period T_0 as $T_n = nT_0$ one may define the operator describing the charge pumped in the n-th period as

$$Q_\alpha^{(n)} = \int_{T_{n-1}}^{T_n} dt\ I_\alpha(t) \tag{2.30}$$

where $I_\alpha = -dN_\alpha/dt$, with $N_\alpha = \sum_k c_{k,\alpha}^\dagger c_{k,\alpha}$, is the current flowing out of lead α. Clearly, the average change pumped in M cycles is $Q_\alpha(M) = MQ_\alpha$ where $Q_\alpha = \langle Q_\alpha^{(n)}\rangle$ is the charge pumped in cycle, independent on n in the stationary state.

Coming now to the noise it is evident that current-current correlations produce both fluctuations in the charge pumped in a single cycle as well as correlations of charge pumped in different cycles. The first is described by $\delta Q_{\alpha\alpha}^{(n)} = \langle (Q_\alpha^{(n)})^2\rangle - \langle (Q_\alpha^{(n)})\rangle^2$. In this Section,

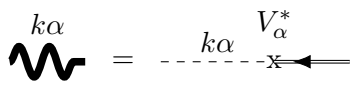

Figure 2.3: This is a visual representation of the diagrammatic expansion of the mixed Green's function on the Keldysh contour. Here we introduced the wobbly line, representing $G^{<}_{d,k\alpha}$ and the other definitions are equal to Fig. (2.2)

however, we will focus on a similar quantity that has the advantage of being similar to the zero frequency component of the noise power spectrum, defined as

$$\delta Q_{\alpha\alpha} = \lim_{M\to+\infty} \frac{(\delta Q_\alpha(M))^2}{M} \tag{2.31}$$

where $(\delta Q_{\alpha\alpha}(M))^2 = \sum_{n,m=1}^{M}(\langle Q_\alpha^{(n)} Q_\alpha^{(m)}\rangle - \langle Q_\alpha^{(n)}\rangle\langle Q_\alpha^{(m)}\rangle$. Using the definition of the operators one may rewrite the latter as

$$\delta Q_{\alpha\alpha} = \lim_{M\to+\infty} \frac{T_0}{T_M}\int_0^{T_M} dt \int_0^{T_M} dt' [\langle I_\alpha(t) I_\alpha(t')\rangle - \langle I_\alpha(t)\rangle\langle I_\alpha(t')\rangle]. \tag{2.32}$$

2.4.1 An alternative derivation of the current's expression

In this section, we recall the known results of the charge pump concerning the resonant level model. Starting from the expression of the Hamiltonian of the dot (Eq. 2.1), the current reads

$$\langle I_\alpha\rangle = -\langle \dot{N}_\alpha\rangle = -i\langle [H, N_\alpha]\rangle = i\sum_k (V_\alpha \langle c^\dagger_{k\alpha} d\rangle - h.c) \tag{2.33}$$

and using the lesser Green's function $G^{<}_{d,k\alpha}(t',t) = i\langle c^\dagger_{k\alpha}(t) d(t')\rangle$ one can write

$$\langle I_\alpha\rangle = 2Re\Big\{ \sum_k V_\alpha G^{<}_{d,k\alpha}(t,t)\Big\}. \tag{2.34}$$

From the diagrammatic expansion of the lesser Green's function (see Fig. (2.3)) entering the definition of the current, it is straightforward to see that, whenever the leads are non-interacting, the latter has the expression [46]

$$G^{<}_{d,k\alpha}(t,t') = \int dt_1 \Big[g^{<}_{k\alpha}(t,t_1)[V_\alpha]^* G^A(t_1,t') + g^r_{k\alpha}(t,t_1)[V_\alpha]^* G^{<}(t_1,t')\Big]. \tag{2.35}$$

Performing now the summation over k using $g^{<}_{k,\alpha}(\epsilon) = 2\pi i\delta(\epsilon-\epsilon_k) f(\epsilon)$ and $g^r_{k,\alpha}(\epsilon) = 1/(\epsilon-\epsilon_k+i0^+)$, where $f(\epsilon) = 1/(\exp[\beta(\epsilon-\mu)]+1)$ is the Fermi function, one has

$$\sum_k G^{<}_{d,k\alpha}(t,t') = \int dt_1 \Big[2\pi\nu_0 i f(t-t_1)[V_\alpha]^* G^A(t_1,t') - \pi\nu_0 i [V_\alpha]^* G^{<}(t_1,t')\Big], \tag{2.36}$$

where $\nu_0 = \sum_k \delta(\epsilon - \epsilon_{k\alpha})$ is the constant density of states and $f(t)$ is the (properly regularized) Fourier transform of the Fermi distribution. Therefore the expectation value of the current operator can be written as

$$\langle I_\alpha \rangle = 2Re\left[i \int dt_1 f(t-t_1) T^a_{\alpha\alpha}(t_1, t') - \frac{i}{2} T^<_{\alpha\alpha}(t,t) \right], \tag{2.37}$$

in terms of the generalized, time-dependent transmission matrices

$$T^{R,A,\gtrless}_{\alpha\beta}(t,t') = 2\pi\nu_0 \sum_k [V_\alpha(t)]^* G^{R,A,\gtrless}(t,t') V_\beta(t'). \tag{2.38}$$

A further simplification of Eq. 2.37 is obtained by expressing of $T^<_{\alpha\alpha}$ in terms of retarded and advanced quantities using

$$G^<(t,t') = \int dt_1 dt_2 G^R(t,t_1) \Sigma^<(t_1,t_2) G^A(t_2,t), \tag{2.39}$$

with

$$\Sigma^<(t,t') = 2\pi\nu_0 i \sum_\alpha V_\alpha(t) f(t-t') [V_\alpha(t')]^*. \tag{2.40}$$

Then one has

$$T^<_{\alpha\alpha}(t,t) = \sum_\beta \int dt_1 dt_2 T^R_{\alpha\beta}(t,t_1) f(t_1-t_2) T^A_{\beta\alpha}(t_2,t). \tag{2.41}$$

Substituting this expression into the current one obtains

$$\begin{aligned} \langle I_\alpha \rangle &= i \int dt_1 [f(t-t_1) T^R_{\alpha\alpha}(t_1,t) - T^A_{\alpha\alpha}(t,t_1) f(t_1-t)] \\ &+ \sum_\beta \int dt_1 dt_2 T^R_{\alpha\beta}(t,t_1) f(t_1-t_2) T^A_{\beta\alpha}(t_2,t). \end{aligned} \tag{2.42}$$

Finally introducing the time-dependent scattering matrices defined as $S_{\alpha\beta} = \delta_{\alpha\beta}\delta(t-t') + iT^R_{\alpha\beta}(t,t')$ one arrives at

$$\langle I_\alpha(t) \rangle = \int dt_1 dt_2 \sum_\beta \left[S_{\alpha\beta}(t,t_1) f_\beta(t_1-t_2) S^\dagger_{\beta\alpha}(t_2,t) - \delta(t-t_1) f_\alpha(t_1-t_2) \delta(t_2-t) \right], \tag{2.43}$$

2.4.2 Brouwer's formula

Let us derive Brouwer's formula from its gradient expansion, applying the techniques of Section A.3. This formula describes the current through a quantum pump at first order in

the gradients. Let us assume the leads to be at equal temperature and chemical potential Starting from expression 2.43, the gradient expansion up to the first order reads

$$\begin{aligned}\langle I_\alpha\rangle &= \int \frac{d\omega}{2\pi} f(\omega)\Big[\sum_\beta \Big\{ S_{\alpha\beta}S^\dagger_{\beta\alpha} + \frac{1}{2i}(\partial_T S_{\alpha\beta}\partial_\omega S^\dagger_{\beta\alpha} - \partial_\omega S_{\alpha\beta}\partial_T S^\dagger_{\beta\alpha})\Big\} - 1\Big] \\ &- \sum_\beta \int \frac{d\omega}{4\pi i}(-f'(\omega))\Big[\partial_T S_{\alpha\beta}S^\dagger_{\beta\alpha} - S_{\alpha\beta}\partial_T S^\dagger_{\beta\alpha}\Big]. \qquad (2.44)\end{aligned}$$

The first term of this sum vanishes due to the gradient expansion of the condition of unitarity of the S-matrix (see Appendix). Therefore we are left only with the last term. Considering the charge pumped in a period T_0

$$Q_\alpha = \int_0^{T_0} dt \langle I_\alpha\rangle, \qquad (2.45)$$

and substituting the expression of the current yields

$$Q_\alpha = -\sum_\beta \int \frac{d\omega}{4\pi i}(-f'(\omega)) \int_0^{T_0} dT \Big\{ \partial_T S_{\alpha\beta}S^\dagger_{\beta\alpha} - S_{\alpha\beta}\partial_T S^\dagger_{\beta\alpha}\Big\}. \qquad (2.46)$$

I must point out that there is no zero-order term. The reason is the absence of any bias or temperature difference between the leads.

In the case we have two parameters (x_1, x_2) that define the pumping cycle, i.e. $S_{\alpha\beta}(t) = S_{\alpha\beta}(x_1(t), x_2(t))$, the dependence on time of the S matrices in the previous expression is to be understood as parametric in the two parameters. One may therefore use Green's theorem to transform the time integral above, which is just an integral over the pumping cycle $(x_1(t), x_2(t))$, into an integral over the area enclosed by the pumping cycle itself. The result is

$$Q_\alpha = \sum_\beta \int \frac{d\epsilon}{4\pi} f'(\epsilon)\Big[\iint_A \frac{dx_1 dx_2}{i}(\partial_{x_2} S_{\alpha\beta}\partial_{x_1} S^\dagger_{\beta\alpha} - \partial_{x_1} S_{\alpha\beta}\partial_{x_2} S^\dagger_{\beta\alpha})\Big]. \qquad (2.47)$$

The scattering matrix entering this expression is the instantaneous scattering matrix depending on the varied parameters in time x_1, x_2. For the resonant level model, where the time-dependent parameters are the level position and the hybridization strength to the leads, one has, therefore, the following expression $(\alpha, \beta = L, R)$

$$S = \begin{pmatrix} 1 - i\Gamma^L G^R & -i\sqrt{\Gamma_L\Gamma_R}G^R \\ -i\sqrt{\Gamma_L\Gamma_R}G^R & 1 - i\Gamma_R G^R \end{pmatrix} \qquad (2.48)$$

with

$$G^R = \frac{1}{\epsilon - \epsilon_d + i\frac{\Gamma}{2}}. \qquad (2.49)$$

2.4.3 The quantum noise

A similar expansion can be derived to obtain the current noise. This expression is analogous to those derived in Ref. [58], i.e. the noise can be separated into two different terms

$$\begin{aligned}
\delta Q_{\alpha\alpha} &= \frac{T_0}{T_m}\int_0^{T_m} dtdt' \int dt_1 dt_2 f(t_1-t')\tilde{f}(t'-t_2)[\delta(t-t_1)\delta(t-t_2) - S^\dagger_{\alpha\alpha}(t_1,t)S_{\alpha\alpha}(t,t_2)] \\
&+ \frac{T_0}{T_m}\int_0^{T_m} dtdt' \int dt_1 dt_2 f(t'-t_2)\tilde{f}(t_1-t')[\delta(t-t_1)\delta(t-t_2) - S^\dagger_{\alpha\alpha}(t_1,t)S_{\alpha\alpha}(t,t_2)] \\
&+ \frac{T_0}{T_m}\int_0^{T_m} dtdt' \int dt_1 dt_2 dt_1' dt_2' f(t_1-t_2')\tilde{f}(t_1'-t_2)\cdot \\
&\quad \sum_{\gamma\delta}[S^\dagger_{\alpha\gamma}(t_1,t)S_{\alpha\delta}(t,t_2)S^\dagger_{\delta\alpha}(t_1',t')S_{\gamma\alpha}(t',t_2') - \delta(t-t_1)\delta(t'-t_1')\delta(t-t_2)\delta(t'-t_2')]
\end{aligned} \tag{2.50}$$

where $\tilde{f}(t,t') = \delta(t-t') - f(t,t')$.

To perform the adiabatic expansion of both terms, let us notice that they have the same structure as a product of convolutions. Then, denoting each convolution with $A(t,t')$ and $B(t',t)$,

$$\frac{T_0}{T_m}\int_0^{T_m} dtdt' A(t,t')B(t',t) = \int_0^{T_m} dT \int_{-T_m}^{T_m} d\tau \int \frac{d\epsilon}{2\pi}\int \frac{d\epsilon'}{2\pi} e^{i(\epsilon-\epsilon')\tau} A(\epsilon,T)B(\epsilon',T) \tag{2.51}$$

Taking $m \to +\infty$ yields

$$\int_0^{T_0} dT \frac{d\epsilon}{2\pi} A(\epsilon,T)B(\epsilon,T) \tag{2.52}$$

and performing an expansion in the gradients as done before for the current one obtains at zero order

$$\delta Q^{(0)}_{\alpha\alpha} = -2\int \frac{d\epsilon}{2\pi}(-\frac{1}{\beta}\frac{\partial f}{\partial \epsilon})\int_0^{T_0} dT\left(1 - S_{\alpha\alpha}(\epsilon,T)S^\dagger_{\alpha\alpha}(\epsilon,T)\right). \tag{2.53}$$

where β is the inverse temperature. This is the average over a period of the instantaneous equilibrium Johnson-Nyquist noise [10].

At first order in the gradients the only non-zero contribution is

$$\begin{aligned}
\delta Q^{(1),th}_{\alpha\alpha} &= \int_0^{T_0} dT \int \frac{d\epsilon}{4\pi i}(-\frac{1}{\beta}\frac{\partial^2 f}{\partial \epsilon^2})\sum_{\beta\neq\alpha}\left[\partial_T S_{\alpha\beta}S^\dagger_{\alpha\beta} - S_{\alpha\beta}\partial_T S^\dagger_{\alpha\beta}\right] \\
&- \int_0^{T_0} dT \int \frac{d\epsilon}{4\pi i}(-\frac{1}{\beta}\frac{\partial f}{\partial \epsilon})\sum_{\beta}\left[\partial_\epsilon S_{\alpha\beta}\partial_T S^\dagger_{\alpha\beta} - \partial_T S_{\alpha\beta}\partial_\epsilon S^\dagger_{\alpha\beta}\right].
\end{aligned} \tag{2.54}$$

this term, which depends on the operation of the pump, is a first-order contribution to thermal noise proportional to the temperature and vanishing at zero temperature [66, 91]. The gradient expansion performed above turns out to miss an important shot noise term and is valid only when $\hbar\Omega \ll k_B T$, where $\Omega = \frac{2\pi}{T_0}$. The finite shot-noise contribution which survives even at zero order was first computed in Ref.[66]. It arises from the emission/absorption of quanta of energy from the scatterer. The expression of this zero-temperature shot noise is

$$\delta Q^{(1),sh}_{\alpha\alpha} = \sum_{q=1}^{\infty} \frac{q}{4\pi} C^{(sym)}_{\alpha\alpha,q}(0) \tag{2.55}$$

where

$$C^{(sym)}_{\alpha\alpha,q}(E) = \frac{C_{\alpha\alpha,q}(E) + C_{\alpha\alpha,-q}(-E)}{2} \tag{2.56}$$

$$C_{\alpha\alpha,q}(E) = \sum_{\gamma\delta} [S^*_{\alpha\gamma}(E) S_{\alpha\delta}(E)]_q [S^*_{\alpha\delta}(E) S_{\alpha\gamma}(E)]_{-q}, \tag{2.57}$$

which arises from the quartic term of Eq. 2.50. The superscript $[]_q$ identifies the Fourier coefficients, defined as

$$[A]_q(E) = \int_0^{T_0} \frac{dt}{T_0} e^{iq\Omega t} A(E,t). \tag{2.58}$$

The derivation of the present shot noise term is described in Appendix C. Moreover, the relevance of the various terms of the noise is discussed in more detail in the Appendix C.1. In Section 2.6 we will analyze the noise obtained together with thermodynamic quantities to gain further insight into the relationship between transport and thermodynamics.

2.5 The quantum pump as an engine

Now that the transport problem is described in its full generality, let us look at a quantum pump as a thermodynamic engine. By varying the parameters $x_i(t)$ over a cycle it is clear that a certain work on the system is being performed, as well as dissipated heat and entropy generated. We note that at least two parameters are varied, as the current in Brouwer's formula is a geometric quantity, i.e. defined by an integral over the area spanned by the cycle.

The goal of this Section will be to give concrete expressions to these quantities for the specific problem of quantum pumping of a resonant level model. Of course, as in the case of transport properties, we will have to proceed in steps, first considering the quasi-static limit, and then proceeding to higher-order contributions in the gradient expansion.

2.5.1 Quasistatic limit

Let us start developing this formalism in the limit of reversible and quasi-static transformations where one can work in the equilibrium gran-canonical framework at fixed temperature β^{-1} and chemical potential μ. Evaluating the grand potential of the total system, $\Omega = -1/\beta \ln \Xi$, where $\Xi = Tr[e^{-\beta(H-\mu N)}]$, in terms of the density of states $\rho(\epsilon)$ of the total system one obtains

$$\Omega_{tot} = -\frac{1}{\beta}\int \frac{d\epsilon}{2\pi}\rho(\epsilon)\ln[1+e^{-\beta(\epsilon-\mu)}]. \tag{2.59}$$

We are now interested in extracting the time-dependent part of this expression when parameters are varied quasi-statically: for a resonant level model in which the time-dependent parameters are $\epsilon_d(t), \Gamma_{L/R}(t)$ this amounts to the replacement in Eq.(2.59) of the total density of states $\rho(\epsilon)$ with the *instantaneous* local spectral function of the dot $A_t(\omega) = A(\omega, [\epsilon_d(t), \Gamma_{L/R}(t)]) = -2\mathrm{Im}[G^r(\omega, [\epsilon_d(t), \Gamma_{L/R}(t)])]$ obtaining an *instantaneous* grand potential

$$\Omega_t = -\frac{1}{\beta}\int \frac{d\epsilon}{2\pi}A_t(\epsilon)\ln[1+e^{-\beta(\epsilon-\mu)}]. \tag{2.60}$$

In fact, the density of states is given as the trace of the spectral function of the system over all the single-particle states n A_{nn}

$$A_t(\epsilon) = \sum_n A_{nn}(\epsilon) \tag{2.61}$$

and we remind that $A_{nn} = -2ImG^R_{nn}$ in terms of the retarded Green function. In the basis of uncoupled dot and leads electron states one can decompose the density of states in terms of the dot and leads contributions

$$A_t(\epsilon) = A(\epsilon) + \sum_{k\alpha} A_{kk,\alpha}(\epsilon), \tag{2.62}$$

where $A(\epsilon)$ is the density of states of the dot (Eq. 2.6). To calculate $A_{kk,\alpha}$ one can write the Dyson equation for the retarded Green function of the leads (Fig. (2.4))

$$G^R_{kk,\alpha}(\epsilon) = g^R_{k\alpha}(\epsilon) + g^R_{k\alpha}(\epsilon)V^2_\alpha(t)G^R(\epsilon)g^R_{k\alpha}(\epsilon), \tag{2.63}$$

so that

$$A_{kk,\alpha} = -2ImG^R_{kk,\alpha}(\epsilon) = -2Img^R_{k\alpha}(\epsilon) + V^2_\alpha(t)(A(\epsilon)Re[g^R_{k\alpha}(\epsilon)^2] - 2ReG^R(\epsilon)Im[g^R_{k\alpha}(\epsilon)^2]. \tag{2.64}$$

Knowing that the free Green function of the leads has the expression

$$g^R_{k\alpha}(\epsilon) = \frac{1}{\epsilon - \epsilon_{k\alpha} + i\eta^+} \tag{2.65}$$

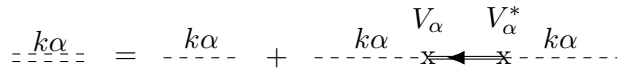

Figure 2.4: Here we introduce the diagrammatic expansion of the bath's Green function, renormalized by the interaction with the dot. The double dashed line represents the dressed Green function $G^C_{kk,\alpha}$

the relation

$$\frac{d}{d\epsilon} g^R_{k\alpha}(\epsilon) = -g^R_{k\alpha}(\epsilon)^2 \tag{2.66}$$

holds and defining $\Sigma_\alpha(\epsilon) = \sum_k |V_\alpha|^2 g^R_{k\alpha}(\epsilon)$ one can rewrite the above density of states as

$$A_t(\epsilon) = A(\epsilon)\left(1 - \frac{d}{d\epsilon} Re(\Sigma_\alpha(\epsilon))\right) + 2Re(G^R(\epsilon))\frac{d}{d\epsilon} Im(\Sigma_\alpha(\epsilon)) + \nu_\alpha(\epsilon), \tag{2.67}$$

where $\nu_\alpha(\epsilon) = -2\sum_k Im(g^R_{k\alpha}(\epsilon))$. Since we work in the wide-band limit, the self-energy has no energy dependence and has the expression

$$\Sigma_\alpha = -\frac{i}{2}\Gamma_\alpha. \tag{2.68}$$

As a consequence, the terms that depend on the derivatives of the self-energy vanish. Furthermore, the free density of states of the leads depends neither on ϵ_d nor on Γ_α so that we can cast it aside. What one is left with is simply the density of states of the dot alone A.

From this expression, one can derive the quasi-static thermodynamic functions $N^{(0)}_t$, $S^{(0)}_t$ and $E^{(0)}_t$, respectively particle number, entropy, energy [13] obtaining

$$N^{(0)}_t = \int \frac{d\epsilon}{2\pi} A_t(\epsilon) f(\epsilon), \tag{2.69}$$

$$S^{(0)}_t = k_B \int \frac{d\epsilon}{2\pi} A_t(\epsilon)\Big[- f\ln f - (1-f)\ln(1-f)\Big], \tag{2.70}$$

$$E^{(0)}_t = \int \frac{d\epsilon}{2\pi} \epsilon\, A_t(\epsilon) f(\epsilon) \tag{2.71}$$

The derivatives of these quantities with respect to time are connected to the reversible energy change $\dot{E}^{(1)}$, the reversible power $\dot{W}^{(1)}$, the heat exchange rate $\dot{\mathcal{Q}}^{(1)}$ and the current $\dot{N}^{(1)}$. In particular, from Eq. (2.62) and Eq. (2.14), in the wide-band limit one can verify the following relation $\partial_\Gamma A = -\partial_\epsilon Re(G^R)$, then the expression for the reversible power $\dot{W}^{(1)} = \dot{\epsilon}_d \partial_{\epsilon_d}\Omega + \sum_\alpha \dot{\Gamma}_\alpha \partial_{\Gamma_i}\Omega$ can be written as

$$\dot{W}^{(1)} = \dot{\epsilon_d} \int \frac{d\epsilon}{2\pi} Af + \dot{\Gamma} \int \frac{d\epsilon}{2\pi} Re(G^R) f. \tag{2.72}$$

Similar calculations lead to the expression of the quasi-static heat exchange rate as

$$\dot{\mathcal{Q}}^{(1)} = T\frac{dS^{(0)}}{dt} = \dot{\epsilon_d}\int \frac{d\epsilon}{2\pi}(\epsilon-\mu)A\partial_\epsilon f + \dot{\Gamma}\int \frac{d\epsilon}{2\pi}(\epsilon-\mu)Re(G^R)\partial_\epsilon f. \tag{2.73}$$

The current out of the dot is

$$\dot{N}^{(1)} = \frac{dN^{(0)}}{dt} = \dot{\epsilon_d}\int \frac{d\epsilon}{2\pi}A\partial_\epsilon f + \dot{\Gamma}\int \frac{d\epsilon}{2\pi}Re(G^R)\partial_\epsilon f. \tag{2.74}$$

Finally, the energy exchange rate

$$\dot{E}^{(1)} = \frac{dE^{(0)}}{dt} = -\dot{\epsilon_d}\int \frac{d\epsilon}{2\pi}\epsilon\partial_\epsilon A f - \dot{\Gamma}\int \frac{d\epsilon}{2\pi}\epsilon f\partial_\epsilon Re(G^R). \tag{2.75}$$

Notice that these quantities satisfy the first law of thermodynamics in the form

$$\dot{E}^{(1)} = \dot{W}^{(1)} + \dot{\mathcal{Q}}^{(1)} + \mu\dot{N}^{(1)}. \tag{2.76}$$

These expressions highlight a similarity of the structure of the terms proportional to $\dot{\epsilon}_d$ and to $\dot{\Gamma}$.

2.5.2 Gradient expansion of thermodynamic quantities

Let us now come to the main results of this Chapter: a self-contained thermodynamic description of the operation of a quantum pump. Quantum pumping is not a quasi-static phenomenon: the quasi-static contribution to the pumped current is simply zero. It is intuitively appealing that the same will be true for certain thermodynamic quantities that are expected to be intimately connected to the flow of a current, such as the heat dissipated and the entropy produced. Therefore in order to address them we will have to extend the present analysis to account for corrections to the quasi-static limit using a gradient expansion. Our goal will be for each generic quantity to express it as expansion in gradients as $\mathcal{O} = \sum_i \mathcal{O}^{(i)}$, where $\mathcal{O}^{(i)}$ contains the i-th time derivative. In order to do so we will first write $\mathcal{O}$ in terms of non-equilibrium Green's functions (Section 2.3) and then perform their adiabatic expansion deriving the next-order corrections to the expressions obtained in the previous section. The expansion we are going to derive is an expansion in gradients precisely as the one obtained for the pumped charge and the noise, i.e. using as small parameters $\dot{\epsilon}_d/\Gamma^2$ and $\dot{\Gamma}_\alpha/\Gamma^2$.

Let us start with the simplest quantity: the particle number in the resonant level. The average number of particles is readily connected to a Green's function using its definition, $N = \langle d^\dagger d\rangle = -iG^<(t,t)$. Therefore one can identify $N^{(i)}$ with the i-th order expansion in the gradients of the lesser Green function (see Section 2.3) which can be calculated starting from the Keldysh equation

$$G^< = \int dt_1 dt_2 G^R(t,t_1)\Sigma^<(t_1,t_2)G^A(t_2,t'). \tag{2.77}$$

Performing a gradient expansion of this one readily obtains the zeroth order terms reported above and

$$N^{(1)} = -\frac{\dot{\epsilon_d}}{2}\int \frac{d\epsilon}{2\pi}\partial_\epsilon f A^2 - \frac{\dot{\Gamma}}{2}\int \frac{d\epsilon}{2\pi}\partial_\epsilon f \frac{A^2}{\Gamma}(\epsilon-\epsilon_d). \tag{2.78}$$

This result can be used to compute the second-order correction to the current out of the dot

$$\begin{aligned}\dot{N}^{(2)} = &-\frac{\dot{\epsilon_d}^2}{2}\int \frac{d\epsilon}{2\pi}\partial_\epsilon^2 f A^2 - \frac{\dot{\Gamma}^2}{2}\int \frac{d\epsilon}{2\pi}\partial_\epsilon f(\epsilon-\epsilon_d)\partial_\Gamma\left(\frac{A^2}{\Gamma}\right)\\ &-\frac{\dot{\epsilon_d}\dot{\Gamma}}{2}\int \frac{d\epsilon}{2\pi}\left[\partial_\Gamma A^2 - \frac{A^2}{\Gamma} + \frac{\partial_\epsilon A^2}{\Gamma}(\epsilon-\epsilon_d)\right]\partial_\epsilon f - \frac{\ddot{\epsilon_d}}{2}\int \frac{d\epsilon}{2\pi}\partial_\epsilon f A^2 - \frac{\ddot{\Gamma}}{2}\int \frac{d\epsilon}{2\pi}\partial_\epsilon f\frac{A^2}{\Gamma}(\epsilon-\epsilon_d).\end{aligned} \tag{2.79}$$

The argument becomes more involved if one wants to calculate the gradient expansion of the entropy. For this sake one needs to substitute in the expression for the entropy introduced the Fermi distribution f with the non-equilibrium distribution ϕ [26] obtained from the Wigner transform of the lesser Green's function $G^<(\epsilon,T) = iA\phi$

$$S = k_B\int \frac{d\epsilon}{2\pi}A\Big[-\phi\ln\phi - (1-\phi)\ln(1-\phi)\Big]. \tag{2.80}$$

A gradient expansion of the lesser Green's function (and a similar one for the retarded one) results in a gradient expansion for the non-equilibrium distribution, hence for the entropy. The results for ϕ are given in Section 2.3. The resulting expansion to the first order of the non-equilibrium distribution gives $S^{(1)}$

$$S^{(1)} = -\frac{k_B\dot{\epsilon_d}}{2}\int \frac{d\epsilon}{2\pi}\left(\frac{\epsilon-\mu}{k_BT}\right)\partial_\epsilon f A^2 - \frac{k_B\dot{\Gamma}}{2}\int \frac{d\epsilon}{2\pi}\left(\frac{\epsilon-\mu}{k_BT}\right)\partial_\epsilon f\frac{A^2}{\Gamma}(\epsilon-\epsilon_d) \tag{2.81}$$

and therefore the entropy production rate to the second order is

$$\begin{aligned}\dot{S}^{(2)} = &\frac{\dot{\epsilon_d}^2}{2T}\int \frac{d\epsilon}{2\pi}(\epsilon-\mu)\partial_\epsilon f\partial_\epsilon A^2 \; - \frac{\dot{\Gamma}^2}{2T}\int \frac{d\epsilon}{2\pi}(\epsilon-\mu)\partial_\epsilon f(\epsilon-\epsilon_d)\partial_\Gamma\left(\frac{A^2}{\Gamma}\right)+\\ &-\frac{\dot{\epsilon_d}\dot{\Gamma}}{2T}\int \frac{d\epsilon}{2\pi}(\epsilon-\mu)\partial_\epsilon f\left[\partial_\Gamma A^2 - \frac{\partial_\epsilon A^2}{\Gamma}(\epsilon-\epsilon_d) + \frac{A^2}{\Gamma}\right] - \frac{\ddot{\epsilon_d}}{2T}\int \frac{d\epsilon}{2\pi}(\epsilon-\mu)\partial_\epsilon f A^2\\ &-\frac{\ddot{\Gamma}}{2T}\int \frac{d\epsilon}{2\pi}(\epsilon-\mu)\partial_\epsilon f\frac{A^2}{\Gamma}(\epsilon-\epsilon_d).\end{aligned} \tag{2.82}$$

Coming to the internal energy, it can be verified that at zero order $E^{(0)} = \langle H_D\rangle^{(0)} + \frac{1}{2}\langle H_V\rangle^{(0)}$, following the choice of Ref. [26]. One may then identify an "effective system" of Hamiltonian $H_{eff} = H_D + \frac{1}{2}H_V$ and an "effective bath" $H_B + \frac{1}{2}H_V$ [13]. This is because

one can verify that this choice gives the correct result, coinciding with $\langle H_D\rangle^{(0)} + \langle H_V\rangle^{(0)} + \langle H_D\rangle^{(0)}$. Therefore, at every order in a gradient expansion, one has

$$E^{(i)} = \langle H_D\rangle^{(i)} + \frac{1}{2}\langle H_V\rangle^{(i)}. \tag{2.83}$$

Let us derive the expression of $\langle H_V\rangle$ up to the first order from the expansion of the mixed Green function. To calculate $\langle H_V\rangle$ we write

$$\langle H_V\rangle = \sum_\alpha V_\alpha(t) \sum_k \Big[\langle d^\dagger c_{k\alpha}\rangle + \langle c^\dagger_{k\alpha} d\rangle\Big] = \sum_\alpha \langle H_V^\alpha\rangle, \tag{2.84}$$

where we define $H_V^\alpha = V_\alpha(t)\sum_k \Big[d^\dagger c_{k\alpha} + c^\dagger_{k\alpha} d\Big]$. It reads

$$\langle H_V^\alpha\rangle = 2V_\alpha(t) \sum_k Im\Big[G^<_{d,k\alpha}(t,t)\Big], \tag{2.85}$$

with $G^<_{d,k\alpha} = i\langle c^\dagger_{k\alpha}(t')d(t)\rangle$, for which the property $G^<_{d,k\alpha}(t,t) = -\big(G^<_{k\alpha,d}(t,t)\big)^*$ holds. The equation of motion for the mixed Green function leads to

$$\begin{aligned}\langle H_V^\alpha\rangle =& 2V_\alpha(t)\sum_k Im\bigg(\int dt'[G^R(t,t')g^<_{k\alpha}(t',t) + G^<(t,t')g^A_{k\alpha}(t',t)]\bigg)\\ =& 2Im\bigg(\int dt'[G^R(t,t')\Sigma^<_\alpha(t',t) + G^<(t,t')\Sigma^A_\alpha(t',t)]\bigg)\end{aligned} \tag{2.86}$$

Moving to the Wigner transform

$$\langle H_V^\alpha\rangle = 2Im\bigg(\int \frac{d\epsilon}{2\pi}[G^R(\epsilon,t) * \Sigma^<_\alpha(\epsilon,t) + G^<(\epsilon,t) * \Sigma^A_\alpha(\epsilon,t)]\bigg). \tag{2.87}$$

The second term $G^<(\epsilon,t) * \Sigma^A_\alpha(\epsilon,t) = G^<(\epsilon,t) * (\frac{i}{2}\Gamma_\alpha)$ dose not contribute. In fact, the zero-order term is real and to the next order one can apply this type of argument

$$\int \frac{d\epsilon}{2\pi} Im\bigg(\frac{i}{2}\partial_\epsilon G^<(\epsilon,t)\frac{i}{2}\dot\Gamma_\alpha\bigg) = \frac{\dot\Gamma_\alpha}{4}\int\frac{d\epsilon}{2\pi}\frac{\partial_\epsilon G^<(\epsilon,t)}{i} = \frac{\dot\Gamma_\alpha}{8\pi}\bigg[\frac{G^<(\epsilon,t)}{i}\bigg]^{+\infty}_{-\infty} = 0. \tag{2.88}$$

Up to the first order in the velocity, the gradient expansion yields

$$\langle H_V^\alpha\rangle = 2Im\bigg(\int\frac{d\epsilon}{2\pi}\bigg[G^R(\epsilon,t)if(\epsilon)\Gamma_\alpha - \frac{i}{2}\partial_t G^R(\epsilon,t)i\partial_\epsilon f\Gamma_\alpha + \frac{i}{2}\partial_\epsilon G^R(\epsilon,t)if(\epsilon)\dot\Gamma_\alpha\bigg]\bigg). \tag{2.89}$$

The gradient expansion of the whole interaction term therefore reads

$$\langle H_V\rangle = 2Im\bigg(\int\frac{d\epsilon}{2\pi}\bigg[G^R(\epsilon,t)if(\epsilon)\Gamma - \frac{i}{2}\partial_t G^R(\epsilon,t)i\partial_\epsilon f\Gamma + \frac{i}{2}\partial_\epsilon G^R(\epsilon,t)if(\epsilon)\dot\Gamma\bigg]\bigg). \tag{2.90}$$

.

As for the internal energy, we will compute the zeroth order in the gradients (quasi-static approximation) in Eq.(2.5.1) and the rate of change to first order in Eq.(2.75). Let us now evaluate the first-order correction of the energy

$$E^{(1)} = -\frac{\dot{\epsilon_d}}{2}\int \frac{d\epsilon}{2\pi}\epsilon\partial_\epsilon f A^2 - \frac{\dot{\Gamma}}{2}\int \frac{d\epsilon}{2\pi}\epsilon\partial_\epsilon f\frac{A^2}{\Gamma}(\epsilon-\epsilon_d), \tag{2.91}$$

whose time derivative reads

$$\begin{aligned}\dot{E}^{(2)} = &\frac{\dot{\epsilon_d}^2}{2}\int \frac{d\epsilon}{2\pi}\epsilon\partial_\epsilon f\partial_\epsilon A^2 - \frac{\dot{\Gamma}^2}{2}\int \frac{d\epsilon}{2\pi}\epsilon\partial_\epsilon f(\epsilon-\epsilon_d)\partial_\Gamma\left(\frac{A^2}{\Gamma}\right)+\\ &+\frac{\dot{\epsilon_d}\dot{\Gamma}}{2}\int \frac{d\epsilon}{2\pi}\left[\epsilon\partial_\epsilon f\partial_\Gamma A^2+\epsilon\frac{\partial_\epsilon A^2}{\Gamma}\partial_\epsilon f(\epsilon-\epsilon_d)\right]-\frac{\ddot{\epsilon_d}}{2}\int \frac{d\epsilon}{2\pi}\epsilon\partial_\epsilon f A^2\\ &-\frac{\ddot{\Gamma}}{2}\int \frac{d\epsilon}{2\pi}\epsilon\partial_\epsilon f\frac{A^2}{\Gamma}(\epsilon-\epsilon_d).\end{aligned} \tag{2.92}$$

The expression for the energy agrees with the energy-resolved one [26]

$$E^{(i)} = \int \frac{d\epsilon}{2\pi}\epsilon A(\epsilon,T)\phi^{(i)}(\epsilon,T). \tag{2.93}$$

The power can be computed according to the definition. One can distinguish two different contributions, relative to H_D and H_V. The first one is

$$\dot{W}_D^{(i)} = \langle\frac{\partial H_D}{\partial\epsilon_d}\rangle^{(i-1)}\dot{\epsilon}_d = \dot{\epsilon}_d N^{(i-1)}. \tag{2.94}$$

Likewise for the components of the coupling

$$\dot{W}_V^{(i)} = \sum_\alpha\langle\frac{\partial H_V}{\partial V_\alpha}\rangle^{(i-1)}\dot{V}_\alpha = \sum_\alpha \dot{V}_\alpha(t)\sum_k(\langle d^\dagger c_{k\alpha}\rangle^{(i)}+h.c.) = \sum_\alpha\frac{\dot{V}_\alpha(t)}{V_\alpha(t)}\langle H_V^\alpha\rangle^{(i)}. \tag{2.95}$$

Changing variable to Γ_α

$$\dot{W}_V^{(i)} = \sum_\alpha\frac{\dot{\Gamma}_\alpha}{2\Gamma_\alpha}\langle H_V^\alpha\rangle^{(i-1)}, \tag{2.96}$$

so that

$$\dot{W}^{(i)} = \dot{W}_V^{(i)} + \dot{W}_D^{(i)}. \tag{2.97}$$

The first order in the gradients of the power was computed in Eq. 2.72. We now use the expansion above to compute the second order correction as

$$\begin{aligned}\dot{W}^{(2)} = &-\frac{\dot{\epsilon_d}^2}{2}\int\frac{d\epsilon}{2\pi}\partial_\epsilon f A^2 - \frac{\dot{\Gamma}^2}{4}\int\frac{d\epsilon}{2\pi}\partial_\epsilon f\partial_\Gamma A + \frac{\dot{\epsilon_d}\dot{\Gamma}}{2}\int\frac{d\epsilon}{2\pi}\partial_\epsilon f\partial_\epsilon A\\ &+\sum_\alpha\frac{\dot{\Gamma}_\alpha^2}{2\Gamma_\alpha}\int\frac{d\epsilon}{2\pi}f\frac{\partial_\epsilon A}{2}.\end{aligned} \tag{2.98}$$

Note the presence of Γ_α at the denominator: this term causes a singularity at $\Gamma_\alpha = 0$, which appears only when multiple heat baths are present.

The heat exchange rate $\mathcal{Q}$ cannot be calculated directly [27] since there are no physical process accounting for dissipation and the Landauer-like picture of transport assumes that dissipation processes take place far away from the system and do not affect its dynamics [51]. The only way it can be derived is from the first law of thermodynamics. The latter reads

$$\dot{E}^{(i)} = \dot{W}^{(i)} + \dot{\mathcal{Q}}^{(i)} + \mu\dot{N}^{(i)}. \tag{2.99}$$

Then, the heat exchange has to be calculated inverting this relation

$$\dot{\mathcal{Q}}^{(i)} = \dot{E}^{(i)} - \dot{W}^{(i)} - \mu\dot{N}^{(i)}. \tag{2.100}$$

Finally, the heat exchange flow reads

$$\begin{aligned}
\dot{\mathcal{Q}}^{(2)} = &-\frac{\dot{\epsilon}_d^2}{2}\int\frac{d\epsilon}{2\pi}(\epsilon-\mu)\partial_\epsilon^2 f A^2 - \frac{\dot{\Gamma}^2}{2}\int\frac{d\epsilon}{2\pi}\partial_\epsilon f(\epsilon-\epsilon_d)(\epsilon_d-\mu)\partial_\Gamma\left(\frac{A^2}{\Gamma}\right)\\
&-\frac{\dot{\Gamma}^2}{4}\int\frac{d\epsilon}{2\pi}\partial_\epsilon^2 f(\epsilon-\epsilon_d)\partial_\Gamma A - \sum_\alpha\frac{\dot{\Gamma}_\alpha^2}{2\Gamma_\alpha}\int\frac{d\epsilon}{2\pi}f\frac{\partial_\epsilon A}{2}\\
&-\frac{\ddot{\epsilon_d}}{2}\int\frac{d\epsilon}{2\pi}(\epsilon-\mu)\partial_\epsilon f A^2 - \frac{\ddot{\Gamma}}{2}\int\frac{d\epsilon}{2\pi}(\epsilon-\mu)\partial_\epsilon f\frac{A^2}{\Gamma}(\epsilon-\epsilon_d)\\
&-\frac{\dot{\epsilon}_d\dot{\Gamma}}{2}\int\frac{d\epsilon}{2\pi}\partial_\epsilon f(\epsilon_d-\mu)\left[\partial_\Gamma A^2 - \frac{A^2}{\Gamma} + \frac{\partial\epsilon A^2}{\Gamma}(\epsilon-\epsilon_d)\right]\\
&+\frac{\dot{\epsilon}_d\dot{\Gamma}}{2}\int\frac{d\epsilon}{2\pi}\partial_\epsilon f(\epsilon-\epsilon_d)\partial_\Gamma A^2 - \frac{\dot{\epsilon}_d\dot{\Gamma}}{4}\int\frac{d\epsilon}{2\pi}\partial_\epsilon^2 f(\epsilon-\epsilon_d)\partial_\epsilon A.
\end{aligned} \tag{2.101}$$

The results obtained for N and $\dot{W}$ are consistent with the ones found in [78].
A final comment on the adiabatic expansion we have just performed is that the entropy production rate is not simply related only to heat production; there is a further contribution that can be identified with dissipated power. In particular this relation holds

$$\dot{S}^{(2)} = \frac{\dot{\mathcal{Q}}^{(2)}}{T} + \frac{\dot{W}^{(2)}}{T}. \tag{2.102}$$

This is because in general, one has this expression

$$\frac{dS}{dt} = \dot{\Sigma} + \frac{\dot{\mathcal{Q}}}{T}, \tag{2.103}$$

where $\dot{\Sigma}$ can be related to the entropy production of the universe and S is the system's entropy. In turn, the change of the entropy of the universe is caused by the mismatch between the corresponding reversible work rate and the work rate in an irreversible process, called unusable energy, i.e.

$$T\dot{\Sigma} = \dot{E}_{un} = \dot{W}_{rev} - \dot{W}, \tag{2.104}$$

which up to second order corresponds to $\dot{W}^{(2)}$ [37].

2.6 Quantum thermodynamics of various pumping cycles

It is now time to put all the pieces of the puzzle together and show how the formulas developed above can be used to gain insight into the physics of quantum pumping by combining information on thermodynamic quantities as well as transport properties (pumped charge and its noise). We will do so for various examples of cycles constructed for a resonant-level model.

2.6.1 The peristaltic cycle

The simplest cycle one can think of is the 'peristaltic' cycle which consists of four strokes as shown in Fig. (2.5): the level initially empty at $+\epsilon_0$ coupled only to Γ_L. It is then lowered to $-\epsilon_0$ and filled with an electron from the left. Afterwards, the coupling is switched to the right and the level is raised again to $+\epsilon_0$ and emptied on the right. Finally, the coupling is reinstated to its initial value. In this cycle, the two time-dependent quantities are ϵ_d and $\delta\Gamma = \Gamma_L - \Gamma_R$. The total decay rate $\Gamma = \Gamma_L + \Gamma_R$ is not changed.

One can calculate the current, using Brouwer's formula (Section 2.4.3). In the limit of low temperature T, the pumped charge is

$$Q_L^{(0)} = \frac{2}{\pi}\left\{ \arctan(x) + \frac{x}{1+x^2} \right\} + O(T^2), \tag{2.105}$$

where $x = \frac{\epsilon_0}{\Gamma/2}$. In the limit $x >> 1$, the pumped charge is quantized, $Q_L^{(0)} \to 1$ (Fig. (2.7)).

The expectation is that the corresponding noise will tend to zero in the quantization limit. We are interested in the zero-temperature limit, which enjoys contributions only from the 'shot' noise (Sec. 2.4.3). The zeroth order contribution to the current noise is just thermal and vanishes in this limit

$$\delta Q_{LL}^{(0)} = 0. \tag{2.106}$$

We evaluate the first-order term in the gradients, containing the relevant shot noise contribution. The result of this calculation gives a current noise which tends to zero in the quantization limit

$$\lim_{x\to\infty} \delta Q_{LL}(x) = 0, \tag{2.107}$$

(see e.g. Fig. (2.6)).

Let us now proceed with the comparison with thermodynamic quantities by integrating the previously calculated ones over a cycle. Integrating over a cycle quantities expanded up to the first order will give a quantity independent of the cycle parametrization, hence geometric. In the present case, however, the integrals are all vanishing, as one can see from the one of the power expanded to first order

$$\dot{W}^{(1)} = \frac{\partial\Omega}{\partial\epsilon_d}\dot{\epsilon}_d + \frac{\partial\Omega}{\partial\Gamma}\dot{\Gamma}, \tag{2.108}$$

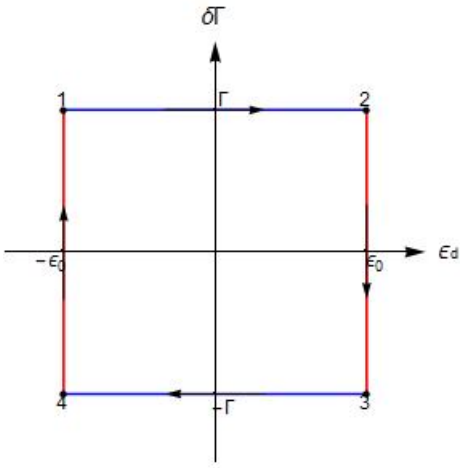

Figure 2.5: The peristaltic cycle: the level initially empty at $+\epsilon_0$ coupled only to Γ_L. It is then lowered to $-\epsilon_0$ and filled with an electron from the left. Afterwards, the coupling is switched to the right and the level is raised again to $+\epsilon_0$ and emptied on the right. Finally, the coupling is reinstated to its initial value.

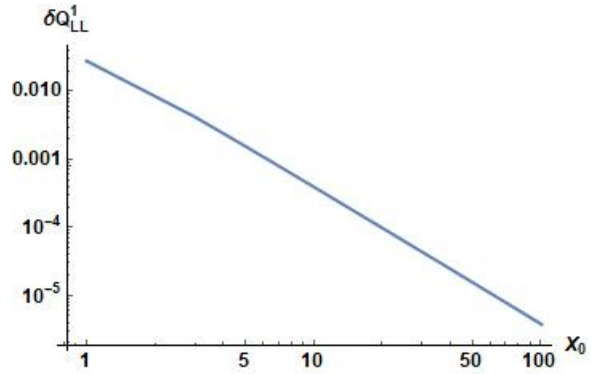

Figure 2.6: The first order of the noise integrated over the peristaltic cycle in the zero-temperature limit (in logarithmic scale). In this case, we have set $v_{\epsilon_d} = |\dot{\epsilon}_d|$ and $v_{\delta\Gamma} = |\dot{\delta\Gamma}|$ to 1. Since the sum of Eq. 2.55 cannot be carried out to infinity numerically, we chose a value of q_{max} as an upper limit to that sum. The latter value was chosen to guarantee convergence and was set to $q_{max} = 10000$.

One can see that, regardless of the values of v_{ϵ_d} and $v_{\delta\Gamma}$, the second order of the noise vanishes in the quantization limit.

which using Green's theorem can be expressed as

$$W^{(0)}_{cycle} = \int_0^{T_0} dt \dot{W}^{(1)} = \iint_A d\epsilon_d d\Gamma \Big[- \frac{\partial^2 \Omega}{\partial \epsilon_d \partial \Gamma} + \frac{\partial^2 \Omega}{\partial \Gamma \partial \epsilon_d} \Big] = 0. \tag{2.109}$$

Similar reasoning can be applied for integrals of all other rates at first order. One can point out that this is a trivial consequence of the absence of any chemical potential or temperature difference.

In contrast, second-order rates integrated over a cycle will not be geometric quantities and will depend on the specific parameterization. In the following, we will consider a linear parameterization so that the rates $\dot{\epsilon}_d$ and $\delta\dot{\Gamma}$ (reminding that $\delta\Gamma = \Gamma_L - \Gamma_R$) are constants along the four strokes. The work would display some divergent integrals, signalling the failure of the gradient expansion for this particular cycle (see Appendix B). The problem concerns indeed the fact that the gradient expansion can be justified only if both $\Gamma_L, \Gamma_R \neq 0$ at all times, which is of course inconsistent with the condition $\delta\Gamma = \pm\Gamma$. One way out is to regularize the cycle, making $\delta\Gamma$ vary from $[-\Gamma + \delta, \Gamma - \delta]$. While the pumped charge and the other terms in the current noise turn out to have a smooth limit as $\delta \to 0$, the work should be computed only for δ small but finite. The work per cycle is

$$W^{(1)}_{cycle} = -v_{\epsilon_d} \int_{-\epsilon_0}^{\epsilon_0} d\epsilon_d \int \frac{d\epsilon}{2\pi} \partial_\epsilon f A^2 + \frac{v_{\delta\Gamma}}{2} \int_{-\Gamma+\delta}^{\Gamma-\delta} d\delta\Gamma \frac{\Gamma}{\Gamma^2 - \delta\Gamma^2} \int \frac{d\epsilon}{2\pi} f \frac{\partial_\epsilon A}{2}. \tag{2.110}$$

Performing the integration over ϵ_d one obtains in the limit $T \to 0$

$$W^{(1)}_{cycle} = v_{\epsilon_d} \Delta W^{(1)}_{\epsilon_d} + v_{\delta\Gamma} \Delta W^{(1)}_{\delta\Gamma}, \tag{2.111}$$

where $v_{\epsilon_d} = |\dot{\epsilon}_d|$, $v_{\delta\Gamma} = |\delta\dot{\Gamma}|$, and the coefficients are

$$\Delta W^{(1)}_{\epsilon_d} = \frac{2}{\pi\Gamma} \Big\{ \arctan x + \frac{x}{1+x^2} \Big\}, \tag{2.112}$$

and

$$\Delta W^{(1)}_{\delta\Gamma} = \frac{1}{\Gamma} \Big[1 - \xi \Big] \frac{1}{\pi} \frac{1}{x^2+1}, \tag{2.113}$$

in terms of the dimensionless variables $x = \frac{\epsilon_0}{\Gamma/2}$ and $\xi = \frac{\delta}{\Gamma}$. Comparing this result with the one obtained for the charge pumped over a cycle, we obtain the following direct relationship $\Delta W^{(1)}_{\epsilon_d} = \frac{v_{\epsilon_d}}{\Gamma} Q^{(0)}_L$. The contribution proportional to $v_{\delta\Gamma}$ is shown in Fig. (2.8) and it is vanishing in the limit $x \to \infty$. Therefore in the limit of charge quantization

$$W^{(1)}_{cycle} = \frac{v_{\epsilon_d}}{\Gamma}, \tag{2.114}$$

the work is finite in the presence of charge quantization and proportional to the pumped charge, in the case of constant velocity.

Let us now compute in the same way the entropy produced over a cycle

$$S^{(1)}_{cycle} = \frac{v_{\epsilon_d}}{T}\int_{-\epsilon_0}^{\epsilon_0} d\epsilon_d \int \frac{d\epsilon}{2\pi}(\epsilon-\mu)\partial_\epsilon f \partial_\epsilon A^2. \tag{2.115}$$

Performing the integrations the result up to the first order in the temperature is

$$S^{(1)}_{cycle} = v_{\epsilon_d}\Delta S^{(1)}_{\epsilon_d}, \tag{2.116}$$

where

$$\Delta S^{(1)}_{\epsilon_d} = \frac{\pi T k_B^2}{3}\frac{128}{\Gamma^3}\frac{x}{(1+x^2)^3} + O(T^3). \tag{2.117}$$

Comparing this expression with the expression of the work, one can observe that while in the limit $x \to \infty$ the work saturates to the value $\frac{v_{\epsilon_d}}{\Gamma}$, the entropy production tends to zero (Fig. (2.9)).

For completeness, we report here also the result for the remaining quantities

$$\mathcal{Q}^{(1)}_{cycle} = -v_{\epsilon_d}\int_{-\epsilon_0}^{\epsilon_0} d\epsilon_d \int \frac{d\epsilon}{2\pi}(\epsilon-\mu)\partial_\epsilon^2 f A^2 - \frac{v_{\delta\Gamma}}{2}\int_{-\Gamma+\delta}^{\Gamma-\delta} d\delta\Gamma \frac{\Gamma}{\Gamma^2-\delta\Gamma^2}\int \frac{d\epsilon}{2\pi} f\frac{\partial_\epsilon A}{2} \tag{2.118}$$

$$E^{(1)}_{cycle} = v_{\epsilon_d}\int_{-\epsilon_0}^{\epsilon_0} d\epsilon_d \int \frac{d\epsilon}{2\pi}\epsilon\partial_\epsilon f \partial_\epsilon A^2 \tag{2.119}$$

$$N^{(1)}_{cycle} = -v_{\epsilon_d}\int_{-\epsilon_0}^{\epsilon_0} d\epsilon_d \int \frac{d\epsilon}{2\pi}\partial_\epsilon^2 f A^2. \tag{2.120}$$

Performing the integrations one obtains that in the limit $x \to \infty$ and $T \to 0$ $N^{(1)}_{cycle} = 0$, $S^{(1)}_{cycle} = 0$ and $\mathcal{Q}^{(1)}_{cycle} = -W^{(1)}_{cycle}$. These conditions define a Non-Equilibrium Steady State (NESS) (see for example [43]). In this condition all the mechanical work is converted into dissipated heat in the leads.

2.6.2 Other examples of cycles

In our analysis of the peristaltic cycle we found that in the limit of quantization, the work per cycle saturates to a value determined by the rate of change of the energy level v_{ϵ_d}. In contrast, the entropy produced per cycle goes to zero (as the noise). The purpose of this section will be to explore other examples of a cycle and study the possibility that these qualitative results could apply to more general situations.

Let's consider a modification of the peristaltic cycle in which the couplings are modified one by one and not together: the level is lowered from $\epsilon_d = \epsilon_0$ to $-\epsilon_0$, while connected mainly to the right lead with $\Gamma_R = \Gamma_0$ and $\Gamma_L = \delta$ ($\xi = \delta/\Gamma_0 \ll 1$). The role of the two couplings is then inverted by first raising Γ_L to Γ_0 and then decreasing Γ_R to δ. It is now the turn of the level to be raised from $-\epsilon_0$ to ϵ_0. Then the Γ_R and Γ_L are exchanged again

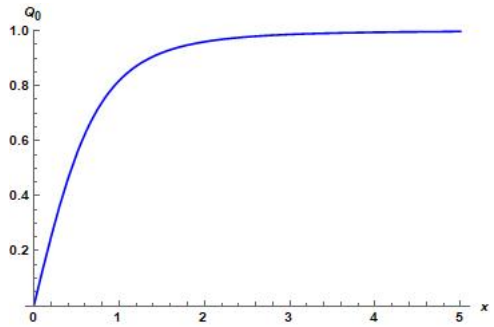

Figure 2.7: The current integrated over a cycle for the left lead w.r.t. the adimensional parameter x. In the limit $x \to \infty$ the quantity displays a quantization to 1.

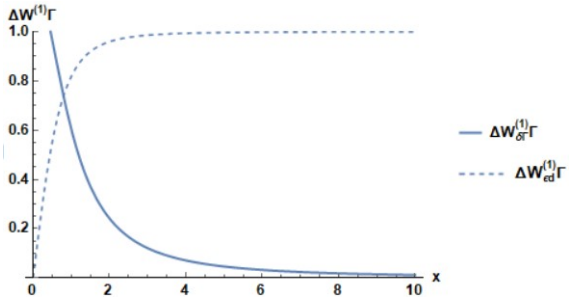

Figure 2.8: $\Delta W^{(1)}_{\epsilon_d}\Gamma$ and $\Delta W^{(1)}_{\delta\Gamma}\Gamma$. The contribution proportional to v_{ϵ_d} tends to 1 for $x \to \infty$, following the direct relation with the pumped charge. In contrast, the contribution proportional to $v_{\delta\Gamma}$ tends to zero in the same limit.

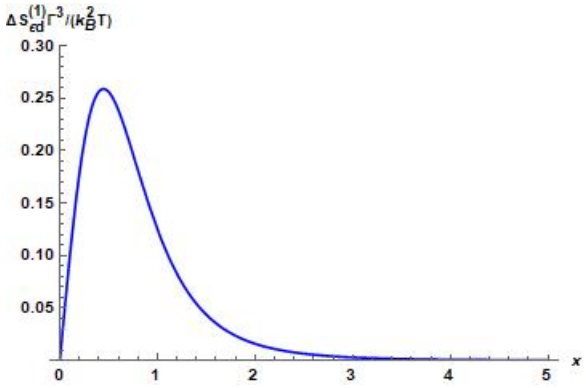

Figure 2.9: The leading order in temperature of the entropy vs. the adimensional parameter x. From this figure, the quantity tends to zero in the quantization limit.

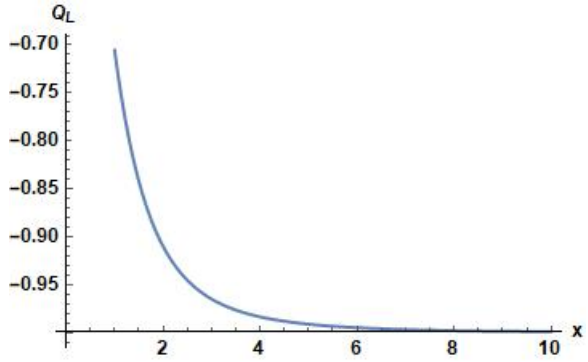

Figure 2.10: The charge pumped from left to right. It is negative because the current flows from left to right. The current displays charge quantization in the large x limit.

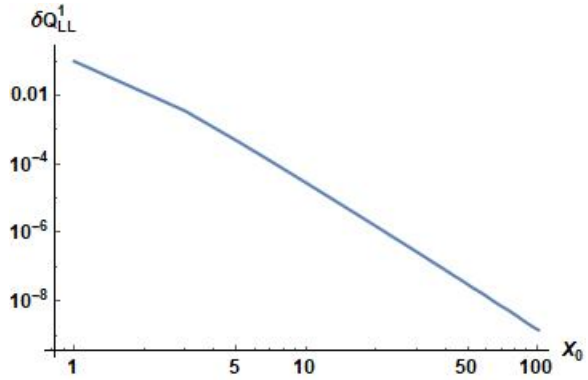

Figure 2.11: The first order of the noise of the current δQ_{LL} (in logarithmic scale). The current noise tends to 0 as $x \to \infty$ as expected, following the quantization requirement.

with the inverse of the above process. The results for the pumped charge are portrayed in Fig. (2.10). It displays indeed charge quantization in the large $x = \epsilon_0/\Gamma$ limit. The current noise can be safely computed for this cycle and the results for the two coefficients which govern the dependence on v_{ϵ_d} and v_Γ are in Fig. (2.11). As one can see both the coefficients tend to $\xi = \frac{\delta}{\Gamma}$ as $x \to \infty$. Therefore $\lim_{\xi\to 0} \lim_{x\to\infty} \delta Q_{\alpha\alpha}(x,\xi) = 0$.

Let us now turn to the work per cycle which has the following expression

$$W^{(1)}_{cycle} = v_{\epsilon d} \Delta W^{(1)}_{\epsilon_d} + v_\Gamma \Delta W^{(1)}_\Gamma, \tag{2.121}$$

where

$$\Delta W^{(1)}_{\epsilon_d} = \frac{2}{\Gamma_0 \pi} \left\{ \arctan(x) + \frac{x}{1+x^2} \right\} \tag{2.122}$$

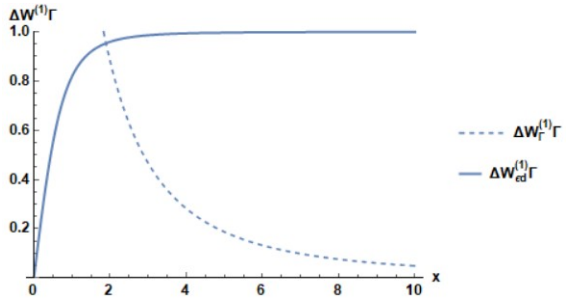

Figure 2.12: The two components of the dissipated power proportional to v_{ϵ_d} and v_Γ for $\xi = 0.001$. The work displays a quantization to $\frac{v_{\epsilon_d}}{\Gamma_0}$ in the limit $x \to \infty$, as the first component is saturated to 1, while the second vanishes in this limit.

and

$$\begin{aligned}\Delta W_\Gamma^{(1)} = \frac{1}{\pi\Gamma_0}\frac{1}{(x^2+1)}\Bigg\{ &- 2x\left[\frac{x}{\xi-2}\right] \\ &- 2x\left[\frac{x}{\xi+2}\right] + 2\log\left[\frac{1-\xi}{\xi}\right] + \log\left[\frac{\xi^2+x^2+2\xi x+1}{\xi^2+x^2-2\xi x+4}\right]\Bigg\} \\ &+ \frac{2}{\pi\Gamma_0}\left(\frac{2-\xi}{x^2+(2-\xi)^2} - \frac{1+\xi}{x^2+(1+\xi)^2}\right)\end{aligned} \tag{2.123}$$

displays a quantization of $\frac{W_{cycle}^{(1)}\Gamma_0}{v_{\epsilon_d}} \to 1$ in the large x limit (see Fig. (2.12)). This appears to be in agreement with what is stated for the peristaltic cycle. Finally, let us focus on the entropy whose first non-zero order reads

$$S_{cycle}^{(1)} = v_\Gamma \Delta S_\Gamma^{(1)} + v_{\epsilon d}\Delta S_{\epsilon_d}^{(1)} + O(T^3). \tag{2.124}$$

where

$$\Delta S_\Gamma^{(1)} = \frac{\pi}{12}\frac{1}{\Gamma^3}(k_B^2 T)\left[\frac{2}{(4x^2+1)^2} - \frac{16}{(x^2+1)^2}\right] \tag{2.125}$$

and

$$\Delta S_{\epsilon_d}^{(1)} = \frac{\pi}{3}(k_B^2 T)\frac{1}{\Gamma^3}\frac{32x}{(1+x^2)^3} \tag{2.126}$$

The two coefficients are in Fig. (2.13). In this case, the entropy also tends to zero in the charge quantization limit. All the other quantities do not add any relevant physical information: as before since $S_{cycle}^{(1)} = 0$, $\mathcal{Q}_{cycle}^{(1)} = -W_{cycle}^{(1)}$ all the external work is converted into dissipated heat. My previous example shows that the main results pertaining to the peristaltic cycle, i.e. work quantization in the limit of quantized charge, no entropy production and zero noise, also pertain to similar cycles.

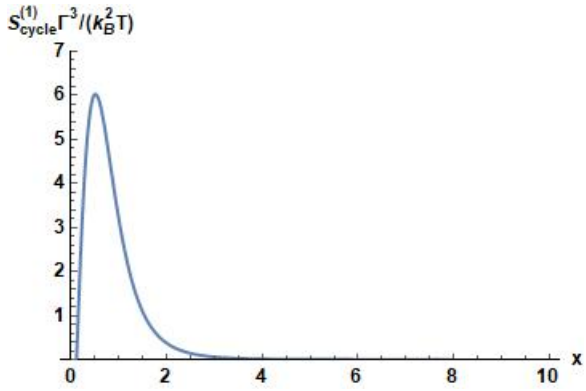

Figure 2.13: The second order in temperature of the entropy for $v_\Gamma = v_{\epsilon_d} = 1$. The two coefficients are summed, as they have the same asymptotic behaviour. One can see they both vanish in the quantization limit.

Let us now focus on another cycle whose peculiarity is to have a maximal pumped charge equal to half an electron charge: the triangular cycle introduced in [45], where Γ_L and Γ_R are time-dependent. In this cycle, at the beginning, the dot is weakly coupled with strength δ to both leads. Then, it is loaded by coupling to the left lead up to $\Gamma_0 \gg \delta$. The next step is to shift the coupling from the left to the right reservoir. Finally, the dot is discharged while returning to the initial state. The energy level of the dot is maintained constant $\epsilon_d = \epsilon_0$ and only the couplings are varied (see Fig. (2.14)). In this example, one has half an electron per period. This means that the current noise has to be finite. The fact that the charge transport is on average equal to 1/2 per cycle, means that half of the times one charge is transported and the other half none. The charge pumped per cycle is plotted in Fig. (2.15) and is given by the expression

$$Q_R^{(1)} = \frac{2}{\pi}\int_{I(C)} dX_L dX_R \frac{X}{[1+X^2]^2} = \frac{1}{\pi}\left[\arctan[X_0] - \frac{X_0}{1+X_0^2}\right], \tag{2.127}$$

where $I(C)$ is the triangular contour in Fig. (2.14). In terms of $X = \frac{\Gamma}{2\epsilon_0}$ and $X_0 = \frac{\Gamma_0}{2\epsilon_0}$. Then, one can define the limiting condition

$$\lim_{X_0\to\infty} Q_R^{(1)} = 1/2. \tag{2.128}$$

Due to the non-integer charge, the adiabatic current noise in Fig. (2.16) is finite in the quantization limit. In this case, the most relevant contribution is from the hypotenuse of the process, where both the couplings are varied and the energy level is half occupied on average. The value reached by the charge noise is

$$\lim_{X_0\to\infty} \delta Q_{RR}^{(1)} = \frac{1}{2}(1-\frac{1}{2}) = \frac{1}{4}. \tag{2.129}$$

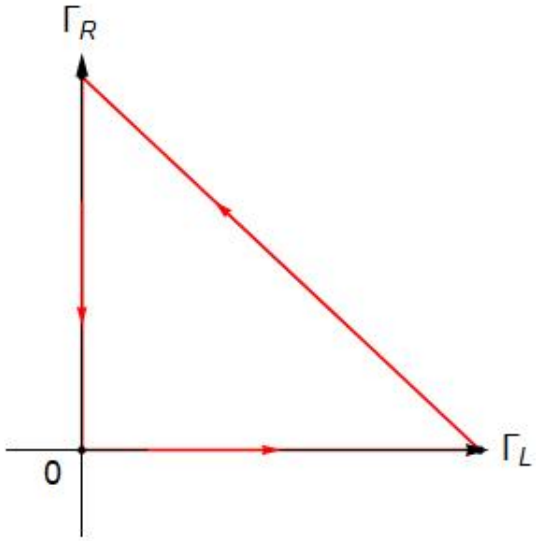

Figure 2.14: The diagram of the cycle with fractional charge quantization.

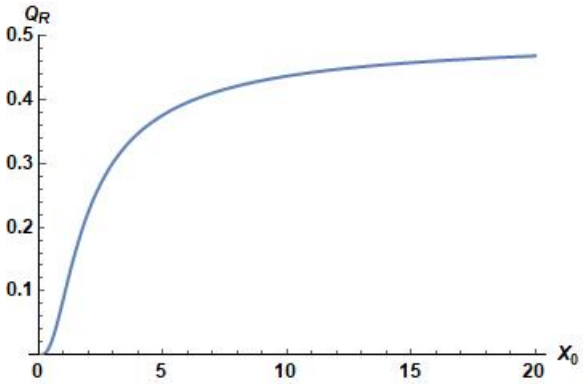

Figure 2.15: The charge pumped with respect to the adimensional parameter X_0, displaying the fractional quantization to the value $\frac{1}{2}$.

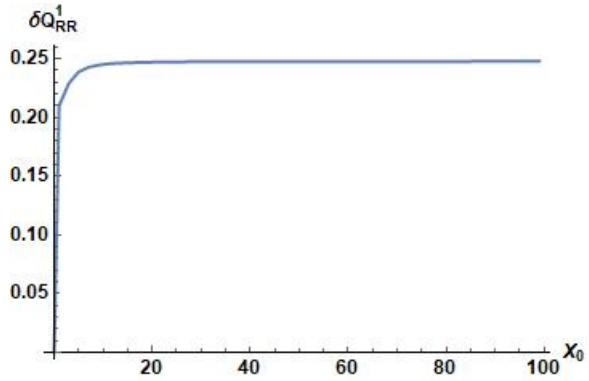

Figure 2.16: The noise with respect to X_0. In this case, one can observe a finite noise in the quantization limit. The limiting value is $\frac{1}{4}$.

The work done per cycle (Fig. (2.17)) is

$$W^{(1)}_{cycle} = v_\Gamma \Delta W^{(1)}_\Gamma + v_{\delta\Gamma} \Delta W^{(1)}_{\delta\Gamma} \tag{2.130}$$

where

$$\Delta W^{(1)}_\Gamma = \frac{1}{\epsilon_0 \pi}\left[\frac{X_0}{1+X_0^2} + \arctan[X_0] - \frac{\delta}{1+\delta^2} - \arctan[\delta]\right] \tag{2.131}$$

and

$$\Delta W^{(1)}_{\delta\Gamma} = \frac{1}{\Gamma}\left[1-\delta\right]\frac{1}{\pi}\frac{2X_0}{X_0^2+1}, \tag{2.132}$$

with $\delta = \frac{\eta}{\Gamma_0}$. One has that, in the quantization limit

$$\frac{W^{(1)}_{cycle}\epsilon_0}{v_\Gamma} \to \frac{1}{2}. \tag{2.133}$$

The entropy integrated over a cycle (Fig. (2.18)) reads

$$S^{(1)}_{cycle} = v_\Gamma \Delta S^{(1)}_\Gamma \tag{2.134}$$

$$\Delta S^{(1)}_\Gamma = \frac{1}{\epsilon_0^3}\frac{\pi}{12}k_B^2 T \frac{2X_0}{(1+X_0^2)^2}. \tag{2.135}$$

Likewise, the entropy in the quantization limit tends to zero.

The results for the two processes we have considered up to now indicate that, when the design of the cycle allows us to define a limiting condition which entails a quantized charge pumped, there are some conclusions we can draw regarding the other quantities relevant to our purposes. In particular, the out-of-equilibrium work performed on the system obeys a similar quantization relation. The entropy integrated over the cycle vanishes in the considered limit. Likewise, the charge noise disappears, as the charge pumped is quantized.

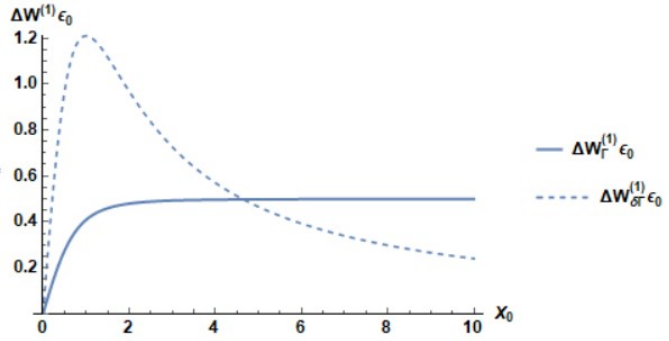

Figure 2.17: The two components of the work with respect to X_0. The figure shows how in the limit $X_0 \to \infty$ the work tends to the value $W^{(1)}_{cycle} \to \frac{1}{2}\frac{v_\Gamma}{\epsilon_0}$

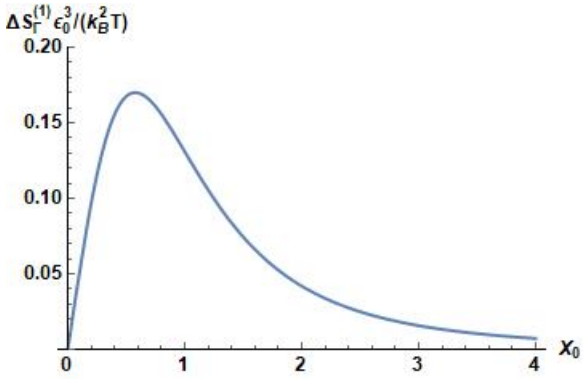

Figure 2.18: The entropy with respect to X_0, vanishing in the quantization limit.

Chapter 3

Electronic Shuttling in Quantum Dots as a nano-electromechanical Clock

- Where we aim at characterizing electronic shuttling as a quantum clock, by evaluating the entropic cost of measuring time.

> *"Thermodynamics is a funny subject. The first time you go through it, you don't understand it at all. The second time you go through it, you think you understand it, except for one or two small points. The third time you go through it, you know you don't understand it, but by that time you are so used to it, it doesn't bother you any more."*
>
> — **Arnold Sommerfeld**

3.1 Introduction

It has been shown that a metallic island between two leads develops a periodic motion regime if a large bias voltage is placed between the latter. Park et al. studied this phenomenon experimentally by employing a C_{60} molecule between two golden electrodes [71]. This is known in the literature as shuttle instability [29, 30, 31, 32] and is manifest even when the size of the island is decreased further and the mechanical motion of the island becomes quantized [29].

This system exhibits a transition between a phase in which the oscillations are damped and the stationary phase is the equilibrium point of the system and a phase in which the oscillations grow until they reach a limit cycle with a fixed amplitude. The mechanism responsible for the sustained oscillations is the non-linearity of the couplings between the

dot and the leads. In addition to that, a Van der Waals force between the molecule and the two leads acts as a restoring force. The driving source is the difference of potential between the leads.

This model is a simple realization of a nano-mechanical electronic clock, as shown in a recent review [36], where its properties have been studied using the master equation technique. Timekeeping is a practice that dates back to ancient civilizations. Quantum clocks have recently received increasing attention, following the seminal article in Ref. [25]. Recent technological developments have rendered this topic relevant and recent studies have shown that quantum clocks can achieve an improved accuracy with respect to purely classical ones [94]. The most important question one could ask is how the precision and the accuracy of the clocks can be quantified and related to other physical quantities, such as the entropy production and the dissipated heat, and identify the fundamental limits on them. Previous studies have highlighted a fundamental trade-off relation between the entropy production and the accuracy of the clocks [25, 36, 41].

The phenomenon of shuttling instability has been studied previously in the limit of large limit cycles and weak coupling in a series of articles [29, 30, 31, 32, 69]. In this Chapter, we seek to go beyond these limits and explore the presence of the phenomena in intermediate and strong coupling. While the transport properties have been studied extensively, a thermodynamical description in the quantum regime has yet to be built. We aim to compute both the transport and the thermodynamic quantities in the adiabatic expansion and to compare the behaviour of the precision and accuracy of timekeeping with the entropy production and other information-theoretic quantities. This question is particularly interesting because this is a quantum clock exhibiting coherent transport and works in a strong coupling regime, resulting in non-trivial correlations with the leads. In this context, it is not guaranteed the TURs would hold.

The structure of the Chapter is the following: we start by studying the equations of motion for the centre of mass in the adiabatic limit, to identify the existence of sustained periodic solutions, dubbed limit cycles, and characterize the dynamics of the system. Then, we will perform a thermodynamic analysis of the stationary phase. We identify how the relevant quantities behave concerning the amplitude of said limit cycle and the bias voltage. Finally, we employ a semi-classical stochastic picture, in order to simulate the effect of the zero-temperature noise on the trajectories of the clock. This allows us to estimate the accuracy, and the precision and to compute the stochastic entropy production. Finally, the current noise and its spectrum are calculated and compared with the other quantities.

3.2 The model

This system (Fig. (3.1)) can be modelled by an Hamiltonian of a movable quantum dot between two leads [29]. The Hamiltonian is divided into an electronic part, which describes the single-level quantum dot, which is assumed to be non-interacting, the coupling with

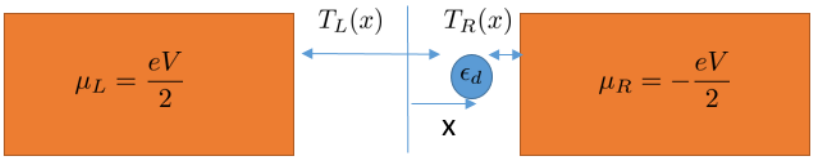

Figure 3.1: The model: a movable quantum dot, placed between two leads. Both the energy level of the dot and the coupling are dependent on the position.

the leads, and a parabolic potential, which models the effective elastic force between the leads and the dot. It reads

$$H = H_{el} + H_{osc}, \tag{3.1}$$

where

$$H_{el} = H_D + H_V + H_{leads} \tag{3.2}$$

and

$$H_D = \epsilon_d(X) c^\dagger c, \tag{3.3}$$

$$H_V = \sum_\alpha H_V^\alpha = \sum_{k\alpha} T_\alpha(X)(a_{k\alpha}^\dagger c + c^\dagger a_{k\alpha}), \tag{3.4}$$

$$H_{leads} = \sum_{k\alpha} \epsilon_{k\alpha} a_{k\alpha}^\dagger a_{k\alpha}, \tag{3.5}$$

and

$$H_{osc} = \frac{1}{2} m\omega^2 X^2 + \frac{P^2}{2m}, \tag{3.6}$$

where c and $a_{k\alpha}$ are the creation-annihilation operators of the dot and the leads' energy levels. X and P are the position and momentum associated with the movable quantum dot. The energy level of the dot obeys a linear displacement relation

$$\epsilon_d(X) = \epsilon_0 - dX, \tag{3.7}$$

where d is proportional to the applied electric field $d = eV\chi$, where χ is the permittivity of the system, and the coupling obeys a non-linear dependence on the position

$$T_{L,R}(X) = T_0 \exp\{\mp X/\lambda\}, \tag{3.8}$$

where λ is a characteristic tunnelling decay length.

As it is customary, we will work in dimensionless units for the momentum $x = X/r_0$ and $p = P/\epsilon_o$ with $r_0 = \sqrt{\frac{\hbar}{m\omega}}$ and $\epsilon_o = \sqrt{m\hbar\omega}$, respectively the length and energy scale of the harmonic oscillator, under which the oscillatory part of the Hamiltonian reads

$$H_{osc} = \frac{1}{2}(x^2 + p^2). \tag{3.9}$$

The other parameters of the problem are re-scaled accordingly using this length and energy scales. We denote the rescaled parameters with the prime index.

3.3 The phase transition

3.3.1 The dynamics of the centre of mass

Let us now study the motion of the centre of mass, in order to characterize the phase transition in the dynamics of the charge shuttle. At the operatorial level, we write this system of differential equations for the variables x and p

$$\begin{cases} \dot{x} = i[H, x] = p \\ \dot{p} = i[H, p] = -x - \frac{\partial H_{el}}{\partial x}. \end{cases} \tag{3.10}$$

By deriving the first equation and substituting the second one obtains Newton's equation of motion for the position $x(t)$ in the form

$$\ddot{x} + x = F(x), \tag{3.11}$$

where

$$F(x) = -\frac{\partial H_{el}}{\partial x}. \tag{3.12}$$

This force term depends on all the operators of the dot and the leads. Therefore, what one can do is to take the expectation value with respect to their associated states. We will perform an adiabatic expansion of the r.h.s up to the first order, which produces a non-linear force term $F^{(0)}(x)$ and a friction-like term $F^{(1)}(x)\dot{x}$. Let us start with the expression of the force, which is

$$F = -\frac{\partial H_{el}}{\partial x} = -\frac{\partial H_{el}}{\partial \epsilon'_d}\frac{\partial \epsilon'_d}{\partial x} - \sum_\alpha \frac{\partial H_{el}}{\partial T'_\alpha}\frac{\partial T'_\alpha}{\partial x}. \tag{3.13}$$

Changing variable implies the following relations for the derivatives $\dot{\epsilon}'_d = -d'\dot{x}$ and $\dot{T}'_\alpha = \lambda'^{-1}(-1)^\alpha T'_\alpha \dot{x}$ with $\alpha = 0(1)$ for right (left). In terms of the operators entering Eq. 3.11-3.13, the expression of the expectation value of the force reads

$$\langle F \rangle = d'\langle c^\dagger c \rangle - \sum_{k\alpha} \lambda'^{-1}(-1)^\alpha (T'_\alpha(t)\langle a^\dagger_{k\alpha} c \rangle + h.c.). \tag{3.14}$$

Using the definitions of the Green's function $G^<(t,t') = i\langle c^\dagger(t')c(t)\rangle$, we can rewrite it as

$$\langle F \rangle = -id'G^<(t,t) - \lambda'^{-1}\sum_\alpha (-1)^\alpha \langle H^\alpha_V \rangle(t), \tag{3.15}$$

with $\alpha = 0, 1$ associated respectively with L, R. Substituting the gradient expansion of $G^<(t,t)$ and $\langle H^\alpha_V \rangle(t)$ (see Appendix D) one obtains the expression of the force at different orders.

As in the previous Chapter, we will use the notation $\mathcal{O}^{(i)}$, for the i-th order of the adiabatic expansion associated with the quantity $\mathcal{O}$. The zero-order term of the force reads

$$F^{(0)} = d' \int \frac{d\epsilon}{2\pi} A \bar{f} - 2 \sum_{\alpha} \lambda'^{-1} (-1)^{\alpha} \int \frac{d\epsilon}{2\pi} Re(G^R) f_{\alpha} \Gamma'_{\alpha}, \tag{3.16}$$

upon defining $\bar{f} = \frac{\Gamma_L f_L + \Gamma_R f_R}{\Gamma}$ as the weighted average of the Fermi distributions of the heat baths, whilst the first order reads

$$\begin{aligned} F^{(1)} = {} & \frac{d'^2}{2} \int \frac{d\epsilon}{2\pi} \partial_{\epsilon} \bar{f} A^2 + d' \sum_{\alpha} \lambda^{-1} (-1)^{\alpha} \Gamma'_{\alpha} \int \frac{d\epsilon}{2\pi} \Big[(\bar{f} - f_{\alpha}) \frac{A^2}{\Gamma'} \\ & - \partial_{\epsilon} \bar{f} \frac{A^2}{\Gamma'} (\epsilon - \epsilon'_d) + \frac{\partial_{\epsilon} A}{2} \partial_{\epsilon} f_{\alpha} \Big] + \lambda'^{-2} \sum_{\alpha\beta} (-1)^{\alpha+\beta} \Gamma'_{\alpha} \Gamma'_{\beta} \int \frac{d\epsilon}{2\pi} \partial_{\Gamma'} A \partial_{\epsilon} f_{\alpha} \\ & + \lambda'^{-2} \sum_{\alpha} \Gamma'_{\alpha} \int \frac{d\epsilon}{2\pi} A \partial_{\epsilon} f_{\alpha}. \end{aligned} \tag{3.17}$$

Notice that the retarded Green function is $G^R = (\epsilon - \epsilon_d + i\Gamma'/2)^{-1}$ (Appendix D) and the spectral function of the dot is $A = \frac{\Gamma'}{(\epsilon - \epsilon'_d)^2 + (\Gamma'/2)^2}$.

3.3.2 The phase portrait

The next step is to evaluate all these integrals in the zero temperature limit, imposing a finite frequency cutoff to ensure the convergence of the integrals. This gives a well-defined equation of motion, which, however, is too complicated to solve analytically. A classic IV-order Runge-Kutta algorithm will be used to evaluate numerically the dynamics in phase space.
The phase portrait of the system is pretty interesting: below a certain critical value eV_C, the trajectories converge to a fixed point (Fig. (3.2)), which is the equilibrium point satisfying the condition $x = F^{(0)}(x)$. Above the critical voltage, the dynamics changes radically (Fig. (3.3)). There is a periodic stationary solution, i.e. a limit cycle, with an amplitude depending on the voltage bias. This cycle acts as an attractive manifold for the dynamics. The ideal shape of this limit cycle is circular in the phase space and it obeys the equation $x(t) = A_C \cos \omega t$.

One interesting question is how the phase transition is affected by the interplay of all the numerous parameters of the system. Let us start with the two parameters controlling the dependence of the energy level ϵ_d and of the tunnelling strength T'_{α} on x, namely λ and χ. In (Fig. (3.4) and (3.5)) one sees how the amplitude of the limit cycle varies with respect to the parameter λ'. The optimal strategy is to choose a combination of λ' and χ' that displays maximally the transition. The question of the presence of the transition, even in the regime of strong coupling, is of great importance. The dependence of A_C on the bias voltage eV for different values of the ratio Γ_0/ϵ_0 is investigated in Fig. (3.6) and

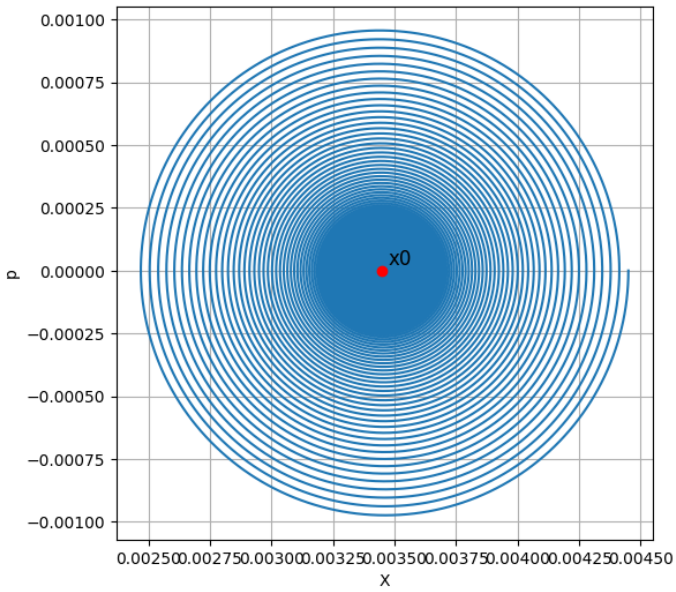

Figure 3.2: The dynamics for $eV < eV_C$ converge to the equilibrium point. For this choice of parameters, the value of eV_C is $0.33\epsilon_o$. The chosen parameters are $\lambda = 5r_o$, $\chi = 0.1/r_o$, $eV = 0.25\epsilon_o$, $\Gamma_0 = \epsilon_0 = 0.1\epsilon_o$, $\Lambda = 100\epsilon_o$. The initial conditions are $(x, p) = (x_0 + \epsilon, 0)$, where x_0 is the equilibrium point and ϵ is set to $0.001r_o$

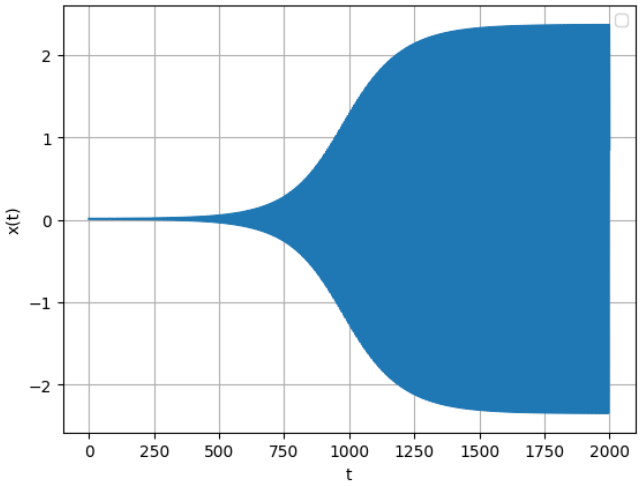

Figure 3.3: The dynamics of $x(t)$ for $eV > eV_C$, converging to the limit cycle. The parameters are the same as Fig. (3.2), but we set $eV = 0.4\epsilon_o$. The initial conditions are $(x, p) = (x_0 + \epsilon, 0)$, where x_0 is the equilibrium point satisfying $x = F_0(x)$ and ϵ assumes the value $0.001r_o$

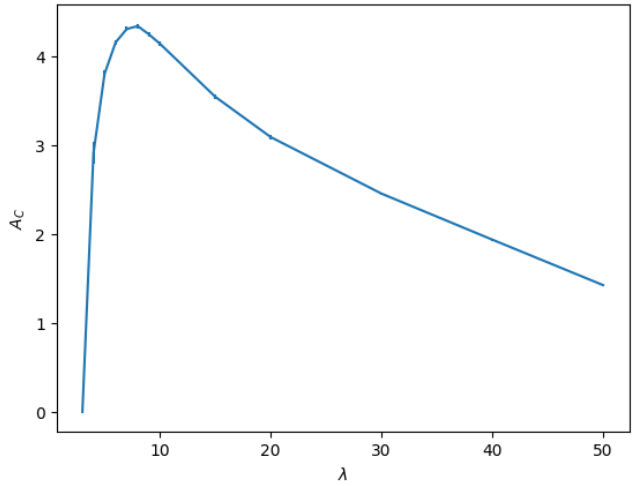

Figure 3.4: The critical amplitude vs. the parameter λ'.We vary λ' and fix $\chi = 0.1/r_o$, as well as $\Lambda = 1000\epsilon_o$, $eV = 5\epsilon_o$ and $\epsilon_0 = \Gamma_0 = 1\epsilon_o$. Note that for values inferior to $\lambda = 4$ there is no limit cycle. This graph allows us to select the values of λ' with maximal visibility of the transition.

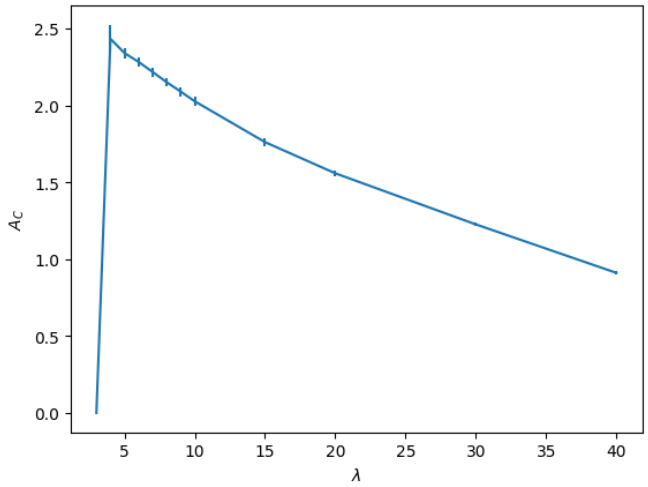

Figure 3.5: The critical amplitude vs. the parameter λ'. We vary λ' and fix $\chi = 0.2/r_0$, as well as $\Lambda = 1000\epsilon_o$, $eV = 5\epsilon_o$ and $\epsilon_0 = \Gamma_0 = 1\epsilon_o$.

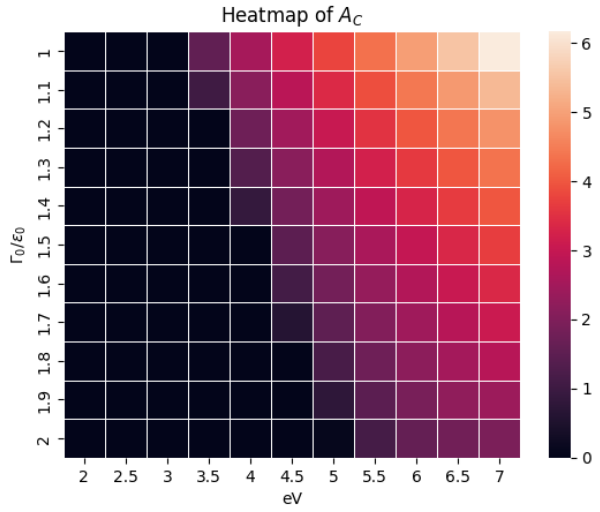

Figure 3.6: A heatmap of the critical amplitude A_C in the region of parameters spanning from $eV = 2\epsilon_o$ to $eV = 7\epsilon_o$ and Γ_0/ϵ_0 from ϵ_o to $2\epsilon_o$. The rest of the parameters coincide with those of Fig. (3.6). From this image, we can visualize the phase transition, noting that in the limit cycle phase, the critical amplitude is finite.

(3.7), pointing out to the absence of a limit cycle phase in the strong coupling limit. One realizes that the relation between the slope of the curves is not simply linear and the latter one tends to zero for $\Gamma_0/\epsilon_0 \to \infty$, as there is no shuttling instability in the strong coupling regime. The critical value of voltage bias seems to follow a linear relation in the considered interval.

3.4 Thermodynamics and transport in the stationary state

The goal of this Section is to characterize electronic shuttling from the thermodynamic point of view. We will start by deriving an expression for all the relevant quantities in the gradient expansion, exactly as done in Chapter 3. We are interested in their behaviour in the stationary state, namely the limit cycle for $V > V_C$.

Let us start by observing that at first order all the thermodynamical quantities can be written in the form

$$A^{(1)} = F[x(t)]\dot{x}(t), \tag{3.18}$$

where $F[x(t)]$ is a generic function of $x(t)$. Therefore when one averages over a period over the limit cycle its result is

$$\int_0^{T_0} dt A^{(1)} = \int_0^{T_0} dt F[x(t)]\dot{x}(t) = \oint_C dx F(x) = 0. \tag{3.19}$$

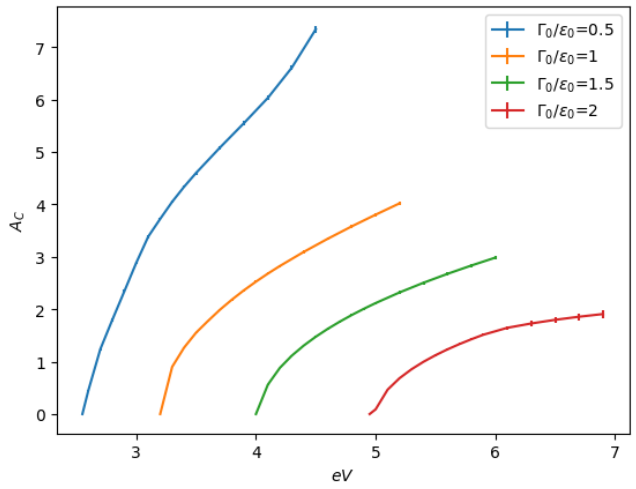

Figure 3.7: The critical amplitude A_C vs. eV for different values of the ratio ϵ_0/Γ_0. We fix $\lambda' = 5$, $\chi' = 0.1$, as well as $\Lambda' = 1000$, $\Gamma'_0 = 1$. The values are $\epsilon_0/\Gamma_0 = 2, 1, 0.67, 0.5$ from left to right. Let us note that for values of the ratio inferior to those depicted in the figure, there is no phase transition, signalling the absence of a shuttle instability in the strong-coupling regime

As a consequence, the only relevant contributions are at zero order. This is a completely different situation with respect to the adiabatic pumping of Chapter 2 because in this case, only a single parameter is time-dependent.

In order to identify the relevant quantities to be computed, one notes that in the context of open systems coupled to thermal baths at different chemical potentials (Ref. [37]), the first law of thermodynamics should be respected in the form

$$\dot{E} = \dot{W} + \dot{\mathcal{Q}} + \sum_{\alpha} \mu_\alpha \dot{N}_\alpha, \tag{3.20}$$

and one has $\mu_L = eV'/2$, $\mu_R = -eV'/2$. $\dot{E}$ is the energy variation rate of the system, $\dot{\mathcal{Q}}$ and $\dot{W}$ respectively the heat and the work rate. The rates $\dot{N}_\alpha$ correspond to the variation in the number of particles in reservoir α, which can be interpreted as

$$\dot{N}_\alpha = -I_\alpha, \tag{3.21}$$

where I_α is the current flowing from reservoir $\alpha = L, R$, so that

$$\sum_{\alpha} \mu_\alpha \dot{N}_\alpha = eV'/2(-I_L) - eV'/2(-I_R) = -eV' \cdot I_L. \tag{3.22}$$

since the two currents are equal and opposite (Section 3.4.1). The other constraint ones has to satisfy (Ref. [37]) defines the entropy production rate $\dot{\Sigma}$, in terms of $\dot{\mathcal{Q}}$ and the

entropy $\dot{S}$,

$$T\dot{S} = \dot{\mathcal{Q}} + \dot{\Sigma}. \tag{3.23}$$

Moreover, at every order the thermodynamic state functions (see [18]) amount to zero when integrated over a cyclic process, namely $\dot{E}$, $\dot{S}$ and $\dot{N}$. The full calculation for $\dot{E}^{(0)}$ is in Appendix F. From the definition, the expression of the work in i-th order reads

$$\dot{W}^{(i)} = F^{(i-1)}\dot{x}(t). \tag{3.24}$$

for $i \geq 1$ and has no zero order contribution. The only finite quantities at zero order are $\dot{\mathcal{Q}}$, $\dot{\Sigma}$ and I_α. Integrating Equation 3.20 over a period T_0 one can infer that

$$\int_0^{T_0} dt\dot{\mathcal{Q}}^{(0)} = \int_0^{T_0} dt \sum_\alpha \mu_\alpha \dot{N}_\alpha^{(0)} = -eV \int_0^{T_0} dt I_L^{(0)}. \tag{3.25}$$

From relation 3.23 it follows that

$$\int_0^{T_0} dt\dot{\Sigma}^{(0)} = -\int_0^{T_0} dt\dot{\mathcal{Q}}^{(0)} = eV' \int_0^{T_0} dt I_L^{(0)} \geq 0, \tag{3.26}$$

result consistent with Ref. [61]. This quantity is always positive, as it should respect the second law of thermodynamics. This is because the current flows from the left lead to the right lead, as a consequence of the sign of the bias.

As pointed out by [29], the evolution of the amplitude of the oscillations should be proportional to the work done over the cycle $\int_0^{T_0} dt\dot{W}[x(t)]$, assuming a solution of the dynamics of the form $x(t) = A\cos\omega t$. Then the value of critical amplitude for the limit cycle A_C can be inferred from the work curves $\int_0^{T_0} dt\dot{W}(A)$ from the condition $\int_0^{T_0} dt\dot{W}(A_C) = 0$. Consequently, we plot the work done over a cycle with respect to the amplitude of oscillations at fixed voltage bias. In the under-critical phase, the work driving the dot position is always positive, i.e. the system is stuck in the $A = 0$ stationary state (Fig. (3.8)). For $V > V_C$, the work is negative for the values below A_C and changes sign for larger A (Fig. (3.9)). This is because the system acquires energy from external resources until it reaches the stationary state. From Fig. (3.10) it is clear that, after an initial transient, the work integrated over a limit cycle stabilizes around 0.

3.4.1 The equilibrium charge transport in the stationary regime

As we explained in the previous Section, the calculation of the entropy production, which is crucial, requires the knowledge of the equilibrium current flowing from each reservoir to the dot. As in Chapter 3, we define the charge transport in terms of the driving period

$$Q_\alpha^{(0)} = \frac{1}{T_0}\int_0^{T_0} dt\langle I_\alpha(t)\rangle, \tag{3.27}$$

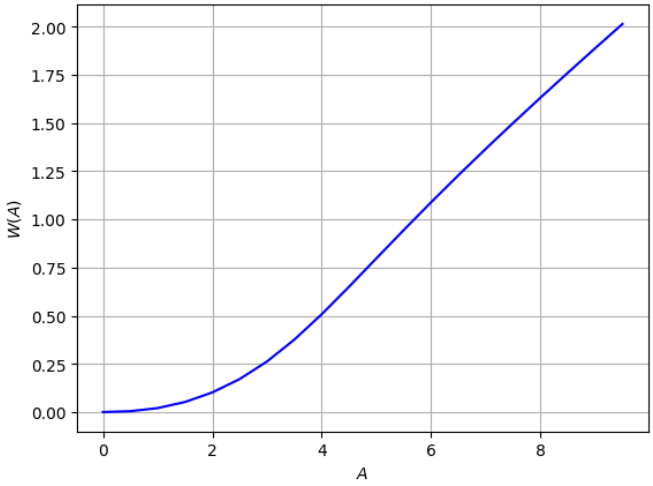

Figure 3.8: The curve of the work $W^{(2)}$ over a cycle vs. A in the under-critical phase. One can see that the work per cycle is always positive for all the values of A.

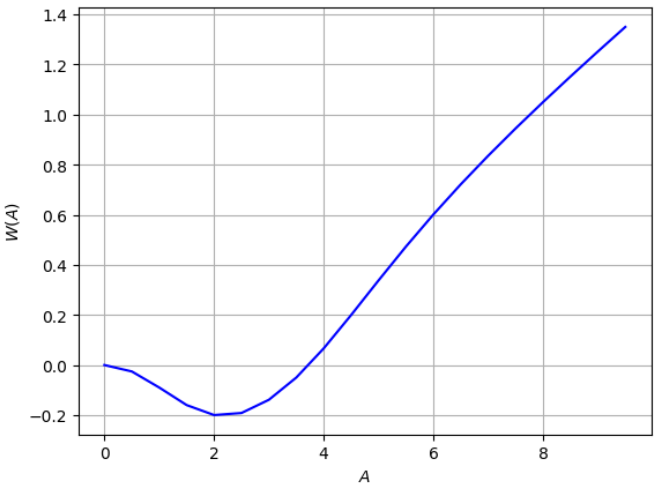

Figure 3.9: The curve of the work $W^{(2)}$ over a cycle vs. A in the upper-critical phase. The zero of this graph provides an imprecise estimation of the value of the limit cycle from the condition $\dot{W}(A_C) = 0$. Below this value, the work per cycle is negative as the amplitude grows, while the sign is reversed for $A > A_C$.

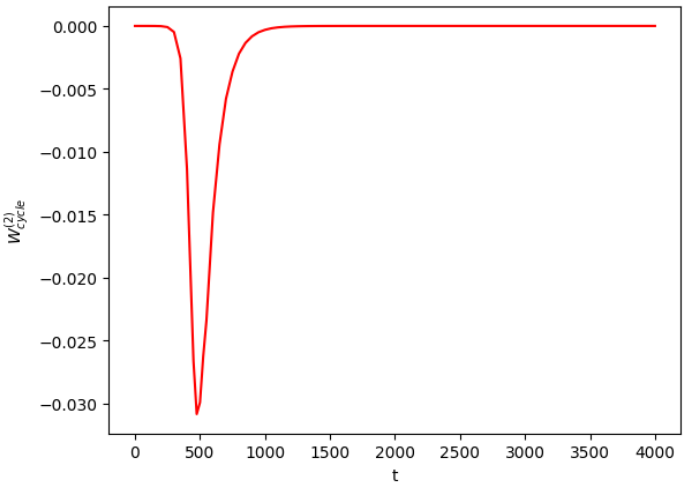

Figure 3.10: The curve of the work $W^{(2)}$ integrated over a cycle $[t, t+T_0]$ vs t for $eV = 0.5$ and the choice of parameters of Fig. (3.3) and the initial conditions $(x, p) = (x_0 + \epsilon, 0)$, $\epsilon = 0.001$. It shows that, after an initial transient in which the system absorbs energy from the external driving, the quantity stabilizes around its stationary value close to zero.

where

$$\langle I_L \rangle = -\langle \dot{N}_L \rangle = \langle \frac{d}{dt} \sum_k a^\dagger_{Lk} a_{Lk} \rangle \tag{3.28}$$

In particular, one would like to compute the left current

$$\langle I_L \rangle = -i\langle [H, N_L] \rangle. \tag{3.29}$$

This commutator reads in terms of the mixed Green function [46]

$$i \sum_{k\in L} T_L [\langle a_{Lk} c - h.c. \rangle] = 2Re\left[\sum_{k\in L} T_L G^<_{d,Lk}(t,t) \right]. \tag{3.30}$$

At zero order the expansion of the charge is (see Appendix D)

$$\begin{aligned} Q^{(0)}_L &= \frac{1}{T_0}\int_0^{T_0} dt I^{(0)}_L = \int_0^{T_0} \frac{dT}{T_0} \int \frac{d\epsilon}{2\pi} 2 \sum_{k\in L} Re\left[G^R(\epsilon, T)\Sigma^<(\epsilon, T) + G^<(\epsilon, T)\Sigma^A(\epsilon, T) \right] \\ &= \int_0^{T_0} \frac{dT}{T_0} \int \frac{d\epsilon}{2\pi} 2Re\left[\frac{A}{2} f_L \Gamma'_L - \frac{A}{2} \bar{f} \Gamma'_L \right] = \frac{\Gamma'_L \Gamma'_R}{\Gamma} \int_0^{T_0} \frac{dT}{T_0} \int \frac{d\epsilon}{2\pi} (f_L - f_R) A \end{aligned} \tag{3.31}$$

where we used the definition of $\bar{f}$. By calculating the right current in the same way, one can readily verify that the relation $Q^{(0)}_L = -Q^{(0)}_R$ holds. From the expression, we note that

this current is maximal when the dot is equidistant between the two leads and tends to for large x, as it is weakly coupled to one of the two leads.

3.5 The characterisation of the noise

So far, we have considered only the deterministic equations of motion of the centre of mass of the shuttle. Now, we would like to incorporate the effect of the noise on the dynamics of the shuttle instability. This is essential for evaluating the performance of this clock. In order to do so, we will employ a stochastic semi-classical approach. First of all, let us rewrite the force term as

$$F(t) = \langle F(t) \rangle + \delta F(t), \tag{3.32}$$

One can interpret $\delta F(t)$ as a noise term. Clearly, per definition, it has the property that $\langle \delta F(t) \rangle = 0$. The key mathematical object we are interested in computing is the correlation function of the noise $\langle \delta F(t) \delta F(t') \rangle$. The latter reads

$$\langle \delta F(t) \delta F(t') \rangle = \langle F(t) F(t') \rangle - \langle F(t) \rangle \langle F(t') \rangle. \tag{3.33}$$

This has to be done by employing the Wick theorem on the Keldysh contour and subsequently performing a gradient expansion. The details of the calculation can be found in the Appendix H.
The results show that the correlation function can be appropriately approximated as a delta function, viz.

$$\langle \delta F(t) \delta F(t') \rangle = D[x(t), p(t)] \delta(t - t'), \tag{3.34}$$

with the noise correlation function $D[x(t), p(t)]$. The full system of stochastic differential equations now reads

$$\begin{cases} \dot{x} = p \\ \dot{p} = -x + F_0(x) + F_1(x) p + \sqrt{D(x,p)} \xi(t), \end{cases} \tag{3.35}$$

with

$$\langle \xi(t) \xi(t') \rangle = \delta(t - t') \tag{3.36}$$

being a realization of white noise with unit variance. In turn, the correlation function is expanded in the quasi-adiabatic limit (Appendix H) as

$$D(x,p) = D^{(0)}(x) + D^{(1)}(x) p. \tag{3.37}$$

This equation can be simulated using a standard Stochastic IV-order Runge-Kutta algorithm [47].

Let us discuss the results one obtains in all the different phases. For $V < V_C$ (cfr. [69]) the probability density is peaked around the equilibrium point. In contrast, for $V > V_C$

the orbits are distributed as an annulus around the limit cycle. However, in this case, the transition is more blurred, as there is an intermediate phase around the critical point, in which the presence of a limit cycle does not prevent a non-negligible probability of the trajectory being around the equilibrium point.

3.5.1 An useful change of variables

Given the structure of the stationary solution, the problem can be efficiently represented with polar coordinates. This change of variables is informative and can shed new light on the dynamics of shuttling instability.
The change of variables is defined as

$$\begin{cases} r = \sqrt{x^2 + p^2} \\ \theta = \arctan[p/x] + \theta_0, \end{cases} \tag{3.38}$$

θ_0 being an arbitrary initial phase. With this choice of variables ([39]), the stochastic differential equations read

$$\begin{cases} \dot{r} = 2\sin\theta F(r,\theta) + \frac{\cos^2\theta}{r} D(r,\theta) + 2\sin\theta\sqrt{D(r,\theta)}\xi_1(t) \\ \dot{\theta} = -1 + \frac{\cos\theta}{r} F(r,\theta) - \frac{\sin\theta\cos\theta}{r^2} D(r,\theta) + \frac{\cos\theta}{r}\sqrt{D(r,\theta)}\xi_2(t), \end{cases} \tag{3.39}$$

where both $\xi_1(t)$ and $\xi_2(t)$ are two different realizations of white noise with unitary variance. The functions $D(r,\theta)$ and $F(r,\theta)$ read

$$F(r,\theta) = F^{(0)} + F^{(1)} r\sin(\theta), D(r,\theta) = D^{(0)} + D^{(1)} r\sin(\theta) \tag{3.40}$$

This new change of variable allows one to identify clearly the radial fixed point. Firstly, if one averages over the noise and considers only the differential equation for r

$$\frac{dr}{dt} = 2\sin\theta F(r,\theta), \tag{3.41}$$

the fixed point condition identifies the critical radius A_C (see Fig. (3.11)). This solution exists only in the limit cycle phase and allows us to give an estimation of A_C. If one includes now the effect of the disorder and averages over the noise, the condition reads

$$\frac{dr}{dt} = 0 = 2\sin\theta F(r,\theta) + \frac{\cos^2\theta}{r} D(r,\theta). \tag{3.42}$$

Evidently, the fixed point tends to shift towards greater values of r (Fig. (3.12)) as the effect of the noise is included.

The RHS of the differential equation (Eq. 3.35) for θ allows one to estimate the average phase modification over a period

$$\dot{\theta} = -1 + \frac{\cos\theta}{r} F(r,\theta) - \frac{\sin\theta\cos\theta}{r^2} D(r,\theta). \tag{3.43}$$

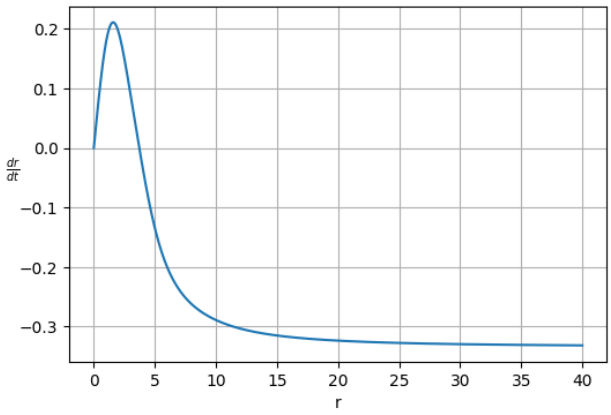

Figure 3.11: This is the r.h.s. of equation (3.41) when averaged over the angular, plotted with respect to the r parameter for $eV = 0.5$, and the same parameters of Fig. (3.2). The zero of this graph identifies the radial fixed point.

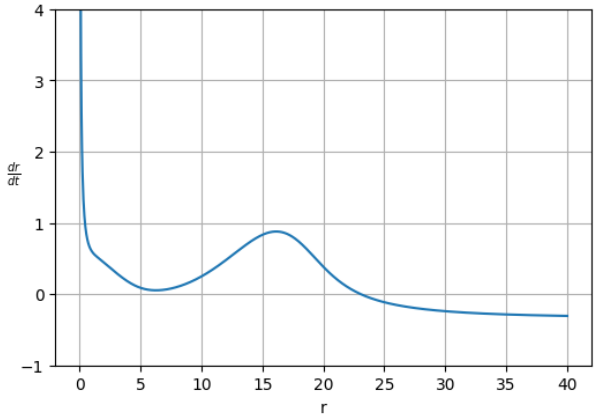

Figure 3.12: This is the RHS of equation (3.42) when averaged over the angular, plotted with respect to the r parameter for $eV = 0.5$, and the same parameter choice of Fig. (3.2). The zero of this graph identifies the radial fixed point when one takes into account the effect of the noise. One can note it is shifted to greater values with respect to Fig. (3.11)

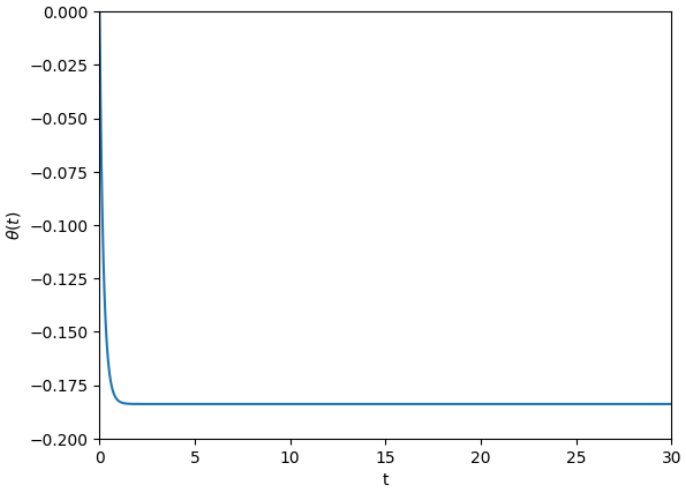

Figure 3.13: The solution for the dynamics of $\theta(t)$ for small radius: exponential convergence to an angular fixed point. The value of the radius is r=0.1, with $eV = 0.5$ and the same choice of parameters of Fig. (3.2)

An important question is whether, if one fixes the radial coordinate to a given value r^*, one has a uniform motion in the θ variable or not. The obtained results signal two different behaviours: for small values of the radius the dynamics tend to converge exponentially to a fixed point (Fig. (3.13)), while at higher values of the radius, the dynamics is nearly uniform (Fig. (3.14)).

The existence of an angular fixed point of the differential equation is the element which allows to discriminate between these two different behaviours. Then, there is a value of the radius r_C above which there is no solution and we demand the latter to be small enough for the probability of the trajectory to be below this radius to be negligible.

3.6 The clock's performance

3.6.1 Precision and accuracy vs. entropy production

Having characterized the noise in the dynamics of the shuttle, now we are in the right place to characterize the performance of the clock and compare it with the relevant thermodynamical quantities. In particular, we will compute the resolution and the accuracy. Then, we will compare it with the entropy production, investigating the relation between the two, to evaluate the thermodynamic cost of time measurement. The choice of parameters we employ is informed by the analysis of the previous sections (3.3.2 and 3.5.1). In particular, one wants the shape of the limit cycle to be close enough to the ideal circular shape. Another important requirement is the visibility of the phase transition for finite

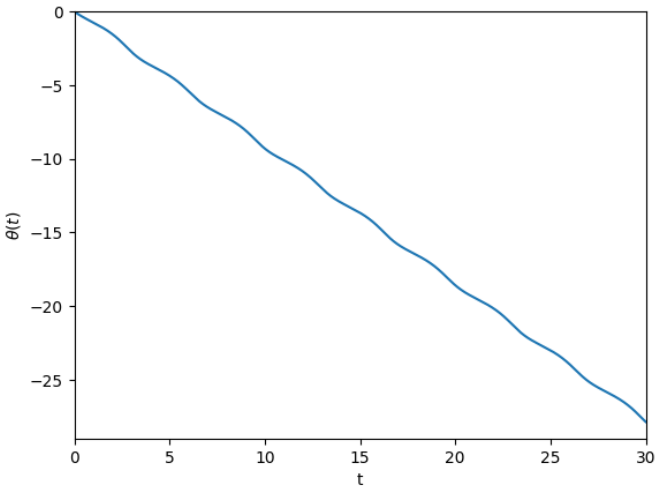

Figure 3.14: The solution for the dynamics of $\theta(t)$ for large radius: almost uniform motion in the angular variable. The value of the radius is r=0.3, with $eV = 0.5$ and the same choice of parameters of Fig. (3.2)

values of the voltage bias. Finally, the motion of the clock should be uniform, as already pointed out. With this choice of parameters, we will compute the only thermodynamic quantity relevant, i.e. the non-equilibrium entropy production, using the results of Section 3.4. Here we plot the average over a period of the entropy production up to the first order obtained in two different ways: from the deterministic trajectories and as the average over the stochastic realization of the noise (Fig. (3.15)).

The results highlight the differences between the two realizations: while in the deterministic entropy production, the two phases are clearly distinguishable, in the stochastic one the transition point is more nuanced, highlighting a superposition between the two phases (as it is evident also from the stochastic thermodynamics perspective [93]).

The other quantities we are interested in computing are precision and accuracy. Once one has the simulated trajectories, the periods of oscillation can be computed by counting how many times the trajectory of $x(t)$ changes sign. Having obtained the average period, which for now we call μ_T, and its variance σ_T^2, we can characterize the precision of the clock, which can be calculated as $1/\mu_T$, and the accuracy as μ^2/σ_T^2 [25] (see Introduction). The resolution is the rate of generation of the ticks, while the accuracy is the expected number of ticks before the clock's reading is off by one tick. We plot the results for different values of the voltage bias in Fig. (3.15) and (3.16) as well as the relative error (Fig. (3.17)) One can draw conclusions about these quantities by quickly comparing the graph of the relative entropy with the ones related to precision and accuracy. There appears to be a direct proportionality between the accuracy and the entropy production, even if the relation is

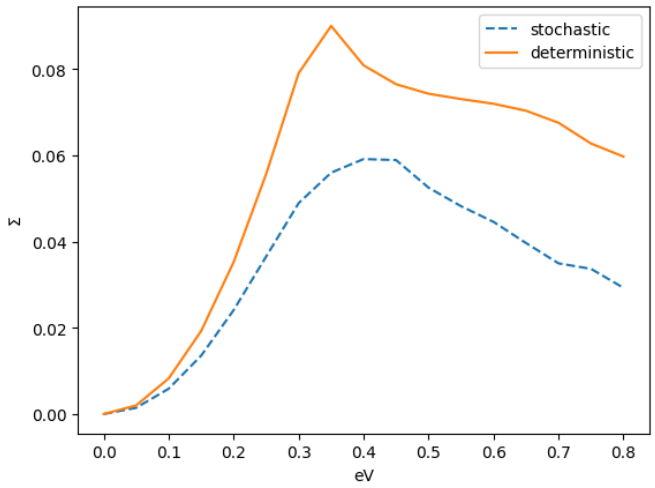

Figure 3.15: The entropy production over deterministic trajectories (solid orange) vs. the stochastic entropy production computed over $N = 100$ trajectories (dashed blue). It is clear that in the deterministic calculation, two curves correspond to the two phases. The entropy grows steadily and peaks around the transition point, after changing its trend. The stochastic entropy production follows the same trend, but the transition is smoothed and its curve lies below because the trajectories tend to drift towards larger values of the radius. From Eq. (3.31) it is clear that the entropy production, being proportional to the charge transport, in the adiabatic limit is maximal when the dot is around $x = 0$.

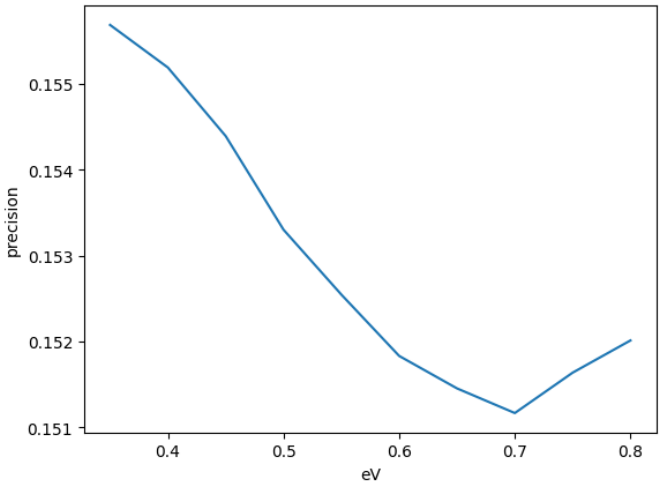

Figure 3.16: The precision of the clock. This quantity decreases for small values of A_C, but after it inverts its tendency. Note that little can be said about the relation between this quantity and the entropy production. N=50000 was the number of trajectories simulated. The set of parameters is the same as Fig. (3.3)

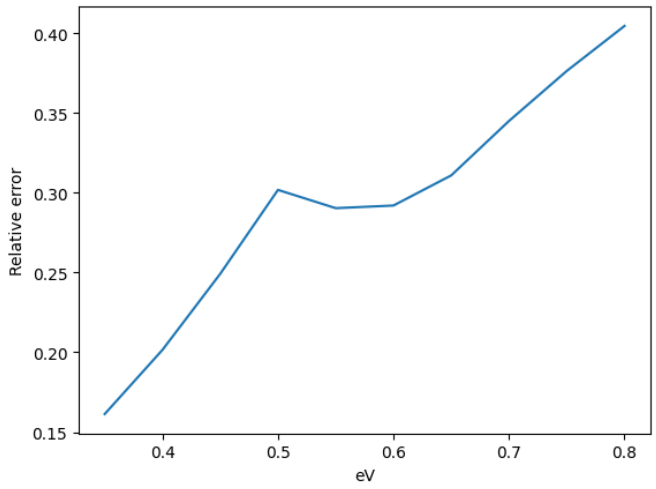

Figure 3.17: The relative error of the clock: its behaviour is the opposite of the observed one in the precision. There is an increase of this quantity along the interval considered.

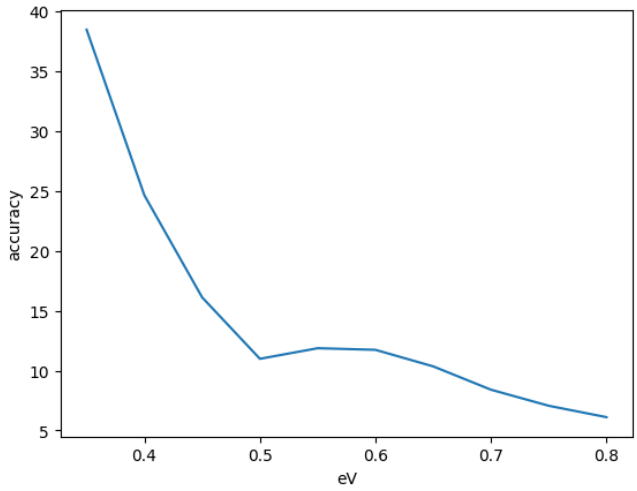

Figure 3.18: The accuracy of the clock. Its behaviour marks a sudden decrease after the transition point, which becomes smoother for larger radii. The accuracy seems to be inversely correlated with the entropy production, even if not linearly.

not linear along all the considered intervals. This aligns completely with our expectations and the results in the literature.

The distribution of the period is different according to the value of the difference of potential. We consider three different values and sample this quantity with N=5000 ensuing periods. In the under-critical phase, for $eV = 0.2$ we obtain a data distribution (Fig. (3.19)), which one can compare with the inverse Gaussian distribution, having the following form

$$IG(T, \mu, \sigma) := \sqrt{\frac{\mu^2}{2\pi\sigma^2 T^3}} \exp\left\{ -\frac{\mu(T-\mu)^2}{2\sigma^2 T} \right\} \tag{3.44}$$

which is the distribution of the return time of a Brownian process [77]. The same considerations apply in the upper-critical phase for values of the voltage close to the transition (Fig. (3.20)). In contrast, at higher voltages, the data binning is not compatible with the Wald distribution, and it becomes more asymmetrical and sharply peaked (Fig. (3.21)).

3.6.2 The Allan variance

Another key quantity to evaluate the performance of a clock is the Allan variance (see Ref. [41],[6]), used to quantify the correlation between the different ticks. The former expresses the deviation of a measured clock signal θ, from a second reference clock, which is assumed to be ideal.

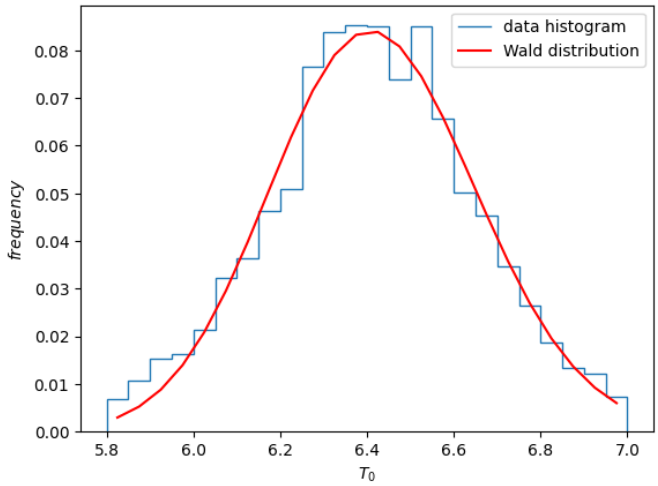

Figure 3.19: This is the distribution of the periods for $eV = 0.20$, when interpolated with the inverse-gaussian or Wald distribution. The interpolation agrees perfectly with the data distribution.

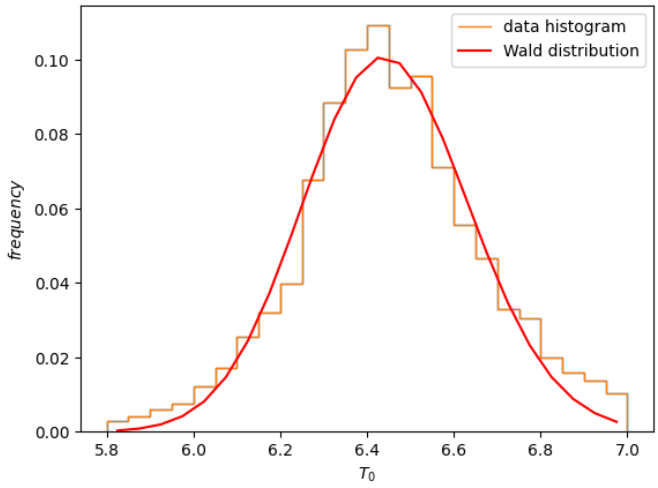

Figure 3.20: This is the distribution of the periods for $eV = 0.40$, in the upper-critical phase, when interpolated with the inverse-gaussian or Wald distribution. The interpolation agrees perfectly with the data distribution and the fit parameters are $\mu = 6.447 \pm 0.007$ and $\sigma = 0.191 \pm 0.006$. These values are compatible with the ones obtained previously in order to calculate the accuracy and the precision.

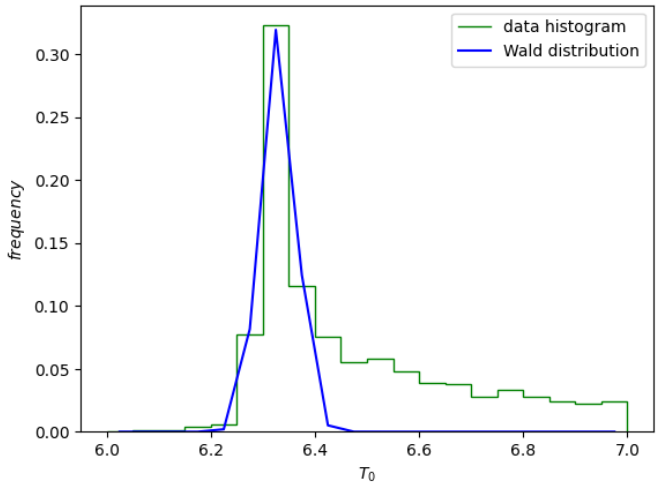

Figure 3.21: This is the distribution of the periods for $eV = 0.70$, in the upper-critical phase, when interpolated with the inverse-gaussian or Wald distribution. The interpolation does not agree with the data distribution. In contrast, it is more sharply peaked and asymmetrical.

The measured deviation from an ideal clock is

$$X(t) = \theta(t) - t. \tag{3.45}$$

If one defines

$$Y(t) = \frac{dX(t)}{dt} \tag{3.46}$$

as the instantaneous difference and integrates it over the period T, obtains the average fractional frequency difference

$$\bar{Y}(t,T) = \frac{1}{T}\int_t^{t+T} dt' Y(t+t'). \tag{3.47}$$

Its variance represents the Allan variance

$$\sigma_Y^2(T) = \frac{1}{2}\{[Y(t+T,T) - Y(t,T)]^2\}. \tag{3.48}$$

The Allan variance of the clock is computed by partitioning the signal in intervals of length T. Then one counts the number of ticks in every region. Let $X_n(T)$ be the latter quantity calculated in the n-th region, then the Allan variance can be estimated as

$$\sigma_Y^2(T) = \frac{1}{2T^2}\{(X_{n-1} + X_{n+1} - 2X_n)^2\} \tag{3.49}$$

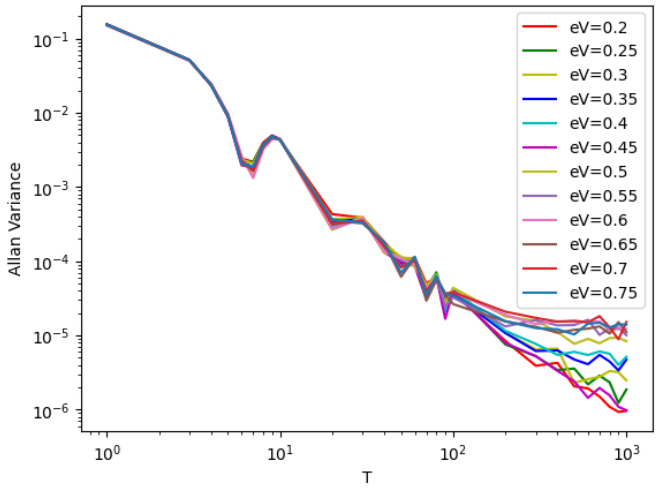

Figure 3.22: The Allan variance for different voltages above and beyond the transition point. The scaling T^{-1} is respected until the time intervals of the order 10^2. After this value, one observes a slower decrease in the variance in the upper-critical phase.

.

The result in Fig. (3.22) highlights for small T an adherence to the renewal process scaling, i.e. $\sigma_Y^2 \sim T^{-1}$ for small scales, with the presence of peaks at multiples of the period of oscillation. The two phases present the same behaviour. However, at medium time scales, there is a significant differentiation between the two phases: in the lower-critical phase, the variance tends to continue to follow the scaling, while in the upper-critical one, there is a slower decrease.

In general, the decrease of the Allan variance over T signals the increased precision of the clock when the integration is performed over larger times. The negative peaks, which appear at multiples of the period, are a consequence of the information yielded by this quantity over the signal of the clock. Moreover, the differentiation of the two phases signals that any possible advantage in medium/longer timescales in timekeeping due to the self-sustained oscillations is eventually lost.

Part II

Part II: Quantum Clocks and Quantum Batteries

Chapter 4

Quantum Clocks and Quantum Batteries

- Where we introduce a new proposal of a quantum clock using the free-energy resources offered by the non-equilibrium stationary state of an integrable spin chain.

"The career of a young theoretical physicist consists of treating the harmonic oscillator in ever-increasing levels of abstraction."

— **Sidney Coleman**

4.1 Introduction

Unlike the physical model presented in the previous chapter, there are quantum timekeeping devices relying on clockwork dynamics defined on a finite-dimensional Hilbert space. The key example is the thermal clock of Erker et. al. [25]. As we will see, said clock relies on the concept of the virtual qubit, introduced first in [15]. This smallest thermal machine is composed of two qubits each interacting with a thermal bath at different temperatures. One then can engineer a thermal state with a negative temperature from the combined Hilbert space of the qubits. The latter enables the production of an inversion of population that can produce work in a nanoscale process. In turn, Erker et.al. used this thermal machine to construct a thermal clock, by adding a ladder of arbitrary (but finite) energy levels with a fixed spacing between them, resonantly coupled to the qubit. Once the top of the ladder is reached, a photon is emitted, which constitutes a clock's signal.

In this Chapter, we examine the new proposal of a quantum clock, inspired by this one, coupled to the non-thermal stationary state of an integrable quantum spin chain, driven away from equilibrium by a quench in one of its parameters. This stationary state, drawn

from a generalized Gibbs ensemble (GGE) [17, 34, 92], has in general a finite ergotropy, and therefore is a non-passive state. Consequently, this spin chain is a particular realization of a quantum battery, providing the external resources for the clock's operation. While a quantum battery is typically characterized by investigating charging power and quantifying extractable work [19, 76, 9, 20] here we study in detail the conditions upon which this work can be used to operate a specific quantum clock.

We will examine particular examples of spin chains, which are relevant for experimental simulations. In the latter ones, the key results indicate the necessity to cross the transition point in the quench protocol, bearing a striking connection with the optimal charging protocol of Ref. [42]. These examples are feasible for experimental simulation using trapped ions [28, 79, 75] with an astonishing level of control.

4.2 What is a quantum clock? Dictionary of general definitions

What is a quantum clock? To answer this question we follow closely the treatment of Ref. [86]. We take a quantum clock to be any system described by the laws of quantum mechanics that provides an estimation of time, intended as the parameter appearing in the non-relativistic Schrodinger equation. This definition encompasses a wide range of physical systems [36, 22, 90, 63, 59]. However, one can identify key characteristics a quantum clock must obey. We will attempt to give some formal definitions and classifications of relevant types of clocks operating with dynamics described from the quantum mechanical point of view. This will identify the key desiderata obeyed by the clock we are going to analyze and how they affect the formal description of its dynamics.

A clock is any object with time-dependent dynamics which can be observed to give an estimation of time. A key requirement for a clock is independence. An independent/ticking clock is one for which the measurement of time information does not disturb the clock or affect the result of future measurements. On a formal level, in the quantum limit, one can define the state of the clock at time t from the density matrix, by tracing out the environment

$$\hat{\rho}(t) = Tr_E[e^{-i\hat{H}_{SE}t}\hat{\rho}^{(0)}_{SE}e^{i\hat{H}_{SE}t}], \tag{4.1}$$

where $\hat{\rho}^{(0)}_{SE}$ is the density matrix describing the state of the system+environment at the initial time. Please note that in the course of this Section, we are using hats on operators to distinguish them from mere numbers.

The measurement operators are defined as Kraus operators $\hat{A}_k$, such that $\sum_k \hat{A}^\dagger_k \hat{A}_k = 1$. A direct consequence of the independence principle is that this density matrix satisfies

$$\hat{\rho}(t) = \sum_k \hat{A}_k \hat{\rho}(t) \hat{A}^\dagger_k \quad \forall t, \tag{4.2}$$

Figure 4.1: The register of a classical clock.

as a direct consequence of the non-disturbance of the measurement from the independence principle. This implies that, if the clock is measured at t_2, then the outcome is independent of what is measured at an earlier time t_1. The principle of independence has a consequence on the structure of the Hilbert space of the clock, leading to the *Koashi-Imoto* decomposition. If we have the degrees of freedom of the "clockwork" $\{\mathcal{H}_{C_n}\}_n$ and those of the display $\{\mathcal{H}_{F_n}\}_n$, and n is the register index. Then, the total Hilbert is subdivided into the relative Hilbert spaces

$$\mathcal{H} = \bigoplus_n \mathcal{H}_{C_n} \otimes \mathcal{H}_{F_n}, \tag{4.3}$$

and the relative density matrix of the clock at time t is block-diagonal in the register index n

$$\hat{\rho}(t) = \bigoplus_n p(n|t)\hat{\rho}(n|t) \otimes \hat{\omega}_n, \tag{4.4}$$

where $p(n|t)$ is a probability distribution and $\hat{\rho}(n|t)$ is a properly normalized density matrix and $\hat{\omega}_n$ is time independent. The measurement operators act only on the display part

$$\hat{A}_k = \bigoplus_n \hat{\mathbb{1}}_n \otimes \hat{A}_{k,n} \tag{4.5}$$

and

$$\hat{\omega}_n = \sum_k \hat{A}_{k,n}\hat{\omega}_n\hat{A}^\dagger_{k,n} \qquad \forall n. \tag{4.6}$$

The corresponding probability to measure an outcome k is

$$P(k) = \sum_n p(n|t) Tr[\hat{A}^\dagger_{k,n} \hat{A}_{k,n} \hat{\omega}_n] = \sum_n p(n|t) a_{k,n}, \tag{4.7}$$

which is a coarse-grained measurement of the probabilities $p(n|t)$. The $a_{k,n}$ is another probability distribution independent of time. This independence requirement justifies neglecting the display part. We can take a minimal clock to be composed only of the "clockwork" part (and the register index)

$$\mathcal{H} = \bigoplus_n \mathcal{H}_{C_n} \tag{4.8}$$

$$\hat{\rho}(t) = \bigoplus_n p(n|t) \hat{\rho}(n|t) \tag{4.9}$$

$$\hat{A}_k = \bigoplus_n \delta_{n,k} \hat{\mathbb{1}}_n. \tag{4.10}$$

The definition of the *essential* clock [86] leads to an even simpler structure in terms of the Hilbert space of the clockwork. The elementary ticking clock has the following structure, which separates the register from the clockwork

$$\mathcal{H} = \mathcal{H}_T \otimes \mathcal{H}_C \tag{4.11}$$

$$\hat{\rho}(t) = \sum_n p(n|t) \hat{\rho}(n|t) \otimes |n\rangle\langle n|_T \tag{4.12}$$

$$\hat{A}_k = \hat{\mathbb{1}}_C \otimes |n\rangle\langle n|_T. \tag{4.13}$$

An important characteristic of an essential clock is self-timing. A clock is *self-timed* if its dynamics is Markovian and does not require keeping the memory of the environment for the past in its evolution. This implies a description by a Lindbladian master equation. In other words, the state at time t depends on the state at time 0 by a dynamical map

$$\hat{\rho}_t = \Lambda_t[\hat{\rho}_0], \tag{4.14}$$

where Λ_t is a family of completely positive, trace-preserving maps, satisfying the property

$$\Lambda_t = \Lambda_s \cdot \Lambda_{t-s} \tag{4.15}$$

for all t,s such that $0 \leq s \leq t$. This implies a Lindbladian dynamics of the form

$$\frac{d}{dt}\hat{\rho}(t) = \mathcal{L}[\hat{\rho}(t)] \tag{4.16}$$

and

$$\hat{\rho}(t) = e^{\Lambda_t t} \hat{\rho}(0). \tag{4.17}$$

The Lindbladian superoperator has the form

$$\mathcal{L}[\hat{\rho}] = -i[\hat{H}, \hat{\rho}] + \sum_k \gamma_k \hat{L}_k \hat{\rho} \hat{L}_k^\dagger - \frac{1}{2} \sum_k \gamma_k \{\hat{L}_k^\dagger \hat{L}_k, \hat{\rho}\}. \tag{4.18}$$

Furthermore, the Hamiltonian is diagonal in the register states n

$$\hat{H} = \bigoplus_n \hat{H}_n \tag{4.19}$$

and the jump operators on the register connect only one state n' for a single state n so that there exists only one pair $\{n, n'\}$such that

$$\hat{\Pi}_n \hat{L}_j \hat{\Pi}_{n'} = \hat{L}_j \tag{4.20}$$

for

$$\hat{\Pi}_n = \bigoplus_n \delta_{k,n} \hat{\mathbb{1}}_n, \tag{4.21}$$

the projector on the n-th subspace of the clockwork. The requirement of clockwork independence states that the clockwork of a ticking clock are independent of the state of the register. This, in turn, implies

$$\mathcal{H}_{C_n} = \mathcal{H}_C \tag{4.22}$$

and

$$\mathcal{H} = \mathcal{H}_C \otimes \mathcal{H}_T. \tag{4.23}$$

The dynamics of the clockwork C is independent of the register state

$$Tr_T[\mathcal{L}[\hat{\rho}_C \otimes |n\rangle\langle n|_T]] = Tr_T[\mathcal{L}[\hat{\rho}_C \otimes |n'\rangle\langle n'|_T]] \qquad \forall n, n'. \tag{4.24}$$

A specific type of clock is the graph clock. This quantum clock is an elementary clock with a graph structure in the clockwork (see Fig. (4.2)). This graph has its transition rates between all the states and the jump operators who are associated with a shift in the register. If the dynamics of such a clock satisfies translational invariance, then the Lindblad operator has the form

$$\mathcal{L}[\hat{\rho}_t] = \sum_\Delta (\mathcal{L}_\Delta \otimes X_\Delta)[\hat{\rho}_t], \tag{4.25}$$

where

$$X_\Delta[|n\rangle\langle n|] = |n + \Delta\rangle\langle n + \Delta| \qquad \forall n. \tag{4.26}$$

As we already pointed out, irreversibility is a property connected to the entropic cost of measuring time. Translated, it means that the state of the register cannot return to the same state two times, for at least a subset of indices of the register. If the clock has the

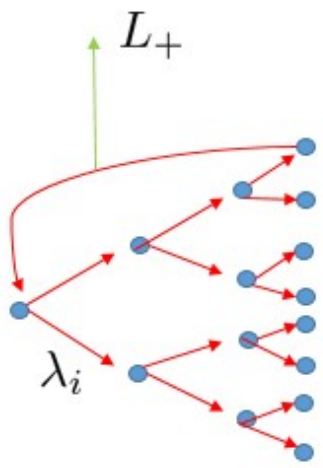

Figure 4.2: This is a scheme of the structure of the clockwork in a graph clock. We have included the transition rates between the states λ_i and the jump operator shifting the register index n.

property that returns to the initial configuration after each tick, it is dubbed a *reset clock*. In that case, the ticks are i.i.d. (independent and identically distributed). A single tick waiting-time distribution is sufficient to describe everything about the clock.

Let us conclude the present section by noting that these definitions identify a particular type of quantum clock and are not obeyed by all the examples of clocks found in the literature. Indeed, as we will see, some clocks can work in the regime of strong coupling with the environment. Moreover, this treatment concerns only registers with finite-dimensional Hilbert space, while certain clocks rely on dynamical systems with dissipative limit cycles. Finally, measurements and coherence can be used as timekeeping resources.

4.3 The thermal clock

Now, let us examine in greater detail the thermal quantum clock by Ref. [25]. This is an essential graph clock and a reset clock, satisfying the requirements exposed in the previous Section 4.2. This clock was introduced as a minimal model of a quantum clock powered by thermal resources, to analyze the fundamental thermodynamic limit of quantum timekeeping.

This quantum clock uses the minimal model of a thermal machine put forward by Brunner et.al. [16]. This thermal machine consists of two qubits each one in contact with a thermal reservoir with fixed temperatures respectively T_c and T_h, satisfying $T_h > T_c$.

Each qubit has its associated energy $E_h > E_c$. The combined Hilbert space of the two qubits is $\{|0\rangle_c|0\rangle_h, |1\rangle_c|0\rangle_h, |0\rangle_c|1\rangle_h, |1\rangle_c|1\rangle_h\}$, with associated energies $0, E_c, E_h, E_c + E_h$. Each qubit is therefore in the thermal state, viz.

$$\tau_i = \frac{1}{1 + e^{-E_i/T_i}}(|0\rangle\langle 0|_i + e^{-E_i/T_i}|1\rangle\langle 1|_i). \tag{4.27}$$

$i = c, h$. As the article shows, by selecting the subset of the combined Hilbert space $\{|0\rangle_v = |1\rangle_c|0\rangle_h, |1\rangle_v = |0\rangle_c|1\rangle_h\}$, one has a virtual qubit, whose energy spacing is $E_v = E_h - E_c$ and whose virtual temperature is defined by the relation

$$T_v = \frac{E_h - E_c}{\frac{E_h}{T_h} - \frac{E_c}{T_c}}. \tag{4.28}$$

This virtual qubit can act as a refrigerator when $T_v < T_c, T_h$, and as a heat pump when $T_v > T_c, T_h$. Interestingly enough, when T_v becomes negative[1], implying $\frac{E_h}{T_h} < \frac{E_c}{T_c}$, this qubit acts as a thermal machine. This is because a population inversion is created in it. This fact means that this qubit can perform work, for example when connected to a ladder of energy level, by lifting its state. The important concept here is population inversion: in quantum mechanics, each process is constrained to have its inverse due to the requirement of the hermiticity of the Hamiltonian. The only way to suppress the inverse process is to make sure the population of the excited state is greater than the one of the ground state in the virtual qubit.

Taking advantage of this concept, Erker et. al. [25] designed a model consisting, for the clockwork part, of a virtual qubit coupled to a ladder of d equally-spaced energy levels. The jump process takes place from the highest energy level to the lowest, with an emission of a photon, constituting the signal of the clock. Therefore, the structure of the ladder is a ring-shaped graph. The Hamiltonian of the model reads

$$H = H_0 + H_{int}, \tag{4.29}$$

where

$$H_0 = \sum_{j=h,c} E_j|1\rangle\langle 1|_j + \sum_{k=0}^{d-1} kE_w|k\rangle_w\langle k|_w \tag{4.30}$$

and

$$H_{int} = g\sum_{k=0}^{d-1}(|1\rangle_c|0\rangle_h|k+1\rangle_w\langle 1|_c\langle 0|_h\langle k+1|_w + h.c.) \tag{4.31}$$

The resonance condition implies that $E_w = E_h - E_c$. A pictorial representation of the setup of this model can be found in Fig. (4.3). As a result of the weak coupling assumption and the absence of initial coherence, the authors justify a semiclassical biased random walk

[1]Please note this is not a thermodynamic temperature, so its definition does not create any problem.

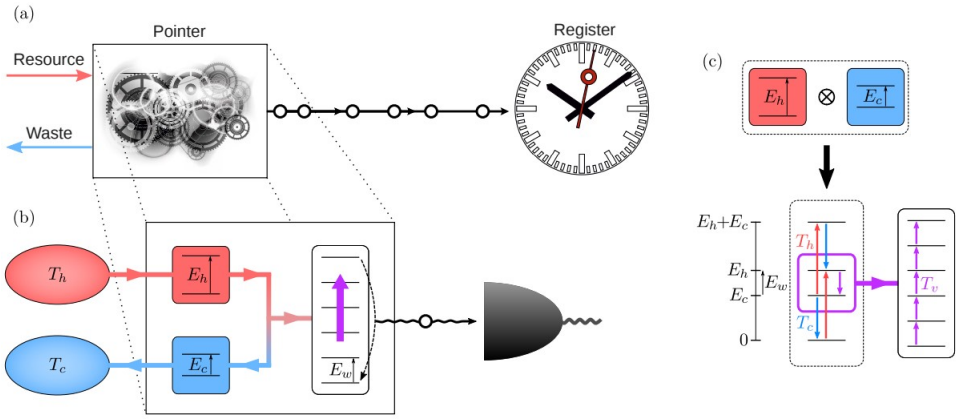

Figure 4.3: A depiction of the thermal clock from [25], involving a virtual qubit weakly coupled to a ladder of d energy levels. The signal of the clock is produced by the spontaneous emission of a photon, taking place once it reaches the top of the ladder. In a) the whole structure of the clock is depicted, distinguishing between the pointer (the clockwork) and the external register. b) represents the structure of the clockwork, with reference to the virtual qubit and the ladder. c) represents the virtual qubit, with special reference to the structure of its Hilbert space.

approximation, resulting in incoherent dynamics of the clockwork. The calculated upward and downward transition rates satisfy the key relation

$$\frac{p_\uparrow}{p_\downarrow} = e^{-\beta_v E_v}. \tag{4.32}$$

This semiclassical analysis allows one to compute the average time it takes to reach the top of the ladder and its dispersion. In this approximation, the state of the ladder can be described using a time-dependent probability distribution $q(n,t)$ [25], where $n \in \mathbb{Z}$. This probability distribution satisfies $q(n,t) > 0$ and $\sum_n q(n,t) = 1$, the normalization condition. The evolution is governed by the master equation

$$\frac{dq(n,t)}{dt} = p_\uparrow q(n-1,t) + p_\downarrow q(n+1,t) - (p_\uparrow + p_\downarrow) q(n,t) \tag{4.33}$$

Now, we denote the mean as μ and the variance as σ^2

$$\mu(t) = \sum_n n q(n,t) \tag{4.34}$$

$$\sigma^2(t) = \sum_n (n - \mu(t))^2 q(n,t). \tag{4.35}$$

The average position of the ladder obeys the following equation

$$\frac{d\mu(t)}{dt} = \sum_n n \frac{dq(n,t)}{dt} = p_\uparrow - p_\downarrow. \tag{4.36}$$

From its definition, the equation for the variance reads

$$\frac{d\sigma^2(t)}{dt} = \sum_n (((n-\mu(t))^2 \frac{dq(n,t)}{dt} - 2(n-\mu(t))\frac{d\mu(t)}{dt} q(n,t). \tag{4.37}$$

Using Eq. 4.36 and the definition of variance, one can infer that

$$\frac{d\sigma^2(t)}{dt} = p_\uparrow + p_\downarrow. \tag{4.38}$$

The average time it takes to reach the top of the ladder is given by the ratio between the ladder dimensionality and the average velocity

$$t_{tick} = \frac{d}{\frac{d\mu(t)}{dt}} = \frac{d}{p_\uparrow - p_\downarrow}. \tag{4.39}$$

The replacement of $d-1$ by d is due to the assumption of large dimensionality of the ladder. The precision, then is defined as the inverse of the average period

$$\nu_{tick} = \frac{1}{t_{tick}} = \frac{p_\uparrow - p_\downarrow}{d}. \tag{4.40}$$

If one integrates the increase rate of the variance over a period, one obtains

$$\Delta\sigma^2(t) = t_{tick}\frac{d\sigma^2(t)}{dt} = d\left(\frac{p_\uparrow + p_\downarrow}{p_\uparrow - p_\downarrow}\right). \tag{4.41}$$

The uncertainty in the time interval between two different ticks

$$\Delta t_{tick} = \frac{\sigma(t - t_{tick})}{\frac{d\mu(t)}{dt}} = \frac{\sqrt{d}}{p_\uparrow - p_\downarrow}\sqrt{\frac{p_\uparrow + p_\downarrow}{p_\uparrow - p_\downarrow}}. \tag{4.42}$$

The definition of accuracy reads

$$N = \left(\frac{t_{tick}}{\Delta t_{tick}}\right). \tag{4.43}$$

Substituting the expressions (Eq. 4.39,4.42) yields

$$N = d\left(\frac{p_\uparrow - p_\downarrow}{p_\uparrow + p_\downarrow}\right). \tag{4.44}$$

The entropy production, according to the standard thermodynamic definition, reads

$$\Delta S_{tick} = d(\beta_c E_c - \beta_h E_h). \tag{4.45}$$

As a consequence, one can write the random walk bias as

$$\frac{p_\uparrow}{p_\downarrow} = e^{\frac{\Delta S_{tick}}{d}}. \tag{4.46}$$

Inserting this expression in the accuracy (Eq. 4.6) one obtains

$$N = d \tanh\left[\frac{\Delta S_{tick}}{2d}\right]. \tag{4.47}$$

When one takes the limit $d \to \infty$, the expression reduces to a linear relation

$$N \to \frac{\Delta S_{tick}}{2}, \tag{4.48}$$

saturating the bounds of the thermodynamic uncertainty relations (Section 1.5). In the limit $\Delta S_{tick} \to \infty$, $N \to d$ yields the maximum accuracy for an incoherent clock.

4.4 The clock and the battery

Inspired by the thermal clock described above, we are going to introduce a new proposal for a quantum clock powered by the stationary state of an integrable quantum spin chain. This stationary state, drawn from a generalized Gibbs ensemble (GGE) [17, 34, 92], in general, has a finite ergotropy [4, 5] and is consequently a particular case of a quantum battery [4, 19, 79, 73]. These integrable models are apt for experimental simulation using trapped ions [28, 79, 75] with an astonishing level of control.

In this case, only a single qubit is necessary, acting as a frequency filter, which is coupled resonantly to the ladder of d equally spaced energy levels, whose dynamics mimics the one described in the previous Section.

The associated Hamiltonian of the model comprises five terms

$$H = H_B + H_Q + H_L + H_{QL} + H_{QB}. \tag{4.49}$$

Here H_Q is relative to the qubit

$$H_Q = \frac{\epsilon_0}{2}\sigma_Q^z \tag{4.50}$$

H_L is the ladder Hamiltonian

$$H_L = \sum_{k=0}^{d-1} k\epsilon_w c_k^\dagger c_k, \tag{4.51}$$

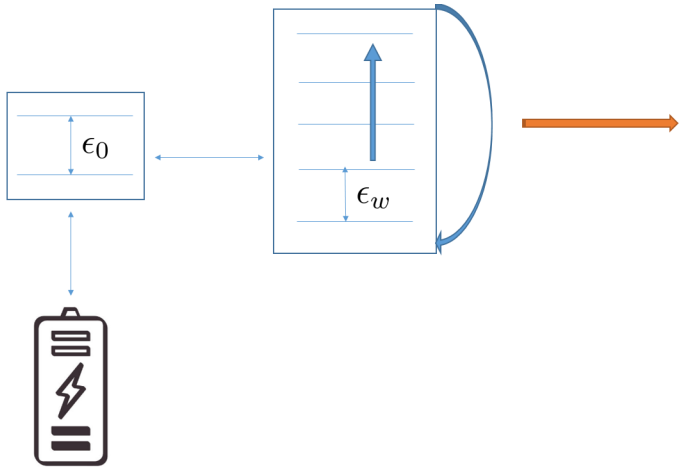

Figure 4.4: The setup of the clock consists of a qubit coupled to a ladder of energy levels of equal spacing ϵ_w. The ladder is resonant with the level spacing of the qubit ϵ_0 so that $\epsilon_0 = \epsilon_w$. The motion of the ladder is biased and each time the top is reached, a photon is released with rate Γ, thus constituting the signal of the clock. The qubit interacts with the battery, which is used as a free energy source to bias the ladder's dynamics.

where the creation-annihilation operators $c_k^\dagger / c_k$ are fermions. The resonance condition is $\epsilon_w = \epsilon_0$, which means that the levels $|1\rangle_Q |k\rangle_L$ has the same energy as $|0\rangle_Q |k+1\rangle_L$. The interaction Hamiltonian between the qubit and the ladder reads

$$H_{QL} = g \sum_{k=0}^{d-1} (\sigma_Q^- c_{k+1}^\dagger c_k + h.c.), \tag{4.52}$$

where g represents the strength of the coupling. The qubit is coupled to the battery through a specific observable of the latter, whose choice is crucial for the clock's operation. In terms of a generic observable A, the qubit-battery interaction term has the expression

$$H_{QB} = \sigma_Q^x A. \tag{4.53}$$

We will explore different examples of integrable quantum spin chains and their coupling to the qubit.

In general terms, the initial state of the spin chain is a fully charged battery, corresponding to the highest excited level of the many-body system. The battery is activated at time $t = 0$ by quenching one of its parameters from λ_i to λ_f. Subsequently, it reaches the stationary regime and we couple to it after this relaxation has taken place. The role of the quench here is to perform work on the battery, analogously to the charging protocol.

A schematic depiction of the clock-battery setup is in Fig. (4.4).

4.5 The dynamics of the clock

In this Section, we will derive the ladder dynamics in the weak coupling regime, namely $g \ll \epsilon_0$.
The following superoperator represents the effect of the battery on the qubit

$$\mathcal{L}_\gamma = \gamma_\downarrow \mathcal{D}[\sigma^-] + \gamma_\uparrow \mathcal{D}[\sigma^+], \tag{4.54}$$

in terms of the qubit raising and lowering operators $\sigma^\pm$, the transition rates of the qubit states due to the effect of the battery $\gamma_{\uparrow,\downarrow}$, and the dissipator

$$\mathcal{D}[A]\rho = A\rho A^\dagger - \frac{1}{2}\{A^\dagger A, \rho\}. \tag{4.55}$$

One describes the dynamics of the clock in the "no-click" subspace. The associated density matrix is $\rho_0(t)$ conditioned on no spontaneous emission having occurred up to time t. We assume the pointer to be in the product state

$$\rho_0(0) = \rho_Q(0) \otimes |0\rangle\langle 0|_w \tag{4.56}$$

with a generic (unimportant) initial condition for the qubit. The evolution of the conditional density operator is described by the equation of motion

$$\frac{d\rho_0}{dt} = i(\rho_0 H_{eff}^\dagger - H_{eff}\rho_0) + \mathcal{L}_\gamma \rho_0, \tag{4.57}$$

where the effective Hamiltonian is

$$H_{eff} = H_0 + H_{int} + H_{se}, \tag{4.58}$$

and $H_0 = H_Q + H_L$ and $H_{int} = H_{QL}$ and the spontaneous emission term, which is non-Hermitian

$$H_{eff} = -\frac{i\Gamma}{2} c_{d-1}^\dagger c_{d-1}. \tag{4.59}$$

4.5.1 The biased random walk model

In the limit $\gamma \gg g, \Gamma$, we use the Nakajima-Zwanzig projection technique to derive an evolution equation for the conditional reduced density operator of the ladder

$$\rho_w(t) = Tr_Q[\rho_0(t)]. \tag{4.60}$$

Let us introduce the projector into the separated state, defined as

$$\mathcal{P}\rho_0(t) = \rho_w(t) \otimes \rho_Q. \tag{4.61}$$

We rewrite the evolution equation of the conditional density matrix as

$$\frac{d\rho_0}{dt} = \mathcal{L}\rho_0, \tag{4.62}$$

where

$$\mathcal{L} = \mathcal{L}_0 + \mathcal{H}_{se} + \mathcal{H}_{int} \tag{4.63}$$

where the Hamiltonian superoperator reads

$$\mathcal{H}_{se}\rho = i(\rho H_{se}^{\dagger} - H_{se}\rho). \tag{4.64}$$

Let's transform the density operator to a dissipative interaction picture defined by $\tilde{\rho(t)} = e^{-\mathcal{L}_0 t}\rho_0(t)$. The corresponding evolution of the superoperators is given by

$$\tilde{\mathcal{H}}_{int}(t) = e^{-\mathcal{L}_0 t}\mathcal{H}_{int}e^{\mathcal{L}_0 t}, \tag{4.65}$$

while the operator $\tilde{\mathcal{H}}_{se}$ stays the same, because it commutes with the operator $\mathcal{L}_0$. Starting from the perturbative argument in the coupling strength of the interaction g and Γ, one can write

$$\frac{d\mathcal{P}\tilde{\rho}_0}{dt} = \tilde{\mathcal{H}}_{se}\mathcal{P}\tilde{\rho}_0(t) + \int_0^t dt'\mathcal{P}\tilde{\mathcal{H}}_{int}(t)\tilde{\mathcal{H}}_{int}(t')\mathcal{P}\tilde{\rho}_0(t'), \tag{4.66}$$

valid up to the second order. One then applies the Born-Markov approximation, on the assumption that $\gamma_{\uparrow,\downarrow} \gg g, \Gamma$. The next steps are expanding the commutator in the basis of the jump operators, whose eigenvalues are the energy differences between the levels of the system, tracing over the qubit states and transforming back to the Schrodinger picture. On the further assumption of no initial coherence, the resulting master equation for the population of the levels p_w is

$$\frac{dp_w}{dt} = p_{\downarrow}\mathcal{D}[B_w]p_w + p_{\uparrow}\mathcal{D}[B_w^{\dagger}]p_w - \frac{\Gamma}{2}(|d-1\rangle_w\langle d-1|_w p_w + p_w|d-1\rangle_w\langle d-1|_w), \tag{4.67}$$

in terms of the ladder jump operators $B_w = c_k^{\dagger}c_{k+1}$. In our case the resulting expression for $p_{\uparrow}$ and $p_{\downarrow}$ is

$$p_{\uparrow} = 2g^2\int_0^{\infty} dt e^{i\epsilon_w t}\langle\sigma^-(t)\sigma^+(0)\rangle \tag{4.68}$$

and

$$p_{\downarrow} = 2g^2\int_0^{\infty} dt e^{-i\epsilon_w t}\langle\sigma^+(t)\sigma^-(0)\rangle. \tag{4.69}$$

The ladder operators evolve according to the adjoint Liouvillian operator $\sigma^-(t) = e^{\mathcal{L}_0^{\dagger}t}\sigma^-(0)$, resulting in $\sigma^-(t) = \exp(-i\epsilon_0 - \gamma_+ t)\sigma_-$, where we define $\gamma_+ = \gamma_{\uparrow} + \gamma_{\downarrow}$. Upon inserting this expression into the definition of $p_{\uparrow,\downarrow}$ we have

$$p_{\uparrow} = \frac{2g^2}{\gamma_+}\langle\sigma^-\sigma^+\rangle_s \tag{4.70}$$

and

$$p_{\downarrow} = \frac{2g^2}{\gamma_+}\langle\sigma^+\sigma^-\rangle_s, \tag{4.71}$$

where these averages are calculated in the stationary state of the qubit.

Using the representation of the qubit density matrix as $\rho(t) = \frac{1}{2}\Big(1 + \langle\vec{\sigma}(t)\cdot\vec{\sigma}\rangle\Big)$ and inserting it into the Lindblad equation for the dynamics of the system qubit+battery only

$$\frac{d\rho_Q}{dt} = i[H_Q, \rho_Q] + \mathcal{L}_\gamma\rho_Q \tag{4.72}$$

one ends with the following evolution equations for the averages of the spin operators

$$\frac{d\langle\sigma^+\rangle}{dt} = -\gamma_+\langle\sigma^+\rangle \tag{4.73}$$

$$\frac{d\langle\sigma^-\rangle}{dt} = -\gamma_+\langle\sigma^-\rangle, \tag{4.74}$$

and for σ_z

$$\frac{d\langle\sigma^z\rangle}{dt} = -\gamma_+\langle\sigma^z\rangle + \gamma_-, \tag{4.75}$$

where $\gamma_- = \gamma_\uparrow - \gamma_\downarrow$. As a consequence, the stationary state has no coherences and

$$\langle\sigma_z\rangle_s = \frac{\gamma_-}{\gamma_+} \tag{4.76}$$

and the diagonal matrix elements are

$$\langle\sigma^+\sigma^-\rangle_s = \frac{1}{2}\left(1 + \frac{\gamma_-}{\gamma_+}\right) \tag{4.77}$$

and

$$\langle\sigma^-\sigma^+\rangle_s = \frac{1}{2}\left(1 - \frac{\gamma_-}{\gamma_+}\right). \tag{4.78}$$

Inserting these expression in the definitions of $p_{\uparrow,\downarrow}$ yields

$$p_{\uparrow} = \frac{g^2}{\gamma_+}\left[1 + \frac{\gamma_-}{\gamma_+}\right] \tag{4.79}$$

and

$$p_{\downarrow} = \frac{g^2}{\gamma_+}\left[1 - \frac{\gamma_-}{\gamma_+}\right]. \tag{4.80}$$

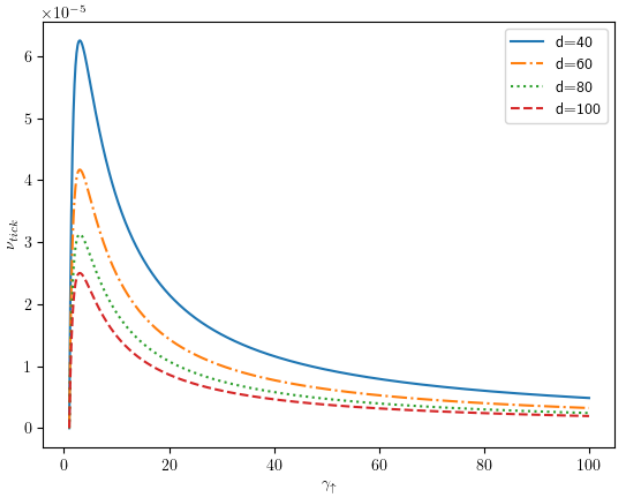

Figure 4.5: The precision of the clock for different values of $\gamma_\uparrow$ and $\gamma_\downarrow = 1$, $g = 0.1$. As one can see, the precision is inversely proportional to the dimensionality of the ladder. The accuracy saturates to a constant value, which is the parameter d, constituting the optimal value for a clock with incoherent dynamics.

4.6 The performance of the clock and the entropy production

One can calculate the key quantities related to the clock's performance by repeating the same analysis of Section 4.3, stemming from the semiclassical approximation. Upon defining $\gamma_\pm = \gamma_\uparrow \pm \gamma_\downarrow$ one can express these quantities in terms of the qubit transition rates, as

$$\nu_{tick} = \frac{p_\uparrow - p_\downarrow}{d} = \frac{2}{d}\frac{g^2\gamma_-}{\gamma_+^2} \tag{4.81}$$

and

$$N = d\left(\frac{p_\uparrow - p_\downarrow}{p_\uparrow + p_\downarrow}\right) = d\frac{\gamma_-}{\gamma_+}, \tag{4.82}$$

(In Figg. 4.5 and 4.6). We can further comment on these expressions by noting that both the accuracy and the precision are proportional to γ_-, which represents the degree to which the random walk is biased and the clock operates at increasing velocity. The dependence on the ladder dimensionality d is such that the accuracy scales as d, while the resolution as d^{-1}. The accuracy saturates to d, the optimal value for a clock with incoherent dynamics.

Now, let us compare the performance of the clock with the entropy production per tick. We can estimate the latter by noting that both the qubit and the battery are in the stationary state, the only way to determine the loss of information due to the clock is by

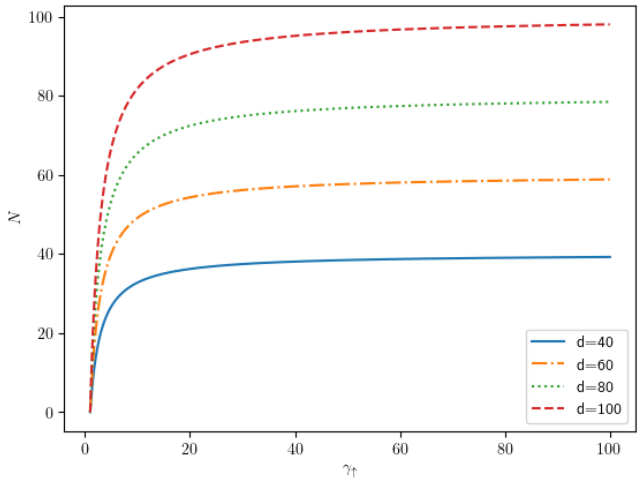

Figure 4.6: The precision of the clock for different values of $\gamma_\uparrow$, with $\gamma_\downarrow = 1$.This image shows that the precision is directly proportional to the dimensionality of the ladder.

observing that the random walk starts on a definite position and then this information is lost. We can use the known results for the entropy production in a biased random walk [54]. By calculating the time-dependent change of the Boltzmann-Gibbs entropy $\dot{S}(t) = -k_B \sum_n \frac{q(n,t)}{dt} \log q(n,t)$

$$\dot{S}(t) = k_B(p_\uparrow - p_\downarrow) \ln \frac{p_\uparrow}{p_\downarrow} + k_B \sum_{n,m=n-1} [p_\uparrow q(m,t) - p_\downarrow q(n,t)] \tag{4.83}$$

One can substitute the master equation (Eq. 4.33)

$$\dot{S}(t) = -k_B \sum_{n=1}^{d} \sum_{m=1}^{d} [p_\uparrow q(n-1,t) + p_\downarrow q(n+1,t) - (p_\uparrow + p_\downarrow) q(n,t)] \ln \left(\frac{q(n,t)}{q(m,t)} \right), \tag{4.84}$$

where the further term at the denominator of the logarithm vanishes due to the condition $\sum_{n=1}^{d} \frac{dq(n,t)}{dt} = 0$. Equivalently

$$\dot{S}(t) = k_B \sum_{m=1}^{d} \sum_{n=m-1}^{d-1} [p_\uparrow q(n,t) - p_\downarrow q(m,t)] \ln \left(\frac{q(n,t)}{q(m,t)} \right). \tag{4.85}$$

This expression can be rewritten as

$$\dot{S}(t) = k_B \sum_{m=1}^{d} \sum_{n=m-1}^{d-1} [p_\uparrow q(n,t) - p_\downarrow q(m,t)] \ln \left(\frac{p_\uparrow q(n,t)}{p_\downarrow q(m,t)} \right) \tag{4.86}$$

$$-k_B \sum_{m=1}^{d} \sum_{n=m-1}^{d-1} [p_\uparrow q(n,t) - p_\downarrow q(m,t)] \ln \frac{p_\uparrow}{p_\downarrow}. \tag{4.87}$$

These two contributions can be recast in the form

$$\dot{S}(t) = \dot{S}_e(t) + \dot{\sigma}(t). \tag{4.88}$$

The first term can be recast as

$$\dot{S}_e(t) = -k_B \sum_{m=1}^{d} \sum_{n=m-1}^{d-1} [p_\uparrow q(n,t) - p_\downarrow q(m,t)] \ln \frac{p_\uparrow}{p_\downarrow} = -k_B [p_\uparrow - p_\downarrow] \ln \frac{p_\uparrow}{p_\downarrow}, \tag{4.89}$$

using the normalization condition. In contrast, the second term is transformed into

$$\dot{\sigma}(t) = k_B (p_\uparrow - p_\downarrow) \ln \left(\frac{p_\uparrow}{p_\downarrow} \right) \tag{4.90}$$

$$+k_B \sum_{m=1}^{d} \sum_{n=m-1}^{d-1} [p_\uparrow q(n,t) - p_\downarrow q(m,t)] \ln \left(\frac{q(n,t)}{q(m,t)} \right). \tag{4.91}$$

The physical interpretation of these two is the following: $S_e(t)$ is the entropy flow into the environment, while the second is the entropy production rate. The second term satisfies $\dot{\sigma}(t) > 0$ and upon the condition of local detailed balance, identifying a non-equilibrium steady state, they satisfy $\dot{\sigma} = -\dot{S}_e$. This is the case we are interested in here.
To obtain the entropy production in a tick of the ladder motion one integrates Eq. 4.83 over time

$$\Delta S_{tick} = k_B t_{tick} (p_\uparrow - p_\downarrow) \ln \frac{p_\uparrow}{p_\downarrow} = d \ln \frac{p_\uparrow}{p_\downarrow}. \tag{4.92}$$

In the case of the thermal clock, this expression yields the correct expression

$$\Delta S_{tick} = d[-\beta_c E_c - \beta_h E_h]. \tag{4.93}$$

In this case, the entropy production reads

$$\Delta S_{tick} = k_B d \left[\ln \left(1 + \frac{\gamma_-}{\gamma_+} \right) - \ln \left(1 - \frac{\gamma_-}{\gamma_+} \right) \right] \tag{4.94}$$

In the limit of small $\gamma_- \simeq 0$, which implies $\gamma_\uparrow \simeq \gamma_\downarrow$ we can approximate this expression as

$$\Delta S_{tick} \simeq 2 d k_B \frac{\gamma_-}{\gamma_+}. \tag{4.95}$$

Comparing this expression with the accuracy (Eq.4.6) we retrieve the key relation of Erker et. al. [25]

$$N = \frac{\Delta S_{tick}}{2} \tag{4.96}$$

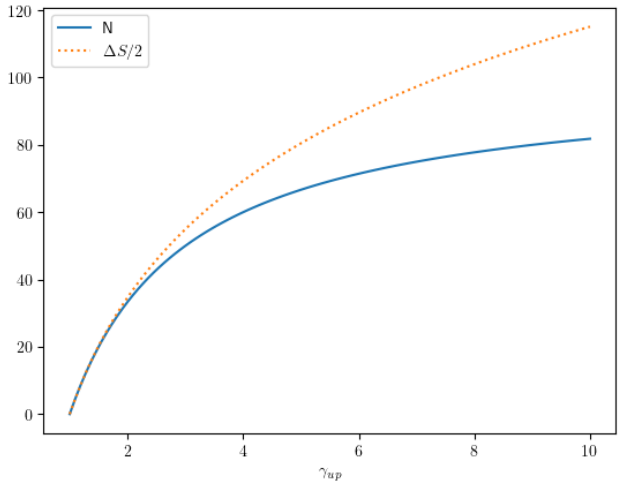

Figure 4.7: The entropy production divided by 2 and the accuracy vs. $\gamma_\uparrow$. We can see clearly that for $\gamma_\uparrow \simeq \gamma_\downarrow$ these two quantities coincide, while for $\gamma_\uparrow >> \gamma_\downarrow$ the entropy production diverges, while the accuracy saturates to d.

in the regime of weak bias[2], saturating the TUR bound. The generic relation between these two quantities reads

$$N = d \tanh\left[\frac{\Delta S_{\text{tick}}}{2d}\right] \tag{4.97}$$

unchanged from the thermal clock's results. That is to say, being an incoherent quantum clock, the relation of Ref. [8] in the context of Brownian clocks holds.

4.7 General Arguments

Let us now examine the conditions in the manifold of parameters of the battery necessary to power the clock, relative to the choice of the coupling observable, now denoted as A on general ground.
The first step is to express the qubit transition rates in the spectral representation (known as Lehmann representation). One can write these rates in the following form [12]

$$\gamma_{\uparrow,\downarrow} = \frac{1}{4}\int_{-\infty}^{\infty} d\tau e^{\mp i\epsilon_0\tau} Tr[\rho_{st} A(\tau/2)A(-\tau/2)], \tag{4.98}$$

where the stationary state of the battery is given by the diagonal ensemble $\rho_{st} = \sum_{k,i} p_k^i |ki\rangle\langle ki|$, with $p_k^i = |\langle ki|\psi_0\rangle|^2$ and $|\psi_0\rangle$ being the initial state. Here, k runs over the energy levels

[2] In Ref. [25] this regime coincides with $\beta_c E_c - \beta_h E_h \to 0$

and i is a degeneracy index. Substituting the expression of this stationary state in the correlation function, one obtains

$$Tr[\rho_{st}A(t)A(0)] = \sum_l p_l \langle l|A(t)A(0)|l\rangle \,. \tag{4.99}$$

By expressing the time dependence of the operator one obtains

$$\sum_l p_l \left\langle l\middle|e^{-iH_B^f t}Ae^{iH_B^f t}A\middle|l\right\rangle . \tag{4.100}$$

Afterwards, we insert a completeness relation and explicit time dependence with the energy eigenstates of the final Hamiltonian

$$\sum_{l,m} p_l e^{-it(E_l-E_m)} \left| \langle l|A|m\rangle \right|^2 . \tag{4.101}$$

From this result, one employs the Lehmann representation (also known as spectral representation)

$$\langle A(t)A(0)\rangle_{st} = \int \frac{d\omega}{2\pi} J(\omega), \tag{4.102}$$

where

$$J(\omega) = \sum_{l,m} p_l \left| \langle l|A|m\rangle \right|^2 \delta(\omega - E_l + E_m). \tag{4.103}$$

Then, the transition rates can be expressed as

$$\gamma_\uparrow = \sum_{l,m} p_l \left| \langle l|A|m\rangle \right|^2 \delta(-\epsilon_0 + E_l - E_m) \tag{4.104}$$

and

$$\gamma_\downarrow = \sum_{l,m} p_l \left| \langle l|A|m\rangle \right|^2 \delta(\epsilon_0 + E_l - E_m). \tag{4.105}$$

Now, let's observe that the delta function admits a solution, respectively when $E_l - E_m > 0$ and $E_l - E_m < 0$. So, one can restrict the sum in the previous expressions

$$\gamma_\uparrow = \sum_{l,m s.t. E_l > E_m} p_l \left| \langle l|A|m\rangle \right|^2 \delta(-\epsilon_0 + E_l - E_m) \tag{4.106}$$

$$\gamma_\downarrow = \sum_{l,m s.t. E_l < E_m} p_l \left| \langle l|A|m\rangle \right|^2 \delta(\epsilon_0 + E_l - E_m). \tag{4.107}$$

Given these expressions, one can write the bias condition $\gamma_\uparrow > \gamma_\downarrow$ (exchanging the indexes) as

$$\sum_{l,ms.t.E_l>E_m} (p_l - p_m)\Big| \langle l|A|m\rangle \Big|^2 \delta(\epsilon_0 - E_l + E_m) > 0. \tag{4.108}$$

So, from this expression, we are in the position to prove three statements:

1. If $p_l > p_m$ at $\epsilon_0 = E_l - E_m$ $\forall |l\rangle, |m\rangle$ s.t. $E_l > E_m$ and $\Big| \langle l|A|m\rangle \Big|^2 \neq 0$, then $\gamma_\uparrow > \gamma_\downarrow$. Such a state is termed "active at resonance".

2. If $p_l \leq p_m$ at $\epsilon_0 = E_l - E_m$ $\forall |l\rangle, |m\rangle$ s.t.$E_l > E_m$ and $\Big| \langle l|A|m\rangle \Big|^2 \neq 0$, then $\gamma_\uparrow \leq \gamma_\downarrow$. This state can be baptized as "passive at resonance" in the subspace of non-vanishing matrix elements.

3. If $\gamma_\uparrow > \gamma_\downarrow$, then the imaginary part of the response function at frequency ϵ_0 $\bar{\chi}''(\epsilon_0) < 0$ (see Appendix I) and the converse is also true.

The proofs of the statements are

1. and 2. follow directly from writing the operating condition as:

$$\sum_{l,m,\text{s.t.},E_l>E_m} (p_l - p_m)\big| \langle l|A|m\rangle \big|^2 \delta(\epsilon_0 - E_l + E_m) > 0 \tag{4.109}$$

3. can be proven by representing the imaginary part of the response function as

$$\bar{\chi}''(\omega) = \sum_{l,m} p_l \Big| \langle l|A|m\rangle \Big|^2 \Big(\delta(\omega + E_l - E_m) - \delta(\omega - E_l + E_m) \Big). \tag{4.110}$$

Clearly, this expression can be rewritten as

$$\bar{\chi}''(\omega) = \sum_{kk'} (p_k - p_{k'}) \Big| \big\langle k \big| A \big| k' \big\rangle \Big|^2 \delta(\omega + E_k - E_{k'}), \tag{4.111}$$

(Section I). Observe that this expression is similar to the transition rates mentioned above. As a matter of fact, one can write the relation $\gamma_\downarrow - \gamma_\uparrow = \bar{\chi}''(\epsilon_0)$. This equation proves directly the statement.

The significance of these results is clear from the fact that, in the absence of degeneracies in the levels satisfying the resonance conditions, statements (1) and (2) indicate that the operating conditions depend solely on the quench parameters, not on the matrix elements of the coupling observable. In the case where degeneracies are present, this no longer holds, but these can be understood as limiting cases. Statement (3) serves as a necessary and sufficient condition, providing a criterion for energy extraction from the battery at the desired frequency.

4.8 Examples of quantum batteries

Let's now study the practical application of these statements by choosing specific examples for the battery. We will analyze, in particular, the Ising and the XX spin chains, in light of their experimental relevance. For these integrable spin chains, the steady-state response function has already been the object of previous studies.

4.8.1 The Quantum Ising chain coupled through the transverse field

The first one is the quantum Ising chain in a transverse field. Its Hamiltonian is given by

$$H_B = -\sum_{j=1}^{L}(J^x\sigma_j^x\sigma_{j+1}^x + J^y\sigma_j^y\sigma_{j+1}^y) - h\sum_{j=1}^{L}\sigma_z. \tag{4.112}$$

Setting $J = 1$, the nearest-neighbor coupling can be parameterized as $J_x = \frac{1+\kappa}{2}$ and $J_y = \frac{1-\kappa}{2}$.
Let's choose the coupling between the battery and the qubit as

$$H_{QB} = g_\sigma\sigma_Q^x\sum_{j=1}^{L}\sigma_j^z. \tag{4.113}$$

This model is exactly solvable through mapping to a free fermionic Hamiltonian ("*fermionization*") [60, 72]. Hereafter, we will illustrate this procedure.

First of all, one defines a mapping to *hard-core bosons* in terms of the spin operators as

$$\begin{cases} \sigma_j^z = 1 - 2b_j^\dagger b_j \\ \sigma_j^+ = b_j^\dagger \\ \sigma_j^- = b_j \end{cases}. \tag{4.114}$$

These hard-core bosons satisfy the commutation relations at different sites, as ordinary bosonic operators do, but they anti-commute at the same site $\{b_j, b_j^\dagger\} = 1$. They verify the hard-core constraint of "no more than one boson in each site" $(b_j^\dagger)^2|0\rangle = 0$. The Hamiltonian, Eq. 4.112 now reads

$$H_B = -\frac{1}{2}\sum_{j=1}^{L}[b_j^\dagger b_{j+1}^\dagger + b_j b_{j+1} + \kappa(b_j^\dagger b_{j+1} + b_j b_{j+1}^\dagger)] - h\sum_{j=1}^{L}(1-2n_j), \tag{4.115}$$

where $n_j = b_j^\dagger b_j$. In this form, it is still not solvable and one needs to implement the Jordan-Wigner transformations. The latter ones relate these hard-core bosonic operators

to fermionic operators on the lattice in one-dimensional systems $b_j = K_j c_j$, where $K_j = e^{i\pi \sum_{j'=1}^{j-1} n_{j'}}$. Spin are mapped into fermions according to

$$\begin{cases} \sigma_j^z = 1 - 2c_j^\dagger c_j \\ \sigma_j^x = K_j(c_j^\dagger + c_j) \\ \sigma_j^y = iK_j(c_j^\dagger - c_j). \end{cases} \tag{4.116}$$

Assuming periodic boundary conditions and an even number of sites, one writes Eq. 4.112 as

$$H_B = -\sum_{j=1}^{L-1}(c_j^\dagger c_{j+1} + c_j^\dagger c_{j+1}^\dagger + h.c.) + h\sum_{j=1}^{L}(2c_j^\dagger c_j - 1). \tag{4.117}$$

Note that in most of the relevant terms in the Hamiltonian, the string operator K_j cancels out. The diagonalization procedure happens by mapping those fermionic operators in the momentum space. Introducing $c_k, c_k^\dagger$ such that $\{c_k, c_k^\dagger\} = 1$, their definition and the inverse transformation read

$$\begin{cases} c_k = \sum_{j=1}^{L} \frac{e^{-i\phi}}{\sqrt{L}} \sum_{j=1}^{L} e^{-ikj} c_j \\ c_j = \sum_{j=1}^{L} \frac{e^{i\phi}}{\sqrt{L}} \sum_k e^{ikj} c_k, \end{cases} \tag{4.118}$$

with an overall phase ϕ, not changing the overall commutation relations. The function of this variable is to highlight the freedom we have in choosing the second axis of the spin in the xy plane. With our choice of boundary conditions, the set of momenta is defined as

$$\Lambda = \left\{ k = +\frac{2n\pi}{L} \text{with n} = -\frac{L}{2} + 1, \ldots, \frac{L}{2} \right\} \tag{4.119}$$

Upon choosing $\phi = 0$, the Hamiltonian now reads

$$H_B = \sum_{k \in \Lambda} H_k, \tag{4.120}$$

where

$$H_k = 2(h - \cos k)(c_k^\dagger c_k - c_{-k} c_{-k}^\dagger) - 2i\kappa \sin k (c_k^\dagger c_{-k}^\dagger - c_{-k} c_k). \tag{4.121}$$

Notice this Hamiltonian commutes for different momenta $[H_k, H_{k'}]\ \forall k \neq k'$. To deal with these combinations of creation/annihilation operators at momentum k and $-k$, one can define a two-dimensional spinor, known as the *two-component Nambu fermionic operator* [60]

$$\vec{\Psi}_k = \begin{pmatrix} c_k \\ c_{-k}^\dagger \end{pmatrix}, \tag{4.122}$$

$$\vec{\Psi}_k^\dagger = \begin{pmatrix} c_k^\dagger & c_{-k} \end{pmatrix}, \tag{4.123}$$

obeying the anti-commutation relations

$$\{\Psi^\dagger_{k,\alpha}, \Psi_{k',\beta}\} = \delta_{kk'}\delta_{\alpha\beta}, \tag{4.124}$$

where the index $\alpha = 1, 2$ runs through the components of the spinor. Eq. 4.112 now reads

$$H_B = \sum_k H_k, \tag{4.125}$$

where

$$H_k = \sum_{\alpha,\alpha'} \Psi^\dagger_{k,\alpha}(\boldsymbol{H}_k)_{\alpha\alpha'}\Psi_{k,\alpha'}. \tag{4.126}$$

The matrix $\boldsymbol{H}_k$ can be represented as

$$\boldsymbol{H}_k = \begin{pmatrix} 2(h-\cos k) & -2i\kappa \sin k \\ 2i\kappa \sin k & -2(h-\cos k) \end{pmatrix}. \tag{4.127}$$

Equivalently, in terms of pseudo-Pauli matrices τ_j

$$\boldsymbol{H}_k = 2(-\kappa J \sin(2\phi)\sin(k)\tau_x + \kappa J \cos(2\phi)\sin(k)\tau_y + (h - J\cos(k))\tau_z). \tag{4.128}$$

This Hamiltonian is diagonalized by a Bogoliubov rotation, and one finds its spectrum of eigenvalues $\epsilon_{k\pm} = \pm|\epsilon_k|$, divided into the positive and negative spectrum (see Fig. (4.8)), with

$$|\epsilon_k| = 2\sqrt{(h-\cos(k))^2 + \kappa^2 \sin^2(k)} \geq 0. \tag{4.129}$$

The unitary matrix of eigenvectors can be expressed as a rotation of angle Θ_k

$$\boldsymbol{U}_k = e^{-i\Theta_k \sigma^y}. \tag{4.130}$$

One defines a new spinor of Bogoliubov fermions

$$\Gamma_k = \begin{pmatrix} \gamma_k \\ \gamma^\dagger_{-k} \end{pmatrix}. \tag{4.131}$$

It is related to the spinor Ψ_k from the relation

$$\Gamma_k = \boldsymbol{U}^\dagger_k \Psi_k. \tag{4.132}$$

In the new basis, the Hamiltonian is, of course, diagonal

$$\boldsymbol{U}_k \boldsymbol{H}_k \boldsymbol{U}^\dagger_k = \begin{pmatrix} \epsilon_k & 0 \\ 0 & -\epsilon_k \end{pmatrix} \tag{4.133}$$

and terms of the transformed eigenstates, now it reads

$$H_k = \sum_k \epsilon_k \Gamma^\dagger_k \sigma^z \Gamma_k = \sum_k \epsilon_k(\gamma^\dagger_k\gamma_k - \gamma^\dagger_{-k}\gamma_{-k} - 1). \tag{4.134}$$

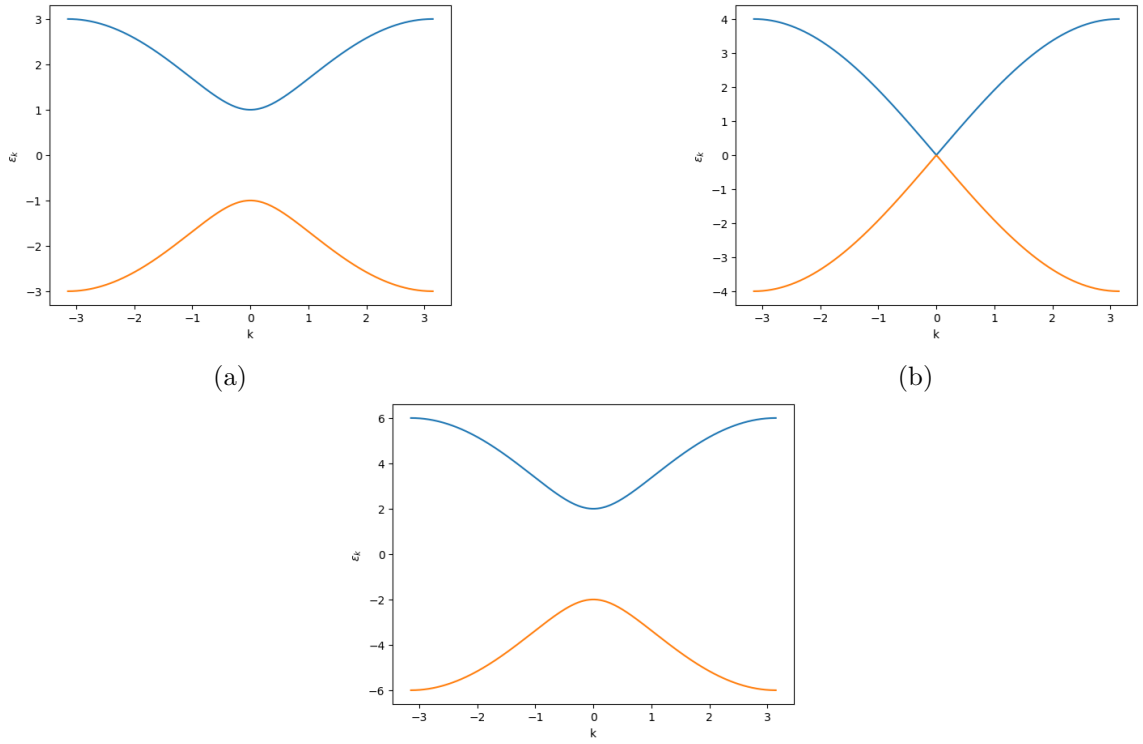

Figure 4.8: The spectrum of the Quantum Ising model at a) h=0.5 (in the ferromagnetic phase), b) h=1 in the critical point, c) h=2 (in the paramagnetic phase). One can see the gap between the two eigenvalue sectors closes at $h = 1$, in the correspondence of the critical point. Visually, there is no difference between the two gapped phases.

The angle of the Bogoliubov transformation is determined by enforcing condition 4.133

$$\tan(2\Theta_k) = \frac{\kappa \sin(k)}{h - \cos(k)}. \tag{4.135}$$

Now, let us arrive at the main object of interest for this analysis: the calculation of the qubit transition rates. From the general definition (Eq. 4.179), one substitutes A, with the observable of our choice, namely the total magnetization along the z-axis

$$\gamma_{\uparrow,\downarrow} = \frac{g_\sigma}{2} \sum_{j=1}^{L} \sum_{j'=1}^{L} \int_{-\infty}^{\infty} ds e^{\mp i\epsilon_0 s} Tr[\rho_{st} \sigma_z^j(s/2) \sigma_z^{j'}(-s/2)]. \tag{4.136}$$

In turn, we need to calculate the correlation function over time of this quantity. First of all, one must use the result for the stationary density matrix and insert a resolution of the

identity

$$\sum_{j=1}^{L}\sum_{j'=1}^{L} Tr[\rho_{st}\sigma_z^j(\tau/2)\sigma_z^{j'}(-\tau/2)] = \sum_{j=1}^{L}\sum_{j'=1}^{L}\sum_{k\alpha}\sum_{k'\beta} p_k^\alpha \langle k\alpha(h_f)|\sigma_j^z(\tau/2)|k'\beta(h_f)\rangle \langle k'\beta(h_f)|\sigma_{j'}^z(-\tau/2)|k\alpha(h_f)\rangle, \tag{4.137}$$

where the state $|k\alpha\rangle = \vec{\Gamma}_{k,\alpha}^\dagger|0\rangle$. Here the total magnetization must be expressed in the basis of $\vec{\Gamma}_{k,(h_f)}$. After a brief calculation, we find the following expression

$$\sum_{j=1}^{L}\sigma_j^z = 2\sum_k \vec{\Psi}_k^\dagger \tau_z \vec{\Psi}, \tag{4.138}$$

where τ_z is the z pseudo-Pauli matrix, by fermionizing the total magnetization and converting it to momentum space. Then, we perform the Bogoliubov rotation

$$\boldsymbol{U}_k \sigma^z \boldsymbol{U}_k^\dagger = 2[\cos(2\Theta_{k,f})\sigma_z + \sin(2\Theta_{k,f})\sigma_x], \tag{4.139}$$

where the Bogoliubov angle respects the definition 4.135 in terms of the final h_f.
Another ingredient of this expression is the overlap between the initial and final states, viz. $p_k^\alpha = |\langle k\alpha(h_f)|\psi_0\rangle|^2$. We take the ground state of the initial Hamiltonian as the initial state. That is to say, the latter is

$$|\psi_0\rangle = \begin{pmatrix}0\\1\end{pmatrix}_{k,(h_i)}, \tag{4.140}$$

such that $\langle\gamma_{k,(h_i)}^\dagger\gamma_{k,(h_i)}\rangle = 0$ and $\langle\gamma_{-k,(h_i)}^\dagger\gamma_{-k,(h_i)}\rangle = 1\ \forall k$. However, the initial state is expressed in the basis of the Bogoliubov spinor of the initial parameters of the quench. In contrast, the state $|ki\rangle$ is expressed in the basis of the final parameters. One must establish the relation between the two bases to solve this conundrum.
We recall the relations

$$\vec{\Gamma}_{k,(h_f)} = \boldsymbol{U}_{k,(h_f)}^\dagger \vec{\Psi}_k \tag{4.141}$$

$$\vec{\Gamma}_{k,(h_i)} = \boldsymbol{U}_{k,(h_i)}^\dagger \vec{\Psi}_k \tag{4.142}$$

Then, in turn

$$\vec{\Gamma}_{k,(h_f)} = \boldsymbol{U}_{k,(h_f)}^\dagger \boldsymbol{U}_{k,(h_i)} \vec{\Psi}_k. \tag{4.143}$$

Conveniently, one can define a new *non-equilibrium Bogoliubov transform* via the subsequent relation

$$\vec{\Gamma}_{k,(h_f)} = \boldsymbol{U}_{k,\Delta}^\dagger \vec{\Gamma}_{k,(h_i)}, \tag{4.144}$$

where

$$\boldsymbol{U}_{k,\Delta}^\dagger = \boldsymbol{U}_{k,(h_f)}^\dagger \boldsymbol{U}_{k,(h_i)} = e^{i\Delta\Theta_k\sigma^y}, \tag{4.145}$$

$\Delta\Theta_k = \Theta_{k,(h_f)} - \Theta_{k,(h_i)}$ is the difference between the Bogoliubov angles. In terms of the latter, one can write the overlaps as

$$p_k^+ = \sin^2(\Delta\Theta_k) \tag{4.146}$$

and

$$p_k^- = \cos^2(\Delta\Theta_k) \tag{4.147}$$

Finally, one can express the time dependence of the operator $\sigma^z(s) = e^{-iH_B^f s}\sigma_z e^{iH_B^f s}$, substitute relations 4.146,4.147 and 4.139 into the correlator (Eq. 4.137), which now reads

$$\frac{4}{L}\sum_k \left[\cos^2(2\Theta_k) + \sin^2(2\Theta_k)(\sin^2(\Delta\Theta_k)e^{-2i|\epsilon_k|\tau} + \cos^2(\Delta\Theta_k)e^{+2i|\epsilon_k|\tau})\right]. \tag{4.148}$$

If one takes the continuum limit, the resulting expression is

$$\frac{2}{\pi}\int_{-\frac{\pi}{2}}^{\frac{\pi}{2}} dk\left[\cos^2(2\Theta_k) + \sin^2(2\Theta_k)(\sin^2(\Delta\Theta_k)e^{-2i|\epsilon_k|\tau} + \cos^2(\Delta\Theta_k)e^{+2i|\epsilon_k|\tau})\right]. \tag{4.149}$$

Let's now take into account each of these terms. Plugging the latter expression into the definition of the transition rates, it is clear that the first term gives a vanishing contribution, as would generate a term proportional to $\delta(\epsilon_0)$ and ϵ_0 is positive. The second term gives the contribution

$$\frac{g_\sigma}{\pi}\int_{-\infty}^{\infty} d\tau \int_{-\frac{\pi}{2}}^{\frac{\pi}{2}} dk \sin^2(2\Theta_k(h_f))\sin^2(\Delta\Theta_k)e^{-2i|\epsilon_k|\tau \mp i\epsilon_0\tau} \tag{4.150}$$

$$= \frac{g_\sigma}{\pi}\int_{-\pi/2}^{\pi/2} dk\delta(2|\epsilon_k| \pm \epsilon_0)\sin^2(2\Theta_k(h_f))\sin^2(\Delta\Theta_k), \tag{4.151}$$

while the third

$$\frac{g_\sigma}{\pi}\int_{-\infty}^{\infty} d\tau \int_{-\frac{\pi}{2}}^{\frac{\pi}{2}} dk \sin^2(2\Theta_k(h_f))\cos^2(\Delta\Theta_k)e^{2i|\epsilon_k|\tau \mp i\epsilon_0\tau} \tag{4.152}$$

$$= \frac{g_\sigma}{\pi}\int_{-\pi/2}^{\pi/2} dk\delta(-2|\epsilon_k| \mp \epsilon_0)\sin^2(2\Theta_k(h_f))\cos^2(\Delta\Theta_k). \tag{4.153}$$

The existence of a solution in the argument of the delta function implies that Eq. (4.150) contributes only to $\gamma_\uparrow$, while Eq. (4.152) to $\gamma_\downarrow$. This leads us to this expression for the transition rates

$$\gamma_\uparrow = \frac{g_\sigma^2}{2\pi}\int_{-\pi/2}^{\pi/2} dk\delta(2|\epsilon_k| - \epsilon_0)\sin^2(2\Theta_k(h_f))\sin^2(\Delta\Theta_k) \tag{4.154}$$

and

$$\gamma_\downarrow = \frac{g_\sigma^2}{2\pi}\int_{-\pi/2}^{\pi/2} dk\delta(2|\epsilon_k| - \epsilon_0)\sin^2(2\Theta_k(h_f))\cos^2(\Delta\Theta_k), \tag{4.155}$$

The zero of the delta function's argument satisfies $\epsilon_k = \frac{\epsilon_0}{2}$, which implies

$$(h_f - \cos k)^2 + \kappa^2 \sin^2(k) = \epsilon_0^2/16. \tag{4.156}$$

This equation admits two solutions $k_\pm = \arccos u_\pm$, i.e.

$$u_\pm = \frac{h_f \pm \sqrt{\kappa^2 h_f^2 - (1-\kappa^2)(\kappa^2 - \epsilon_0^2/16)}}{1-\kappa^2} \tag{4.157}$$

The solutions in Eq. 4.157 require the argument of the square root to be positive. The latter condition can be rewritten as

$$\epsilon_0^2 \geq \kappa^2 - \frac{\kappa^2}{1-\kappa^2}h_f^2 \tag{4.158}$$

If one assumes to be in the paramagnetic phase $h_f > 1$ and only the k_- solution exists, the condition is always verified. The other conditions that must be verified are $0 \leq u_\pm \leq 1$. The two conditions translate into

$$\epsilon_0^2/16 \geq (h_f - 1)^2 \tag{4.159}$$

and

$$\epsilon_0^2/16 \leq h_f^2 + \kappa^2. \tag{4.160}$$

From the physical point of view, these two conditions imply that the energy level must be between the energy gap between the two sectors and the max excursion between the lowest and the highest energy levels, corresponding respectively to $2\epsilon_{k=0}$ and $2\epsilon_{k=\pm\frac{\pi}{2}}$.

Most importantly, let's analyze the bias condition for the clock $\gamma_\uparrow > \gamma_\downarrow$. By comparing the two expressions Eq. 4.184 and 4.185, one can see they translate into

$$\cos(2\Delta\Theta_k)|_{k=k^-} < 0 \tag{4.161}$$

in terms of the difference between the Bogoliubov angles. This difference can be rewritten using standard trigonometric relations

$$\cos(2\Delta\Theta_k) = \cos(2\Theta_k(h_f))\cos(2\Theta_k(h_i)) + \sin(2\Theta_k(h_f))\sin(2\Theta_k(h_i)). \tag{4.162}$$

From the conditions defining the Bogoliubov rotation, one infers the relations $\cos(2\Theta_k) = \frac{h-\cos k}{\epsilon_k}$ and $\sin(2\Theta_k) = \frac{\kappa\cos k}{\epsilon_k}$. The resulting expression of Eq. 4.161 is

$$\frac{(h_f - \cos k)(h_i - \cos k) + \kappa^2\cos^2 k}{\epsilon_{k,(h_f)}\epsilon k,(h_i)}. \tag{4.163}$$

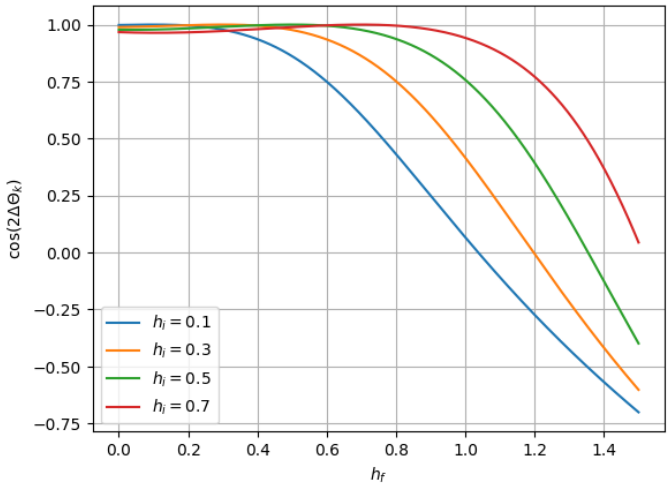

Figure 4.9: The l.h.s. of Eq. 4.109 is plotted for different values of h_i in the paramagnetic phase. The quantity is negative only for h_f in the ferromagnetic phase. The existence of the solution is examined in Fig. (4.10)

One can see that the only relevant solution for quenches from the ferromagnetic to the paramagnetic phase is u_-. By substituting it into the latter equation we arrive at

$$8\frac{(h_f-u_-)(h_i-u_-)+\kappa^2(1-u_-^2)}{\epsilon_0\sqrt{\epsilon_0^2/4-4(h_f-u_-)^2+4(h_i-u_-)^2}}<0 \tag{4.164}$$

Since $0<u_-<1$ Eq. 4.164 implies that if $h_i<1$, then $h_f>1$, indicating that the quench protocol must cross the phase transition point (this is confirmed by Fig. (4.9)), in a striking similarity with the charging protocol of [42]

4.8.2 The XX spin chain

Now, let's consider a further example of an integrable model. We choose a system of tight-binding hard-core bosons hopping on a ring lattice with L sites with a staggered on-site potential. Its Hamiltonian is given by

$$H_B(\phi)=t\sum_{j=1}^{L}(e^{i\phi}b_j^\dagger b_{j+1}+h.c.)+V\sum_{j=1}^{L}(-1)^j n_j, \tag{4.165}$$

in terms of hard-core bosonic operators $b_j^\dagger/b_j$ and upon defining the number operator $n_j=b_j^\dagger b_j$. The field ϕ represents an external magnetic field, which we can set to zero for

simplicity, from now on.
The Hamiltonian of the qubit-battery interaction is chosen as

$$H_{QB} = g_J(\sigma_Q^x J_{\phi=0}), \tag{4.166}$$

where g_J is the coupling strength and the current in the ring $J_{\phi=0}$ is defined as

$$J_{\phi=0} = -\partial_\phi H|_{\phi=0} \tag{4.167}$$

and has the following expression

$$J_{\phi=0} = -it\sum_{j=1}^{L}(b_j^\dagger b_{j+1} - h.c.). \tag{4.168}$$

This Hamiltonian (Eq. 4.165) is integrable. Using the mapping of Eq. 4.114 it results in

$$H_B = t\sum_{j=1}^{L}(\sigma_j^x\sigma_{j+1}^x + \sigma_j^y\sigma_{j+1}^y) - \frac{V}{2}\sum_{j=1}^{L}(-1)^j\sigma_j^z, \tag{4.169}$$

which in the literature is known as the XX model with the addition of an external staggered magnetic field. We can employ the same Jordan-Wigner transformation of the past Section (Eq. 4.116), resulting in

$$H_B = t\sum_{j=1}^{L}(c_j^\dagger c_{j+1} + h.c.) + V\sum_{j=1}^{L}c_j^\dagger c_j. \tag{4.170}$$

In the momentum space (Eq. 4.118) we have

$$H_B = \sum_{k\in\Lambda}(2t\cos k c_k^\dagger c_k + V c_k^\dagger c_k) \tag{4.171}$$

Represented in the compact form

$$H_B = \sum_{k\in\Lambda}\vec{\Psi}_k^\dagger H_K \vec{\Psi}_k, \tag{4.172}$$

where

$$\vec{\Psi}_k = \begin{pmatrix} c_k \\ c_{-k} \end{pmatrix} \tag{4.173}$$

and

$$H_k = 2t\cos k\tau^z + V\tau^x, \tag{4.174}$$

in terms of the spin 1/2 pseudo-Pauli matrices τ^α ($\alpha = x, y, z$). The diagonalization through Bogoliubov transformations is defined with the angle

$$\tan[2\Theta_k] = \frac{V}{2t\cos k} \tag{4.175}$$

and results in the expression

$$H_B = \sum_k \epsilon_k \vec{\Gamma}_k^\dagger \tau^z \vec{\Gamma}_k, \tag{4.176}$$

with the spinor

$$\vec{\Gamma}_k = \begin{pmatrix} \gamma_k \\ \gamma_{-k} \end{pmatrix} \tag{4.177}$$

and

$$\epsilon_k = \sqrt{4t^2\cos^2 k + V^2} \tag{4.178}$$

is the associated energy spectrum (Fig. (4.11)) The phase diagram of this model is the

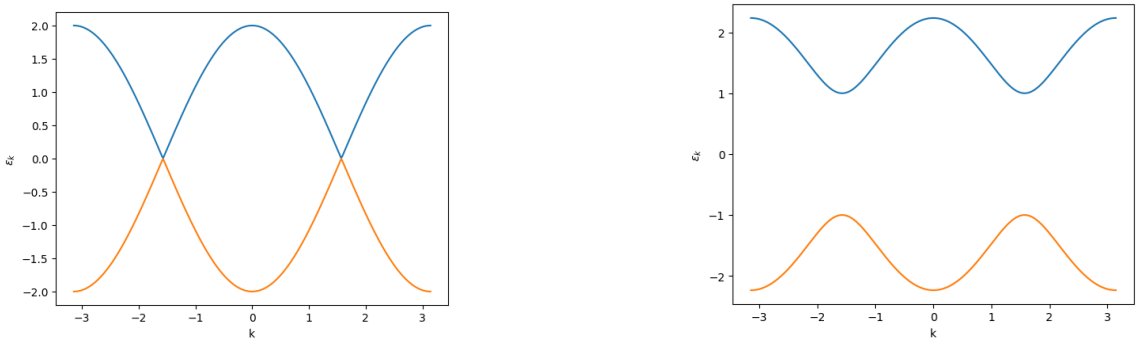

(a) (b)

Figure 4.10: The spectrum of the XX model with a staggered on-site potential. We set $t = 1$ for simplicity. In a) we have the gapless spectrum at $V = 0$, while in b) we have the spectrum in the gapped insulating phase at $V = 1$.

following: in the critical point $V = 0$ we have a gapless superfluid phase, while for $V \neq 0$ the spectrum is gapped and the model has an associated insulating behaviour.

Now, let us calculate the rate of the dissipative process associated with the qubit's dynamics, namely $\gamma_{\uparrow,\downarrow}$. We write these rates in the following form [12]

$$\gamma_{\uparrow,\downarrow} = \frac{1}{4}\int_{-\infty}^{\infty} ds e^{\mp i\epsilon_0 s} Tr[\rho_{st} J_{\phi=0}(s/2) J_{\phi=0}(-s/2)], \tag{4.179}$$

As before, we need to work out the expression of the current in the ring at $\phi = 0$ in terms of Bogoliubov fermions. We write Eq. 4.168 as

$$J_{\phi=0} = -it \sum_{j=1}^{L} \left(c_j^\dagger c_{j+1} - c_{j+1}^\dagger . c_j \right) \tag{4.180}$$

In momentum space, it admits the following representation

$$J_{\phi=0} = -2t \sum_k \sin(k) c_k^\dagger c_k, \tag{4.181}$$

or, more compactly,

$$J_{\phi=0} = \vec{\Psi}_k^\dagger J_k \vec{\Psi}_k, \tag{4.182}$$

where

$$J_k = -2t \sum_k \sin k \tau^z. \tag{4.183}$$

As in the previous Section (Sec. 4.8.1), the result is proportional to τ^z. Therefore, the subsequent passages are exactly the same as in the Ising chain, apart from the prefactor.

Let us jump then to the final results

$$\gamma_\uparrow = \frac{g_J^2}{2\pi} \int_{-\pi/2}^{\pi/2} dk \delta(2|\epsilon_k| - \epsilon_0) \sin^2(2\Theta_k(V_f)) \sin^2(\Delta\Theta_k) \tag{4.184}$$

and

$$\gamma_\downarrow = \frac{g_J^2}{2\pi} \int_{-\pi/2}^{\pi/2} dk \delta(2|\epsilon_k| + \epsilon_0) \sin^2(2\Theta_k(V_f)) \cos^2(\Delta\Theta_k). \tag{4.185}$$

The zero solution of the argument of the delta function is the following

$$k^* = \arccos \sqrt{\frac{\epsilon_0^2/4 - V_f^2}{4t^2}}. \tag{4.186}$$

To guarantee the existence of a solution to the previous relation, one must require that

$$0 < \frac{\epsilon_0^2/4 - V_f^2}{4t^2} < 1 \tag{4.187}$$

This relation can be interpreted physically as requiring that ϵ_0 lies in the range between the gap between the two sectors of the eigenvalues and the distance between the lowest and the highest eigenstates in energy.
From the expression of the rates we have an additional condition, namely

$$\epsilon_0^2/4 - V_f^2 + V_i^2 > 0, \tag{4.188}$$

which is always verified given the validity of Eq. 4.187.
Again, the operating condition of the clock reads

$$\cos(2\Delta\Theta_k)|_{k^*} < 0. \tag{4.189}$$

Substituting the relations $\sin(2\Theta_k) = \frac{V}{\epsilon_k}$ and $\cos(2\Theta_k) = \frac{2t\cos k}{\epsilon_k}$, one obtains

$$\frac{(2t\cos k)^2 + V_i V_f}{\epsilon_k(V_f)\epsilon_k(V_i)}. \tag{4.190}$$

When using the resonance condition (Eq. 4.186), we can see the relation 4.189 implies

$$\epsilon_0^2/4 - V_f^2 + V_i V_f < 0. \tag{4.191}$$

The latter leaves as a consequence that $V_i V_f < 0$. Then, the take-home message of this analysis is that the required quench must cross the critical point $V = 0$, which characterizes the transition from the superfluid to the insulating phase and the opening of the gap between the two energy sectors.

4.9 The battery's lifespan

In this Section, we try to answer the following question: how much time does the quantum battery last? The answer to this question is relatively simple, here we try to give a rough estimate. The main piece of information we are interested is how this quantity scales with the battery's size. Let us start by observing that the total number of ticks over the battery lifespan is given by the energy available in the battery divided by the energy of the photon emitted $E_{ph} = (d-1)\epsilon_0$

$$N_p = \frac{E_{av}}{E_{ph}}. \tag{4.192}$$

Therefore the total time is

$$T^* = \frac{E_{av}\tau}{E_{ph}} \tag{4.193}$$

The energy available in the battery can be estimated from the amount of energy available at the right frequency of the

$$E_{av} = \sum_k 2\epsilon_k \delta(2\epsilon_k - \epsilon_0)\cos^2(\Delta\Theta_k) \tag{4.194}$$

In the continuum limit, this quantity reads

$$E_{av} = \frac{L}{2\pi}\int dk 2\epsilon_k \delta(2\epsilon_k - \epsilon_0)\cos^2(\Delta\Theta_k) \tag{4.195}$$

Upon defining the density of states as $\rho(\epsilon) = \int dk \delta(k - \epsilon)$ and appropriately regularizing this expression, we have

$$E_{av} = \frac{L}{2\pi} \epsilon_0 \rho(\epsilon_0/2) \cos^2(\Delta\Theta_k)|_{k=k*}, \tag{4.196}$$

leading to the result

$$T^* = -\frac{\gamma_+}{\bar{\chi}''(\epsilon_0)} \frac{L}{2\pi} \rho(\epsilon_0/2) \cos^2(\Delta\Theta_k) \Big|_{k=k^*}, \tag{4.197}$$

where $\rho(\epsilon) = \left| \frac{\partial \epsilon_k}{\partial k} \right|^{-1}$ is the constant density of states of the spin chain. The main take-home message of this expression is the extensivity of the total lifespan, even if one considers coupling through a global observable, like in the cases presented in the examples. If the coupling occurs through a local observable, more transitions could be accessible and we expect the result to be super-extensive. Note that the average energy dissipation rate is related to the imaginary part of the response function $-\bar{\chi}''(\epsilon_0)$ [80] and the total lifespan is inversely proportional to this quantity. Finally, we should stress that this is only a rough estimate, as the condition of the rate of energy extraction being constant is not guaranteed in the initial and final transient of the battery's operation.

Chapter 5

Conclusions and Outlook

"Explicit expliceat. Bibere scriptor eat"-"It is finished. Let it be finished, and let the writer go out for a drink"

— An anonymous monk

In the first part of this Thesis, we introduced and examined two different, but related, transport problems in the context of quantum dots interacting with multiple baths. In both cases, the key challenge was to develop a complete and consistent thermodynamic picture, starting from the resonant level model and using diagrammatic techniques. This analysis transcends the standard weak coupling approximation, accounting for the hybridization between the dot and the leads. The dot is an externally driven system, in which both its level and the coupling with the leads are time-dependent and controlled via external gate voltage. In this context, it is not viable to find exact analytical solutions, and one must resort to approximate solutions. In particular, we used the tool of adiabatic expansion to evaluate finite-time correction to the adiabatic limit. This setup allowed us to build connections with the transport properties. We studied all this in the context of single-level non-interacting quantum dots. However, the methods developed here could in principle be generalized to other time-dependent transport problems, such as transport through multilevel dots or even interacting systems [33, 83].

First of all, we introduced charge pumping in non-interacting quantum dots. By completing periodic processes in the manifold of time-dependent parameters, one is able to achieve a finite charge transport, even in the absence of any bias between the leads. We examined the subsystem of processes in which a set of limiting conditions is defined, allowing for a quantized transport to be achieved. Focusing on specific cycles and comparing transport to thermodynamic quantities we have shown that whenever a quantized charge is attained one expects, together with zero charge noise, zero entropy and a saturated work per cycle proportional to the speed with which the quantity associated with the quantization limit is varied. The results obtained are relative to this specific model but nonetheless

offer insight into the phenomenon of adiabatic pumping and its thermodynamical implications, which can be relevant in other contexts (for example Thouless pumps).

In Chapter 3, we presented the quantum shuttle, a similar problem, in which a spatial degree of freedom is present and the time-dependent quantities depend parametrically through the dot's position. The problem has been addressed from a wide variety of perspectives. First, a complete characterization of the dynamical properties of this model has been attained. Taking into account the quantum noise, which affects the dynamics of the system in a semi-classical picture, this has allowed us to calculate the precision and accuracy and to draw its relations with the entropy production, which is the most relevant quantity for our purposes, and other information-theoretical quantities. The results of this comparison highlight a direct proportionality, but not a linear relation, between accuracy and entropy production, as indicated in the previous literature. The findings of Section 3.6 differ from the previous literature on this subject, as in the present we study a different regime of validity. The relevance of the adiabatic approximation is discussed in Appendix G, where it is found to be more appropriate for smaller values of the radius. In contrast, the semiclassical treatment of Ref. [36] requires large limit cycles and weak coupling.
The methods and the results developed here are significant as they illustrate a rich and non-trivial behaviour in the thermodynamic significance of the clock's performance, while the presence of a trade-off relation between accuracy and entropy production is confirmed.

In Part II, we introduced a novel setup of a quantum clock connected to a quantum battery. The battery, an integrable many-body system, is driven out of equilibrium by a quench in one of its parameters. After the relaxation process, it reaches a non-thermal stationary state, from which it is possible to extract energy under determinate conditions. We used this fact to couple this system to a quantum clock relying on a discrete Hilbert space, inspired by previous examples in the literature. The accuracy/entropy production relation in this framework is investigated and coincides with known results about Brownian clocks. Our main concern has been to examine all the conditions in the parameter manifold guaranteeing the clock's operation. This allowed us to establish a direct relation between the negative of the imaginary part of the response function of the associated coupling observable and bias condition in the ladder's dynamics. By examining relevant examples, we found these conditions constrain the quench to take place crossing the critical point of the integrable system. However, it remains unclear whether this is a universal condition in terms of the model and the choice of a particular class of observables, such as the order parameter. Moreover, the impact of the choice of local observables on this analysis and in particular on the battery's lifespan has to be examined.

Bibliography

[1] Matteo Acciai et al. "Constraints between entropy production and its fluctuations in nonthermal engines". In: *Phys. Rev. B* 109 (7 Feb. 2024), p. 075405. DOI: 10.1103/PhysRevB.109.075405. URL: https://link.aps.org/doi/10.1103/PhysRevB.109.075405.

[2] Alexander Aeppli et al. "Clock with 8×10^{-19} Systematic Uncertainty". In: *Phys. Rev. Lett.* 133 (2 July 2024), p. 023401. DOI: 10.1103/PhysRevLett.133.023401. URL: https://link.aps.org/doi/10.1103/PhysRevLett.133.023401.

[3] Kushagra Agarwal, Himanshu Rai, and Sandip Mondal. "Quantum dots: an overview of synthesis, properties, and applications". In: *Materials Research Express* 10.6 (June 2023), p. 062001. DOI: 10.1088/2053-1591/acda17. URL: https://dx.doi.org/10.1088/2053-1591/acda17.

[4] Robert Alicki and Mark Fannes. "Entanglement boost for extractable work from ensembles of quantum batteries". In: *Phys. Rev. E* 87 (4 Apr. 2013), p. 042123. DOI: 10.1103/PhysRevE.87.042123. URL: https://link.aps.org/doi/10.1103/PhysRevE.87.042123.

[5] A. E. Allahverdyan, R. Balian, and Th. M. Nieuwenhuizen. "Maximal work extraction from finite quantum systems". In: *Europhysics Letters* 67.4 (Aug. 2004), p. 565. DOI: 10.1209/epl/i2004-10101-2. URL: https://dx.doi.org/10.1209/epl/i2004-10101-2.

[6] D.W. Allan. "Statistics of atomic frequency standards". In: *Proceedings of the IEEE* 54.2 (1966), pp. 221–230. DOI: 10.1109/PROC.1966.4634.

[7] A. Andreev and A. Kamenev. "*Counting Statistics of an Adiabatic Pump*". In: *Phys. Rev. Lett.* 85 (2000), p. 1294. DOI: 10.1103/PhysRevLett.85.1294.

[8] Andre C. Barato and Udo Seifert. "Cost and Precision of Brownian Clocks". In: *Phys. Rev. X* 6 (4 Dec. 2016), p. 041053. DOI: 10.1103/PhysRevX.6.041053. URL: https://link.aps.org/doi/10.1103/PhysRevX.6.041053.

[9] Felipe Barra, Karen V Hovhannisyan, and Alberto Imparato. "Quantum batteries at the verge of a phase transition". In: *New Journal of Physics* 24.1 (Jan. 2022), p. 015003. DOI: 10.1088/1367-2630/ac43ed. URL: https://dx.doi.org/10.1088/1367-2630/ac43ed.

[10] Ya.M. Blanter and M. Büttiker. "Shot noise in mesoscopic conductors". In: *Physics Reports* 336.1 (2000), pp. 1–166. ISSN: 0370-1573. DOI: https://doi.org/10.1016/S0370-1573(99)00123-4. URL: https://www.sciencedirect.com/science/article/pii/S0370157399001234.

[11] D. Bluvstein et al. "Controlling quantum many-body dynamics in driven Rydberg atom arrays". In: *Science* 371.6536 (2021), pp. 1355–1359. DOI: 10.1126/science.abg2530. eprint: https://www.science.org/doi/pdf/10.1126/science.abg2530. URL: https://www.science.org/doi/abs/10.1126/science.abg2530.

[12] H.P. Breuer and F. Petruccione. *The Theory of Open Quantum Systems*. Oxford University Press, 2002. ISBN: 9780198520634.

[13] A. Bruch et al. "*Quantum Thermodynamics of the driven resonant model*". In: *Phys. Rev. B* 93 (2016), p. 115318. DOI: 10.1103/PhysRevB.93.115318.

[14] Anton Bruch et al. "Quantum thermodynamics of the driven resonant level model". In: *Phys. Rev. B* 93 (11 Mar. 2016), p. 115318. DOI: 10.1103/PhysRevB.93.115318. URL: https://link.aps.org/doi/10.1103/PhysRevB.93.115318.

[15] Nicolas Brunner et al. "Virtual qubits, virtual temperatures, and the foundations of thermodynamics". In: *Phys. Rev. E* 85 (5 May 2012), p. 051117. DOI: 10.1103/PhysRevE.85.051117. URL: https://link.aps.org/doi/10.1103/PhysRevE.85.051117.

[16] Nicolas Brunner et al. "Virtual qubits, virtual temperatures, and the foundations of thermodynamics". In: *Phys. Rev. E* 85 (5 May 2012), p. 051117. DOI: 10.1103/PhysRevE.85.051117. URL: https://link.aps.org/doi/10.1103/PhysRevE.85.051117.

[17] Pasquale Calabrese, Fabian H L Essler, and Maurizio Fagotti. "Quantum quenches in the transverse field Ising chain: II. Stationary state properties". In: *Journal of Statistical Mechanics: Theory and Experiment* 2012.07 (July 2012), P07022. DOI: 10.1088/1742-5468/2012/07/P07022. URL: https://dx.doi.org/10.1088/1742-5468/2012/07/P07022.

[18] Herbert B. Callen. *Thermodynamics and an Introduction to Thermostatistics*. 2nd. Wiley, 1991. ISBN: 978-0471862567.

[19] Francesco Campaioli, Felix A Pollock, and Sai Vinjanampathy. "Quantum batteries". In: *Thermodynamics in the Quantum Regime: Fundamental Aspects and New Directions* (2018), pp. 207–225.

[20] A.G. Catalano et al. "Frustrating Quantum Batteries". In: *PRX Quantum* 5 (3 July 2024), p. 030319. DOI: 10.1103/PRXQuantum.5.030319. URL: https://link.aps.org/doi/10.1103/PRXQuantum.5.030319.

[21] Roberta Citro and Monika Aidelsburger. "Thouless pumping and topology". In: *Nature Reviews Physics* 5.2 (2023), pp. 87–101. ISSN: 2522-5820. DOI: 10.1038/s42254-022-00545-0. URL: https://doi.org/10.1038/s42254-022-00545-0.

[22] Oisin Patrick Culhane et al. "Powering an autonomous clock with quantum electromechanics". In: *New Journal of Physics* (2023).

[23] D.Thouless. "*Quantization of Particle Transport*". In: *Phys. Rev. B* 27 (1983), p. 6083. DOI: 10.1103/PhysRevB.27.6083.

[24] Fernanda Deus, Alexis R Hernández, and Mucio A Continentino. "Adiabatic charge and spin pumping through interacting quantum dots". In: *Journal of Physics: Condensed Matter* 24.35 (Aug. 2012), p. 356001. DOI: 10.1088/0953-8984/24/35/356001. URL: https://dx.doi.org/10.1088/0953-8984/24/35/356001.

[25] Paul Erker et al. "Autonomous Quantum Clocks: Does Thermodynamics Limit Our Ability to Measure Time?" In: *Phys. Rev. X* 7 (3 Aug. 2017), p. 031022. DOI: 10.1103/PhysRevX.7.031022. URL: https://link.aps.org/doi/10.1103/PhysRevX.7.031022.

[26] M. Esposito et al. "*Quantum Thermodynamics: A Nonequilibrium Green's Function Approach*". In: *Phys. Rev. Lett.* 114 (2015), p. 080602. DOI: 10.1103/PhysRevLett.114.080602.

[27] Massimiliano Esposito, Maicol A. Ochoa, and Michael Galperin. "Nature of heat in strongly coupled open quantum systems". In: *Phys. Rev. B* 92 (23 Dec. 2015), p. 235440. DOI: 10.1103/PhysRevB.92.235440. URL: https://link.aps.org/doi/10.1103/PhysRevB.92.235440.

[28] K Kim et.al. "Quantum simulation of the transverse Ising model with trapped ions". In: *New Journal of Physics* 13.10 (Oct. 2011), p. 105003. DOI: 10.1088/1367-2630/13/10/105003. URL: https://dx.doi.org/10.1088/1367-2630/13/10/105003.

[29] D. Fedorets. "Quantum description of shuttle instability in a nanoelectromechanical single-electron transistor". In: *Phys. Rev. B* 68 (3 July 2003), p. 033106. DOI: 10.1103/PhysRevB.68.033106. URL: https://link.aps.org/doi/10.1103/PhysRevB.68.033106.

[30] D. Fedorets et al. "Quantum Shuttle Phenomena in a Nanoelectromechanical Single-Electron Transistor". In: *Phys. Rev. Lett.* 92 (16 Apr. 2004), p. 166801. DOI: 10.1103/PhysRevLett.92.166801. URL: https://link.aps.org/doi/10.1103/PhysRevLett.92.166801.

[31] D. Fedorets et al. "Spintronics of a Nanoelectromechanical Shuttle". In: *Phys. Rev. Lett.* 95 (5 July 2005), p. 057203. DOI: 10.1103/PhysRevLett.95.057203. URL: https://link.aps.org/doi/10.1103/PhysRevLett.95.057203.

[32] D. Fedorets et al. "Vibrational instability due to coherent tunneling of electrons". In: *Europhysics Letters* 58.1 (Apr. 2002), p. 99. DOI: 10.1209/epl/i2002-00611-3. URL: https://dx.doi.org/10.1209/epl/i2002-00611-3.

[33] Davide Fioretto and Alessandro Silva. "Phase Coherence, Inelastic Scattering, and Interaction Corrections in Pumping Through Quantum Dots". In: *Phys. Rev. Lett.* 100 (23 June 2008), p. 236803. DOI: 10.1103/PhysRevLett.100.236803. URL: https://link.aps.org/doi/10.1103/PhysRevLett.100.236803.

[34] Laura Foini, Leticia F. Cugliandolo, and Andrea Gambassi. "Fluctuation-dissipation relations and critical quenches in the transverse field Ising chain". In: *Phys. Rev. B* 84 (21 Dec. 2011), p. 212404. DOI: 10.1103/PhysRevB.84.212404. URL: https://link.aps.org/doi/10.1103/PhysRevB.84.212404.

[35] Ken Funo et al. "Shortcuts to Adiabatic Pumping in Classical Stochastic Systems". In: *Phys. Rev. Lett.* 124 (15 Apr. 2020), p. 150603. DOI: 10.1103/PhysRevLett.124.150603. URL: https://link.aps.org/doi/10.1103/PhysRevLett.124.150603.

[36] G.J.Milburn. "The thermodynamics of clocks". In: *Contemporary Physics* 61 (2 2020), pp. 69–95.

[37] G.Landi and M.Paternostro. "*Irreversible entropy production, from quantum to classical*". In: *Rev. Mod. Phys.* 93 (2021), p. 035008. DOI: 10.1103/RevModPhys.93.035008.

[38] G.Stefanucci and R. Van Leeuwen. *Nonequilibrium Many-Body Theory of Quantum Systems*. Cambridge University Press, 2013. ISBN: 978-0-521-76617-3.

[39] Crispin Gardiner. Springer, 2009. ISBN: 978-3540707127.

[40] J. Gemmer, M. Michel, and G. Mahler. *Quantum Thermodynamics, Emergence of Thermodynamic Behavior Within Composite Quantum Systems*. Vol. 657. Springer Lecture Notes in Physics, 2004. ISBN: 978-3-540-44513-5. DOI: https://doi.org/10.1007/b98082.

[41] J. Goold et al. "*The role of quantum information in thermodynamics—a topical review*". In: *J. Phys. A: Math. Theor.* 49 (2016), p. 143001. DOI: 10.1088/1751-8113/49/14/143001.

[42] Riccardo Grazi et al. "Enhancing energy storage crossing quantum phase transitions in an integrable spin quantum battery". In: *arXiv preprint arXiv:2402.09169* (2024).

[43] S. de Groot and P.Mazur. Non-Equilibrium Thermodynamics. Dover Publications Inc. New York, 1984. ISBN: 978-94-007-5460-7.

[44] M. Hasegawa and T. Kato. "*Nonadiabatic Correction and Adiabatic Criteria of Noninteracting Quantum Dot Systems*". In: *J. Phys. Soc. Jpn.* 91 (2022), p. 074705. DOI: https://doi.org/10.7566/JPSJ.91.074705.

[45] M. Hasegawa and other. "*Adiabatic almost-topological pumping of fractional charges in noninteracting quantum dots*". In: *Phys. Rev. B* 100 (2019), p. 125420. DOI: 10.1103/PhysRevB.100.125420.

[46] H. Haug and A. P. Jauho. *Quantum Kinetics in Transport and Optics of Semiconductors*. Springer, 2007. ISBN: 9783540735618. DOI: https://doi.org/10.1007/978-3-540-73564-9.

[47] Rebecca L. Honeycutt. "Stochastic Runge-Kutta algorithms. I. White noise". In: *Phys. Rev. A* 45 (2 Jan. 1992), pp. 600–603. DOI: 10.1103/PhysRevA.45.600. URL: https://link.aps.org/doi/10.1103/PhysRevA.45.600.

[48] H. Smith J.Rammer. "Quantum field-theoretical methods in transport theory of metals." In: *Review of Modern Physics* 58.2 (1986).

[49] M. W. Jack, N. J. López-Alamilla, and K. J. Challis. "Thermodynamic uncertainty relations and molecular-scale energy conversion". In: *Phys. Rev. E* 101 (6 June 2020), p. 062123. DOI: 10.1103/PhysRevE.101.062123. URL: https://link.aps.org/doi/10.1103/PhysRevE.101.062123.

[50] C. Jarzynski. "Nonequilibrium Equality for Free Energy Differences". In: *Phys. Rev. Lett.* 78 (14 Apr. 1997), pp. 2690–2693. DOI: 10.1103/PhysRevLett.78.2690. URL: https://link.aps.org/doi/10.1103/PhysRevLett.78.2690.

[51] Michael Galperin Jiayang Zhou Anqi Li. "Quantum Thermodynamics: Inside-Outside Perspective". In: *unpublished* (). DOI: https://doi.org/10.48550/arXiv.2308.06893. URL: arXiv:2308.06893.

[52] Alex Arash Sand Kalaee, Andreas Wacker, and Patrick P. Potts. "Violating the thermodynamic uncertainty relation in the three-level maser". In: *Phys. Rev. E* 104 (1 July 2021), p. L012103. DOI: 10.1103/PhysRevE.104.L012103. URL: https://link.aps.org/doi/10.1103/PhysRevE.104.L012103.

[53] Or Katz, Marko Cetina, and Christopher Monroe. "Programmable N-Body Interactions with Trapped Ions". In: *PRX Quantum* 4 (3 July 2023), p. 030311. DOI: 10.1103/PRXQuantum.4.030311. URL: https://link.aps.org/doi/10.1103/PRXQuantum.4.030311.

[54] Henning Kirchberg and Abraham Nitzan. "Energy Conversion and Entropy Production in Biased Random Walk Processes—From Discrete Modeling to the Continuous Limit". In: *Entropy* 25.8 (2023). ISSN: 1099-4300. DOI: 10.3390/e25081218. URL: https://www.mdpi.com/1099-4300/25/8/1218.

[55] R. Kosloff. "*Quantum Thermodynamics: A Dynamical Viewpoint*". In: *Entropy* 15 (2013), pp. 2100–2128. DOI: 10.3390/e15062100.

[56] Jonas Larson. "Floquet analysis perspective of driven light–matter interaction models". In: *J. Opt. Soc. Am. B* 41.8 (Aug. 2024), pp. C235–C246. DOI: 10.1364/JOSAB.524005. URL: https://opg.optica.org/josab/abstract.cfm?URI=josab-41-8-C235.

[57] L. S. Levitov. "Counting statistics of charge pumping in an open system". In: (2001). arXiv: cond-mat/0103617 [cond-mat.mes-hall]. URL: https://arxiv.org/abs/cond-mat/0103617.

[58] M.L.Polianski et al. "*Noise through quantum pumps*". In: *Phys. Rev. B* 65 (2002), p. 245314. DOI: 10.1103/PhysRevB.65.245314.

[59] Sreenath K Manikandan. "Autonomous quantum clocks using athermal resources". In: *Physical Review Research* 5.4 (2023), p. 043013.

[60] Glen Bigan Mbeng, Angelo Russomanno, and Giuseppe E Santoro. "The quantum Ising chain for beginners". In: *arXiv preprint arXiv:2009.09208* 59 (2020).

[61] Pankaj Mehta and Natan Andrei. "Nonequilibrium Quantum Impurities: From Entropy Production to Information Theory". In: *Phys. Rev. Lett.* 100 (8 Feb. 2008), p. 086804. DOI: 10.1103/PhysRevLett.100.086804. URL: https://link.aps.org/doi/10.1103/PhysRevLett.100.086804.

[62] Florian Meier et al. "Precision is not limited by the second law of thermodynamics". In: (2024). arXiv: 2407.07948 [quant-ph].

[63] GJ Milburn and TJ Milburn. "A quantum optomechanical Mach clock". In: *arXiv preprint arXiv:1708.02369* (2017).

[64] M. Moskalets and M. Buttiker. "*Adiabatic quantum pump in the presence of external ac voltages*". In: *Phys. Rev. B* 69 (2004), p. 205316. DOI: 10.1103/PhysRevB.69.205316.

[65] M. Moskalets and M. Buttiker. "*Dissipation and noise in adiabatic quantum pumps*". In: *Phys. Rev. B* 66 (2022), p. 035306. DOI: 10.1103/PhysRevB.66.035306.

[66] M. Moskalets and M. Buttiker. "*Floquet scattering theory for current and heat noise in large amplitude adiabatic pumps*". In: *Phys. Rev. B* 70 (2004), p. 245305. DOI: 10.1103/PhysRevB.70.245305.

[67] M. Moskalets and M. Buttiker. "*Floquet scattering theory of quantum pumps*". In: *Phys. Rev. B* 66 (2002), p. 205320. DOI: 10.1103/PhysRevB.66.205320.

[68] M. Moskalets and M. Buttiker. "*Time-resolved noise of adiabatic quantum pumps*". In: *Phys. Rev. B* 75 (2007), p. 035315. DOI: 10.1103/PhysRevB.75.035315.

[69] Tomá š Novotný, Andrea Donarini, and Antti-Pekka Jauho. "Quantum Shuttle in Phase Space". In: *Phys. Rev. Lett.* 90 (25 June 2003), p. 256801. DOI: 10.1103/PhysRevLett.90.256801. URL: https://link.aps.org/doi/10.1103/PhysRevLett.90.256801.

[70] P.W.Brouwer. "*Scattering approach to parametric pumping*". In: *Phys. Rev. B* 58 (1998), R10135(R). DOI: 10.1103/PhysRevB.58.R10135.

[71] J. et.al. Park. "Nanomechanical oscillations in a single-C60 transistor". In: *Nature* 407 (2000), pp. 57–60. DOI: https://doi.org/10.1038/35024031.

[72] Pierre Pfeuty. "The one-dimensional Ising model with a transverse field". In: *Annals of Physics* 57.1 (1970), pp. 79–90. ISSN: 0003-4916. DOI: https://doi.org/10.1016/0003-4916(70)90270-8. URL: https://www.sciencedirect.com/science/article/pii/0003491670902708.

[73] Giulia Piccitto and Alessandro Silva. "Dynamical phase transition in the transverse field Ising chain characterized by the transverse magnetization spectral function". In: *Phys. Rev. B* 100 (13 Oct. 2019), p. 134311. DOI: 10.1103/PhysRevB.100.134311. URL: https://link.aps.org/doi/10.1103/PhysRevB.100.134311.

[74] Patrick Pietzonka. "Classical Pendulum Clocks Break the Thermodynamic Uncertainty Relation". In: *Phys. Rev. Lett.* 128 (13 Apr. 2022), p. 130606. DOI: 10.1103/PhysRevLett.128.130606. URL: https://link.aps.org/doi/10.1103/PhysRevLett.128.130606.

[75] Mu et.al. Qiao. "Tunable quantum simulation of spin models with a two-dimensional ion crystal". In: *Nature Physics* 20 (4 2024).

[76] James Q Quach, Giulio Cerullo, and Tersilla Virgili. "Quantum batteries: The future of energy storage?" In: *Joule* 7.10 (2023), pp. 2195–2200.

[77] Sidney Redner. *A guide to first passage properties*. Cambridge University Press, 2001. ISBN: 978-0521652483.

[78] Alberto Rolandi and Martí Perarnau-Llobet. "Finite-time Landauer principle beyond weak coupling". In: *Quantum* 7 (Nov. 2023), p. 1161. ISSN: 2521-327X. DOI: 10.22331/q-2023-11-03-1161. URL: http://dx.doi.org/10.22331/q-2023-11-03-1161.

[79] Davide Rossini et al. "Quantum quenches, linear response and superfluidity out of equilibrium". In: *EPL* 107.3 (2014), p. 30002. DOI: 10.1209/0295-5075/107/30002. eprint: 1310.4757 (cond-mat.stat-mech).

[80] Angelo Russomanno, Alessandro Silva, and Giuseppe E. Santoro. "Linear response as a singular limit for a periodically driven closed quantum system". In: *Journal of Statistical Mechanics: Theory and Experiment* 2013 (2013). URL: https://api.semanticscholar.org/CorpusID:118426539.

[81] Avraham Schiller and Alessandro Silva. "Adiabatic pumping through a quantum dot in the Kondo regime: Exact results at the Toulouse limit". In: *Phys. Rev. B* 77 (4 Jan. 2008), p. 045330. DOI: 10.1103/PhysRevB.77.045330. URL: https://link.aps.org/doi/10.1103/PhysRevB.77.045330.

[82] Udo Seifert. "Stochastic thermodynamics, fluctuation theorems and molecular machines". In: *Reports on Progress in Physics* 75.12 (Nov. 2012), p. 126001. DOI: 10.1088/0034-4885/75/12/126001. URL: https://dx.doi.org/10.1088/0034-4885/75/12/126001.

[83] Eran Sela and Yuval Oreg. "Adiabatic Pumping in Interacting Systems". In: *Phys. Rev. Lett.* 96 (16 Apr. 2006), p. 166802. DOI: 10.1103/PhysRevLett.96.166802. URL: https://link.aps.org/doi/10.1103/PhysRevLett.96.166802.

[84] E.M. Sevick et al. "Fluctuation Theorems". In: *Annual Review of Physical Chemistry* 59.Volume 59, 2008 (2008), pp. 603–633. ISSN: 1545-1593. DOI: https://doi.org/10.1146/annurev.physchem.58.032806.104555. URL: https://www.annualreviews.org/content/journals/10.1146/annurev.physchem.58.032806.104555.

[85] Vaibhav Sharma and Erich J. Mueller. "Driven-dissipative control of cold atoms in tilted optical lattices". In: *Phys. Rev. A* 103 (4 Apr. 2021), p. 043322. DOI: 10.1103/PhysRevA.103.043322. URL: https://link.aps.org/doi/10.1103/PhysRevA.103.043322.

[86] Ralph Silva, Nuriya Nurgalieva, and Henrik Wilming. *Ticking clocks in quantum theory*. 2023. arXiv: 2306.01829 [quant-ph]. URL: https://arxiv.org/abs/2306.01829.

[87] Janine Splettstoesser et al. "Adiabatic Pumping through Interacting Quantum Dots". In: *Phys. Rev. Lett.* 95 (24 Dec. 2005), p. 246803. DOI: 10.1103/PhysRevLett.95.246803. URL: https://link.aps.org/doi/10.1103/PhysRevLett.95.246803.

[88] M. Switkes et al. "An Adiabatic Quantum Electron Pump". In: *Science* 283.5409 (1999), pp. 1905–1908. DOI: 10.1126/science.283.5409.1905. eprint: https://www.science.org/doi/pdf/10.1126/science.283.5409.1905. URL: https://www.science.org/doi/abs/10.1126/science.283.5409.1905.

[89] Philip Taranto et al. "Landauer Versus Nernst: What is the True Cost of Cooling a Quantum System?" In: *PRX Quantum* 4 (1 Mar. 2023), p. 010332. DOI: 10.1103/PRXQuantum.4.010332. URL: https://link.aps.org/doi/10.1103/PRXQuantum.4.010332.

[90] D. Wahyu Utami et al. "Quantum noise in the electromechanical shuttle: Quantum master equation treatment". In: *Phys. Rev. B* 74 (1 July 2006), p. 014303. DOI: 10.1103/PhysRevB.74.014303. URL: https://link.aps.org/doi/10.1103/PhysRevB.74.014303.

[91] M. Vavilov. *Phd Thesis:* Influence of Microwave Radiation on Transport Properties of Mesoscopic Systems. 2001.

[92] Lev Vidmar and Marcos Rigol. "Generalized Gibbs ensemble in integrable lattice models". In: *Journal of Statistical Mechanics: Theory and Experiment* 2016.6 (June 2016), p. 064007. DOI: 10.1088/1742-5468/2016/06/064007. URL: https://dx.doi.org/10.1088/1742-5468/2016/06/064007.

[93] Christopher W Wächtler et al. "Stochastic thermodynamics of self-oscillations: the electron shuttle". In: *New Journal of Physics* 21.7 (July 2019), p. 073009. DOI: 10.1088/1367-2630/ab2727. URL: https://dx.doi.org/10.1088/1367-2630/ab2727.

[94] Mischa P. Woods et al. "Quantum Clocks are More Accurate Than Classical Ones". In: *PRX Quantum* 3 (1 Feb. 2022), p. 010319. DOI: 10.1103/PRXQuantum.3.010319. URL: https://link.aps.org/doi/10.1103/PRXQuantum.3.010319.

Appendix

Appendix A

Methods for non-equilibrium quantum dynamics

In this Chapter, we will briefly introduce the main techniques we apply in the following sections to calculate thermodynamic and transport quantities through nanostructures, namely the Keldysh-Schwinger non-equilibrium Green's function technique and the scattering matrix theory.

A.1 Contour-ordered Green functions

The non-equilibrium Green function (NEGF) technique has been introduced to calculate observables in systems driven out of equilibrium by an external perturbation [46, 38]. The general setup we will be working on is that of a Hamiltonian containing an out-of-equilibrium term, which is in general time-dependent

$$H = h + H^{neq}(t). \tag{A.1}$$

The part of the Hamiltonian not dependent on time h can have a quadratic part H_0 and an interacting part H_{int}

$$h = H_0 + H^{int}. \tag{A.2}$$

One further assumption we will make consists in requiring the system to be in equilibrium for times prior to the initial time t_0. That is to say, the perturbation $H_{neq}(t)$ is switched on at time t_0 and, before time t_0, the system is described by the initial density matrix

$$\rho(h) = \frac{\exp(-\beta h)}{Tr[\exp(-\beta h)]} \tag{A.3}$$

In the following, for simplicity, we assume $H_{int} = 0$. Using this expression, our task will be to calculate time-dependent expectation values in the Heisenberg representation,

such as

$$\langle O_H(t)\rangle = Tr[O_H(t)\rho(h)], \tag{A.4}$$

where the subscript H means that the observable evolves in time according to the Heisenberg picture with the full Hamiltonian. In order to transform this expression into one more suitable for diagrammatic expansion, we express all this in terms of averages with respect to the free Hamiltonian H_0. Since

$$T\exp\left[-i\int_{t_0}^{t} dt' H(t')\right] = \exp[-ih(t-t_0)]T\exp\left[-i\int_{t_0}^{t} dt' H^{neq}(t')\right], \tag{A.5}$$

the time dependence can be transformed from the full Hamiltonian H to the equilibrium part h in the following way

$$O_H(t) = U_h^{\dagger}(t,t_0)O_h(t_0)U_h(t_0,t), \tag{A.6}$$

where

$$U_h(t,t_0) = T\left\{\exp\left[-i\int_{t_0}^{t} dt' H_h^{neq}(t')\right]\right\}, \tag{A.7}$$

where we have introduced the interaction representation of the Hamiltonian

$$H_h^{neq}(t) = \exp[ih(t-t_0)]H^{neq}\exp[-ih(t-t_0)] \tag{A.8}$$

and T is the time-ordering operator arranging the latest times to the left.
Expanding the time-ordered exponential, one obtains terms of this fashion

$$\bar{T}\left\{H^{neq}(t_1)\dots H^{neq}(t_n)\right\}O_h(t_0)T\left\{H^{neq}(t_1')\dots H^{neq}(t_n')\right\}, \tag{A.9}$$

where all $\{t_i\}$ and $\{t_i'\}$ are between t_0 and t. This disposition hints at a more convenient way to rewrite the expectation value (Eq. A.6), by introducing the appropriate contour γ (in Fig. **??**), with its definition

$$C = C_- \oplus C_+ = (t_0,t)\oplus(t,t_0), \tag{A.10}$$

viz

$$O_H(t) = T_\gamma\left[\exp\left(-i\int_C d\tau H_h^{neq}(\tau)\right)O(t)\right]. \tag{A.11}$$

The time ordering along the contour γ, T_γ, has this meaning: the operators with time labels that occur later on the contour have to stand left to operators with earlier time labels. This expression, if $H^{int} = 0$, can be used as a basis for perturbation theory. The key object to perform a perturbative expansion is the contour-ordered Green function, defined as

$$G_C(t_1,t_1') = -i\langle T_C(\psi_H(t_1)\psi_H^{\dagger}(t_1'))\rangle, \tag{A.12}$$

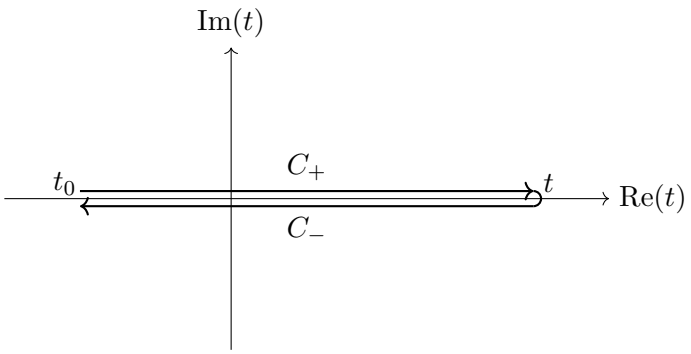

Figure A.1: The "closed time path" contour C

where ψ_H are fermionic operators, so that

$$G_C(t_1,t_1') = \begin{cases} G^T(t_1,t_1') & \text{for } t_1,t_1' \in C_+ \\ G^{\bar{T}}(t_1,t_1') & \text{for } t_1,t_1' \in C_- \\ G^{>}(t_1,t_1') & \text{for } t_1 \in C_- \text{ and } t_1' \in C_+ \\ G^{<}(t_1,t_1') & \text{for } t_1 \in C_+ \text{ and } t_1' \in C_- \end{cases} \tag{A.13}$$

where we defined the time-ordered Green's function

$$\begin{aligned} G^T(t_1,t_1') &= -i\langle T(\psi_H(t_1)\psi_H(t_1'))\rangle = \\ &= -i\theta(t_1-t_1')\psi_H(t_1)\psi_H^\dagger(t_1'), \end{aligned} \tag{A.14}$$

the anti-time-ordered Green's function

$$\begin{aligned} G^{\bar{T}}(t_1,t_1') &= -i\langle \bar{T}(\psi_H(t_1)\psi_H(t_1'))\rangle = \\ &= -i(\theta(t_1-t_1')\psi_H(t_1)\psi_H^\dagger(t_1')), \end{aligned} \tag{A.15}$$

the "lesser" Green's function

$$G^{<}(t_1,t_1') = +i\langle \psi_H(t_1')\psi_H^\dagger(t_1)\rangle \tag{A.16}$$

and the "greater" Green's function

$$G^{>}(t_1,t_1') = -i\langle \psi_H^\dagger(t_1)\psi_H(t_1')\rangle. \tag{A.17}$$

Note that only three of the Green's functions are linearly-independent, as the following relation holds

$$G^T(t_1,t_1') + G^{\bar{T}}(t_1,t_1') = G^{<}(t_1,t_1') + G^{>}(t_1,t_1'). \tag{A.18}$$

For studying non-equilibrium dynamics, the most suitable Green's functions, as we will see, are the lesser-greater functions and the advanced and retarded Green's functions. Their definition is

$$G^r(t_1, t_1') = \theta(t_1 - t_1')(G^>(t_1, t_1') - G^<(t_1, t_1')) \tag{A.19}$$

and

$$G^a(t_1, t_1') = \theta(t_1' - t_1)(G^>(t_1, t_1') - G^<(t_1, t_1')) \tag{A.20}$$

They obey the relation

$$G^> - G^< = G^r - G^a \tag{A.21}$$

To obtain a suitable form for performing a perturbative expansion of the said Green functions, one must transform to the interaction picture with respect to the free Hamiltonian H_0.

$$G(t_1, t_1') = -i\langle S_H^C \psi_h(t_1)\psi_h^\dagger(t_1')\rangle \tag{A.22}$$

where

$$S_H^C = \exp\left[-i \int_C d\tau H_h^{neq}(\tau)\right] \tag{A.23}$$

$$G(t_1, t_1') = -i\frac{Tr[\rho_0 T_C(S_C^{neq}\psi_{H_0}(t_1)\psi_{H_0}^\dagger(t_1'))]}{Tr[\rho_0 T_C(S_C^{neq})]} \tag{A.24}$$

where

$$\rho_0 = \frac{\exp(-\beta H_0)}{Tr[\exp(-\beta H_0)]} \tag{A.25}$$

and

$$S_C^{neq} = \exp\left(-i \int_C d\tau H_{H_0}^{neq}(\tau)\right) \tag{A.26}$$

A.2 Analytic continuation techniques

Now, from the aforementioned diagrammatic expansion of Green's functions, one usually obtains expressions in the form of Dyson's equations or similar, similar to the equilibrium ones, to which the educated reader is more familiar. These expressions usually involve convolutions, viz. terms with the structure

$$C(t, t') = \int_C d\tau A(t, \tau)B(\tau, t'). \tag{A.27}$$

In this expression, A, B and C represent objects on the contour, such as Green's functions or self-energies. If one is in the situation of t being on C_+ and t' on C_-, then we are in the presence of a "lesser" function. Once given expressions of this type, it appears

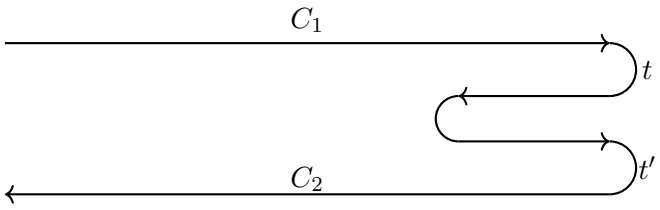

Figure A.2: The doubling of the contour integral

complicated to extract $C(t,t')$ and $C^{a,r}(t,t')$ Let us deform the contour, into an upper and a lower contour C_1 and C_2, as shown in Fig. **??**. Then, one can represent C as

$$C^<(t,t') = \int_{C_1} dt_1 A^<(t,t_1)B(t_1,t') + \int_{C_2} dt_1 A(t,t_1)B^<(t_1,t') \tag{A.28}$$

The sign $<$ means that in the contour t stand before t_1, because firstly we integrate over C_1 and after over C_2. Subsequently, we can write the second term as

$$\begin{aligned}\int_{C_2} d\tau A(t,t\tau)B^<(\tau,t') = \int_{-\infty}^{t} dt_1 A^<(t,t_1)B^<(t_1,t') + \int_{t}^{-\infty} dt_1 A^>(t,t_1)B^<(t_1,t') \\ = \int_{-\infty}^{\infty} dt_1 A^r(t,t_1)B^<(t_1,t')\end{aligned} \tag{A.29}$$

Again, the same reasoning can be applied to the first one, yielding

$$C^<(t,t') = \int_{-\infty}^{\infty} dt_1 [A^r(t,t_1)B^<(t_1,t') + A^<(t,t_1)B^a(t_1,t')] \tag{A.30}$$

That is the first of Langreth's rules.
Now, we will simply list the rest of the rules, which can be proven in similar ways

$$C^r(t,t') = \int_{-\infty}^{\infty} dt_1 A^r(t,t_1)B^r(t_1,t') \tag{A.31}$$

$$C^>(t,t') = \int_{-\infty}^{\infty} [A^r(t,t_1)B^>(t_1,t') + A^>(t,t_1)B^a(t_1,t')]$$

$$C^a(t,t') = \int_{-\infty}^{\infty} dt_1 A^a(t,t_1)B^a(t_1,t')$$

A.3 The gradient expansion

Through diagrammatics, one often is able to obtain a perturbative analysis of the studied problem. However, the equations obtained can be untractable and it is not always possible to obtain an exact solution for the Green's function. For this reason, approximation

schemes are much needed. One of these approximation schemes applicable when a separation of scales is present is the gradient expansion. The first step to implement it is to introduce the Wigner time coordinates

$$\begin{aligned} T &= \frac{t+t'}{2}, \\ \tau &= t-t' \end{aligned} \tag{A.32}$$

This transformation [48] separates the "slow" degrees of freedom of the "time-centre of mass" from the "fast" coordinate of the difference of times varying on a microscopic scale. Thus, one seeks to treat exactly the second and approximately the first. Then one passes to the Fourier transform with respect to ϵ, the relative coordinate of τ.
Let us return to our convolution structure

$$C(t,t') = \int ds A(t,s)B(s,t') \tag{A.33}$$

In the Fourier transform

$$C(\epsilon,T) = \int d\tau e^{-i\epsilon\tau} C(T+\tau/2, T-\tau/2) \tag{A.34}$$

Performing a Taylor expansion in T, for the Fourier transform one obtains this result

$$C(\epsilon,T) = A(\epsilon,T)\, G_{\epsilon,T} B(\epsilon,T), \tag{A.35}$$

where

$$G_{\epsilon,T} = e^{\frac{1}{2i}(\overleftarrow{\partial_T}\overrightarrow{\partial_\epsilon} - \overleftarrow{\partial_\epsilon}\overrightarrow{\partial_T})} = \sum_n \frac{1}{(2i)^n}\frac{1}{n!}(\overleftarrow{\partial_T}\overrightarrow{\partial_\epsilon} - \overleftarrow{\partial_\epsilon}\overrightarrow{\partial_T})^n. \tag{A.36}$$

Expanding the Wigner transform up to first order in the gradients one obtains

$$C(\epsilon,T) = A(\epsilon,T)B(\epsilon,T) + \frac{1}{2i}(\partial_T A(\epsilon,T)\partial_\epsilon B(\epsilon,T) - \partial_\epsilon A(\epsilon,T)\partial_T B(\epsilon,T)). \tag{A.37}$$

A.4 Introduction to Scattering Matrices

In this Section, we present the time-dependent scattering matrices, useful for describing transport through a scattering medium. In this context, we are particularly interested in the problem of a scatterer subject to a periodic perturbation, when the time dependence enters through a collection of parameters in the Hamiltonian.
The configuration we seek to describe physically is one of two (or more) leads (fermionic baths in equilibrium), denoted by index i, connected by a scatterer, through many channels, denoted by the Greek indexes α, β (see Fig. A.3).
The scattering matrix relates the creation/annihilation operators of the ingoing operators

Figure A.3: This represents the basic setup concerning the scattering through a quantum pump

in the channels of the leads [58], denoted by an index α, $a_\alpha(t)/a^\dagger_\alpha(t)$ to the outgoing operators $b_\alpha(t)/b^\dagger_\alpha(t)$, in the following manner

$$b_\alpha(t) = \sum_\beta \int_{-\infty}^{\infty} dt' S_{\alpha\beta}(t,t') a_\beta(t') \tag{A.38}$$

$$b^\dagger_\alpha(t) = \sum_\beta \int_{-\infty}^{\infty} dt' a^\dagger_\beta(t') (S_{\beta\alpha}(t',t))^\dagger \tag{A.39}$$

Where α and β are the indexes related respectively to the ingoing and outgoing channels. The scattering matrix has the further property

$$(S(t',t)_{\beta\alpha})^\dagger = S^*_{\alpha\beta}(t,t'). \tag{A.40}$$

The causality requirement implies that $S(t,t') = 0$ for $t < t'$. The unitarity condition reads

$$\sum_\beta \int dt_1 S_{\alpha\beta}(t,t_1) S^\dagger_{\alpha\beta}(t_1,t') = \delta(t-t'). \tag{A.41}$$

Let us now evaluate, as an example, the current through the scatterer from lead $i = L, R$, as an illustration of the operation of this method. In terms of the ingoing/outgoing operators reads

$$I_i(t) = \sum_{\alpha\in i} [a^\dagger_\alpha(t) a_\alpha(t) - b^\dagger_\alpha(t) b_\alpha(t)] \tag{A.42}$$

in units of the fundamental charge e.
Now, let us average with respect to the states of the leads. Substituting relation Eq. A.38, one obtains the expression of the current, i.e.

$$\langle I_\alpha(t)\rangle = \int dt_1 dt_2 \sum_\beta \Big[S_{\alpha\beta}(t,t_1) f_\beta(t_1-t_2) S^\dagger_{\beta\alpha}(t_2,t) - \delta(t-t_1) f_\alpha(t_1-t_2)\delta(t_2-t) \Big], \tag{A.43}$$

where we used the relations

$$\begin{aligned} \langle a^\dagger_\alpha(t) a_\beta(t')\rangle &= f_\alpha(t-t')\delta_{\alpha\beta} \\ \langle a_\alpha(t) a^\dagger_\beta(t')\rangle &= \tilde{f}_\alpha(t'-t)\delta_{\alpha\beta}, \end{aligned} \tag{A.44}$$

and $f(t-t')$ is the Fourier transform of the Fermi distribution function associated to each bath $f(\epsilon) = 1/(1+\exp(\beta(\epsilon-\mu))$, while $\tilde{f}(t) = \delta(t) - f(t)$.

Appendix B

The adiabaticity conditions of the quantum pump

In this section, we will analyze the conditions on the instantaneous velocity and acceleration according to which the physical process one is considering can be adiabatic. Following the method put forward by [44], we will extend the adiabatic expansion of the charge pumped up to the third order and require that the first order in the expansion of the charge current is much bigger than the higher order corrections. The first-order instantaneous current can be rewritten in the form

$$Q_\alpha^{(1)} = \frac{1}{T_0}\int_0^{T_0} dt \sum_i A_{\alpha,i}(t)\frac{dx_i}{dt}. \tag{B.1}$$

This is the adiabatic term, which can be interpreted in a geometrical manner (Brouwer's formula). The second order has two contributions

$$Q_\alpha^{(2)} = \frac{1}{T_0}\int_0^{T_0} dt\Big(\sum_i B_{\alpha,i}^{(1)}(t)\frac{d^2x_i}{dt^2} + \sum_{i,j} B_{\alpha,i,j}^{(2)}(t)\frac{dx_i}{dt}\frac{dx_j}{dt}\Big). \tag{B.2}$$

Using integration by part, the second order correction becomes

$$B_{\alpha,i,j} = B_{\alpha,i,j}^{(2)} - \frac{\partial B_{\alpha,i}^{(1)}(t)}{\partial x_j}. \tag{B.3}$$

Exactly in the same way, from the third order one can distinguish 2 different terms:

$$\langle I_\alpha^{(3)}(t)\rangle = \langle I_\alpha^{(3v)}(t)\rangle + \langle I_\alpha^{(3a)}(t)\rangle, \tag{B.4}$$

$$\langle I_\alpha^{(3v)}(t)\rangle = \sum_{i,j,k} C_{\alpha,i,j,k}(t)\frac{dx_i}{dt}\frac{dx_j}{dt}\frac{dx_k}{dt}, \tag{B.5}$$

$$\langle I_\alpha^{(3a)}(t)\rangle = \sum_{i,j} D_{\alpha,i,j}(t)\frac{d^2x_i}{dt^2}\frac{dx_j}{dt}. \tag{B.6}$$

In order for the process to be adiabatic, one must require the first order in the expansion of the charge current to be much bigger than the higher order corrections:

$$|\langle I_\alpha^{(1)}(t)\rangle| \gg |\langle I_\alpha^{(2)}(t)\rangle|, |\langle I_\alpha^{(3v)}(t)\rangle|, |\langle I_\alpha^{(3a)}(t)\rangle|. \tag{B.7}$$

let us translate this condition in terms of the coefficients. In this way, one can rewrite the adiabaticity condition for the second-order correction defining a velocity limit $v_{lim,\alpha}^{(2)}(t)$ for which it must be true that

$$|v(t)| \ll v_{lim,\alpha}^{(2)}(t). \tag{B.8}$$

The velocity limit can be defined as

$$v_{lim,\alpha}^{(2)}(t) = \frac{|A_\alpha(t)|}{|B_\alpha(t)|}, \tag{B.9}$$

$$A_\alpha(t) = \sum_i A_{\alpha,i}(t)\tilde{v}_i(t), \tag{B.10}$$

$$B_\alpha(t) = \sum_{i,j} B_{\alpha,i,j}(t)\tilde{v}_i(t)\tilde{v}_j(t), \tag{B.11}$$

where $\tilde{v}_i = \frac{v_i}{|v_i|}$. For the third order correction in similar way

$$v_{lim,\alpha}^{(3)}(t) = \sqrt{\frac{|A_\alpha(t)|}{|C_\alpha(t)|}}, \tag{B.12}$$

$$C_\alpha(t) = \sum_{i,j,k} C_{\alpha,i,j,k}(t)\tilde{v}_i(t)\tilde{v}_j(t)\tilde{v}_k(t). \tag{B.13}$$

So, in the end one must require that

$$v(t) \ll \min[v_{lim}^{(2)}, v_{lim}^{(3)}, ...]. \tag{B.14}$$

Now, let us examine these conditions on our peristaltic cycle, for which $x_1 = \epsilon_d$ and $x_2 = \delta\Gamma$.
one can extract an energy scale $\frac{1}{\Gamma^2}$ and express in terms of the adimensional variables $x = \epsilon_d/\Gamma$ and $y_0 = \delta_\Gamma/\Gamma$

$$|A_{\alpha,1}| = \frac{2}{\pi\Gamma}\frac{1 \pm y_0}{2}\left|\frac{1}{x^2+1} + \frac{2x^2}{(1+x^2)^2} - \frac{2}{(1+x^2)^2}\right|. \tag{B.15}$$

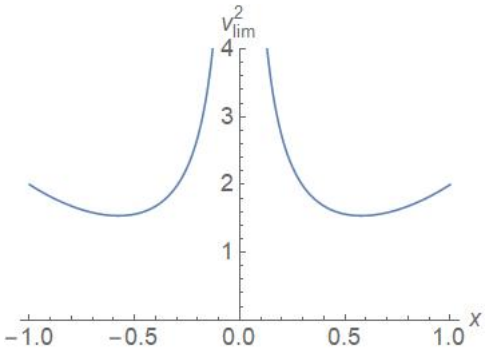

Figure B.1: The adimensional function $f_2(x, y_0)$ with respect to the variable x, for $y_0 = 1$

In the same way, one can compute $A_{\alpha,2}$. The result is

$$|A_{\alpha,2}| = \frac{1}{4\pi\Gamma}\left|\frac{x_0}{1+x_0^2}\right|, \tag{B.16}$$

in terms of $x_0 = \epsilon_0/\Gamma$. The results of the second-order coefficients are

$$B_{\alpha,11}(t) = \frac{2}{\pi\Gamma^3}\frac{1 \pm y_0}{2}\partial_\epsilon A^2. \tag{B.17}$$

The resulting condition for the derivative of ϵ_d is

$$\frac{\dot{\epsilon_d}}{\Gamma^2} \ll f_2(x, y_0), \tag{B.18}$$

where f_2 is an adimensional function which is in fig.B.1 .

Now, let us analyze the third-order corrections for the velocity. One can obtain the expression of the coefficient

$$\begin{aligned} C_{\alpha,111} = \frac{1}{2\pi\Gamma^5}\frac{1 \pm y_0}{2}\Bigg\{\left(\frac{1}{(x-i)^6} + \frac{1}{(x+i)^6}\right) + i\frac{2}{1+x^2}\left(-\frac{1}{(x-i)^5} + \frac{1}{(x+i)^5}\right) \\ -i\frac{2}{(1+x^2)^2}\left(-\frac{1}{(x-i)^3} + \frac{1}{(x+i)^3}\right) - \frac{8}{(1+x^2)^4}\Bigg\}. \end{aligned} \tag{B.19}$$

The coefficient $C_{\alpha,222}$ is also equal to 0.

Therefore, one can express the condition $v(t) \ll v^{(3)}_{lim}$ as

$$\frac{\dot{\epsilon}_d}{\Gamma^2} \ll f_3(x, y_0), \tag{B.20}$$

where $f_3(x, y_0)$ is in B.2. Finally, let us consider the limits on acceleration. From the

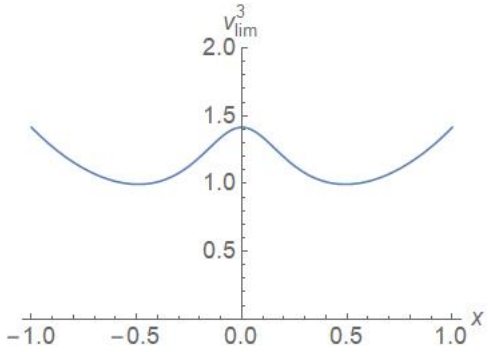

Figure B.2: The adimensional function $f_3(x, y_0)$ with respect to the variable x, for $y_0 = 1$

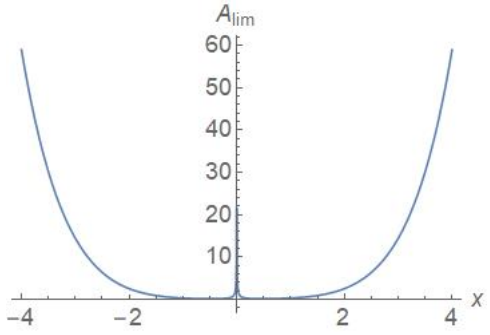

Figure B.3: The adimensional function $g(x, y_0)$ with respect to the variable x, for $y_0 = 1$

adiabatic expansion, one can infer that the coefficient $D_{\alpha 11}$ is

$$D_{\alpha 11} = \frac{1}{3\pi}\frac{1 \pm y0}{2}\left\{\left(\frac{1}{(x-i)^5} + \frac{1}{(x+i)^5}\right) - i\frac{2}{1+x^2}\left(\frac{1}{(x+i)^4} - \frac{1}{(x-i)^4}\right) - i\frac{34}{(1+x^2)^2}\left(\frac{1}{(x+i)^2} - \frac{1}{(x-i)^2}\right)\right\}. \tag{B.21}$$

The resulting condition on the acceleration is

$$\frac{\ddot{\epsilon}_d}{\Gamma^3} \ll g(x, y_0) \tag{B.22}$$

$g(x, y_0)$ is in (fig.B.3). These results appear to justify the claim that the adiabatic expansion is well-defined along the entire cycle, provided that the appropriate bounds on the derivatives of the time-dependent quantities are respected. However, repeating the same reasoning with the current noise and the thermodynamic rates would signal that there are divergences when one of the couplings with the two baths is switched off: $\Gamma_L = 0$ or $\Gamma_R = 0$.

Appendix C

Derivation of the shot noise term in the first order of the adiabatic expansion

To derive the "shot" noise term in the first order of the adiabatic expansion of the current fluctuations, which is not present in the gradient expansion of the latter quantity, we will link up with the approach employed in [66], namely the adiabatic expansion of the Floquet scattering matrix. Furthermore, we show that this approach yields the same results for the adiabatic expansion of all the other thermodynamics and transport quantities we have considered in Chapter 2.
The definition of the two-times scattering matrix relates the outgoing states to the ongoing ones

$$b_\alpha(t) = \sum_\beta \int_{-\infty}^{\infty} dt_1 S_{\alpha\beta}(t, t_1) a_\beta(t_1). \tag{C.1}$$

If one performs the Fourier transform of this expression, what he obtains is

$$b_\alpha(\epsilon) = \sum_\beta \int_{-\infty}^{\infty} \frac{d\omega}{2\pi} S_{\alpha\beta}(\epsilon, \epsilon+\omega) a_\beta(\epsilon+\omega), \tag{C.2}$$

adopting the ingoing energy ϵ as a reference. But we have to note that the scattering matrix elements are periodic in their arguments $S(t, t') = S(t, t' + T_0)$. So, it's more appropriate to use a Fourier series expansion

$$b_\alpha(\epsilon) = \sum_\beta \sum_{n=-\infty}^{\infty} S^F_{\alpha\beta}(\epsilon, \epsilon_n) a_\beta(\epsilon_n), \tag{C.3}$$

where $\epsilon_n = \epsilon + n\Omega$, and $\Omega = \frac{2\pi}{T_0}$. The matrix $S^F(\epsilon, \epsilon_n)$ is dubbed "Floquet scattering matrix" and described in a series of articles, most prominently [67].

The definition of the current noise is

$$\delta I_{\alpha\alpha}(t,t') = \langle \Delta I_\alpha(t) \Delta I_\alpha(t') \rangle \tag{C.4}$$

and $\Delta I_\alpha(t) = I_\alpha(t) - \langle I_\alpha(t) \rangle$. It can be rewritten as

$$\delta I_{\alpha\alpha}(t,t') = \langle I_\alpha(t) I_\alpha(t') \rangle - \langle I_\alpha(t) \rangle \langle I_\alpha(t') \rangle. \tag{C.5}$$

The current operator, in turn, reads

$$I_\alpha(t) = b_\alpha^\dagger(t) b_\alpha(t) - a_\alpha^\dagger(t) a_\alpha(t). \tag{C.6}$$

In the Fourier transform, the noise of the current turns into

$$\begin{aligned} \delta I_{\alpha\alpha}(t,t') = \int \frac{dE dE' dE'' dE'''}{(2\pi)^4} e^{i(E-E')t} e^{i(E''-E''')t'} \Big[\langle (b_\alpha^\dagger(E) b_\alpha(E') - a_\alpha^\dagger(E) a_\alpha(E')) \\ (b_\alpha^\dagger(E'') b_\alpha(E''') - a_\alpha^\dagger(E'') a_\alpha(E''')) \rangle - (\langle b_\alpha^\dagger(E) b_\alpha(E') \rangle - \langle a_\alpha^\dagger(E) a_\alpha(E') \rangle) \\ (\langle b_\alpha^\dagger(E'') b_\alpha(E''') \rangle - \langle a_\alpha^\dagger(E'') a_\alpha(E''') \rangle) \Big]. \end{aligned} \tag{C.7}$$

We consider the charge-pumped fluctuations, which are defined as

$$\delta Q_{\alpha\alpha} = \int_0^{T_0} dT \int_{-\infty}^{\infty} d\tau \delta(T + \frac{\tau}{2}, T - \frac{\tau}{2}). \tag{C.8}$$

In the latter, we employ the Wick theorem and cancel the disconnected averages, then insert Eq. C.3. The expression is further simplified by employing the representation of the delta function $\delta(\alpha) = \int_{-\infty}^{\infty} dt e^{i\alpha t}$. We obtain all the expressions of [66]

$$\delta Q_{\alpha\alpha} = \delta Q_{\alpha\alpha}^{th} + \delta Q_{\alpha\alpha}^{sh} \tag{C.9}$$

$$\delta Q_{\alpha\alpha}^{th} = 2T_0 \int \frac{d\epsilon}{2\pi} f(\epsilon) \tilde{f}(\epsilon) \sum_n (1 - |S_{\alpha\alpha}^F(\epsilon_n, \epsilon)|^2) \tag{C.10}$$

and

$$\begin{aligned} \delta Q_{\alpha\alpha}^{sh} = T_0 \int \frac{d\epsilon}{(2\pi)^2} \sum_{\gamma\delta} \sum_n \sum_m \sum_p \frac{(f(\epsilon_n) - f(\epsilon_m))^2}{2} (S_{\alpha\gamma}^{F*}(\epsilon, \epsilon_n) S_{\alpha\delta}^F(\epsilon, \epsilon_m) \\ S_{\alpha\delta}^{F*}(\epsilon_p, \epsilon_m) S_{\alpha\gamma}^F(\epsilon_p, \epsilon_n)) \end{aligned} \tag{C.11}$$

The Floquet scattering matrix has the following adiabatic expansion

$$S^F(E_n, E) = S_n(E) + \frac{n\Omega}{2} \frac{\partial}{\partial \epsilon} S_n(E) + \Omega A_n + O(\Omega^2), \tag{C.12}$$

with $S_n(E)$ the n-th Fourier coefficient of the scattering matrix defined as

$$S_n(E) = \int_0^{T_0} \frac{dt}{T_0} e^{in\Omega t} S(E) \tag{C.13}$$

and A_n is the first order correction of the quantity. By substituting the expansion, one obtains the zero and first-order thermal noise

$$\delta Q_{\alpha\alpha}^{0,th} = 2k_B T \int_{-\infty}^{\infty} \frac{d\epsilon}{2\pi} \Big(- \frac{df}{d\epsilon} \Big) \Big[T_0 - \int_0^{T_0} dT |S_{\alpha\alpha}(E)|^2 \Big] \tag{C.14}$$

and

$$\delta Q_{\alpha\alpha}^{1,th} = k_B T \int_{-\infty}^{\infty} \frac{d\epsilon}{4\pi i} \int_0^{T_0} dT \Big(- \frac{df}{d\epsilon} \Big) \sum_{\beta \neq \alpha} \frac{dI_{\alpha\alpha}}{dE} \tag{C.15}$$

where $\frac{dI_{\alpha\alpha}}{dE}$ is the spectrally resolved current, with its definition

$$\frac{dI_{\alpha\alpha}}{dE} = \Big(\frac{\partial S_{\alpha\alpha}^*}{\partial t} S_{\alpha\alpha} - \frac{\partial S_{\alpha\alpha}}{\partial t} S_{\alpha\alpha}^* \Big). \tag{C.16}$$

These two expressions can correspond with the ones obtained from the gradient expansion. The shot noise term has different expressions according to the regime in which one considers it. In the zero temperature limit $k_B T \ll \Omega$ and $k_B T \ll \Gamma^{-1}$. In the zero temperature limit, the difference $(f(E_n) - f(E_m))^2 \simeq \theta(E_m - \mu) - \theta(E_n - \mu)$. Taking the other scattering matrix elements at the zero order

$$\delta Q_{\alpha\alpha}^{1,sh} = \sum_{q=1}^{\infty} \frac{q\Omega}{8\pi^2} C_{\alpha\alpha}^{(sym)}(\mu). \tag{C.17}$$

In the high-temperature limit, instead, one can formally write the difference as $(f(E_n) - f(E_m))^2 \simeq \Big(- \frac{df}{d\epsilon} \Big) |n - m| \Omega$. Then this "high-temperature shot noise" reads

$$\delta Q_{\alpha\alpha}^{2,sh} = \int_{-\infty}^{\infty} \frac{d\epsilon}{8\pi^2} \Big(\frac{df}{d\epsilon} \Big)^2 \sum_{q=1}^{\infty} (q\Omega)^2 C_{\alpha\alpha}^{(sym)}(E) \tag{C.18}$$

Note that this belongs to the second order in the adiabatic expansion. This expression can be understood by rewriting it in terms of the derivatives and compared with the gradient expansion. In fact, one has that

$$\sum_q q\Omega [A]_q = \frac{1}{i} \partial_t A(\epsilon). \tag{C.19}$$

Then

$$\delta Q_{\alpha\alpha}^{(2,sh)} = -\int_0^{T_0} dT \int \frac{d\epsilon}{16\pi}(\partial_\epsilon f(\epsilon))^2 \Big\{ 2\sum_\beta \Big[\partial_T^2 S_{\alpha\beta} S_{\alpha\beta}^\dagger + S_{\alpha\beta}\partial_T^2 S_{\alpha\beta}^\dagger - 2\partial_T S_{\alpha\beta}\partial_T S_{\alpha\beta}^\dagger \Big] - 2\sum_{\gamma\delta}(\partial_T S_{\alpha\delta} S_{\alpha\delta}^\dagger - S_{\alpha\delta}\partial_T S_{\alpha\delta}^\dagger)(\partial_T S_{\alpha\gamma} S_{\alpha\gamma}^\dagger - S_{\alpha\gamma}\partial_T S_{\alpha\gamma}^\dagger) \Big\}. \tag{C.20}$$

The relevance of all these terms is discussed in the next section of the Appendix.
Using this formalism of the Floquet scattering matrix, we now show how to derive the expansion of all the quantities we have analyzed in Chapter 3. In terms of the operators, the current reads [67]

$$I_\alpha(t) = \int \frac{dE dE'}{(2\pi)^2} e^{i(E-E')t}(b_\alpha^\dagger(E) b_\alpha(E') - a_\alpha^\dagger(E) a_\alpha(E')). \tag{C.21}$$

The charge pumped is the integral over t of this quantity. After substituting the definition of the Floquet scattering matrix, one has the following expression

$$Q_\alpha = T_0 \int \frac{dE}{2\pi} \sum_\beta \sum_n (|S_{\alpha\beta}^F(E, E_n)|^2 f(E_n) - f(E)). \tag{C.22}$$

When shifting the energy variables $E \to E - n\Omega$

$$Q_\alpha^{(1)} = T_0 \int \frac{dE}{2\pi} \sum_\beta \sum_n |S_{\alpha\beta}^F(E_n, E)|^2 (f(E) - f(E_n)). \tag{C.23}$$

The difference of Fermi functions $f(E) - f(E_n) \to n\Omega\Big(-\frac{df}{d\epsilon}\Big)$, formally assuming $k_B T \gg \Omega$. However, one can demonstrate that this gives the correct result in the zero temperature limit as well. Inserting eq. C.12, one obtains the following expression

$$Q_\alpha^{(1)} = T_0 \int \frac{dE}{2\pi} \sum_\beta \sum_n \Big(-\frac{df}{d\epsilon}\Big) n\Omega |S_{\alpha\beta}^n(E)|^2 \tag{C.24}$$

Using relation C.19, we obtain our previous expression of the pumped charge

$$Q_\alpha^{(1)} = \int_0^{T_0} dt \int \frac{dE}{2\pi} \sum_\beta \Big(\frac{\partial S_{\alpha\beta}^*}{\partial t} S_{\alpha\beta} - S_{\alpha\beta}^* \frac{\partial S_{\alpha\beta}}{\partial t} \Big). \tag{C.25}$$

The variation of the number of particles is obtained from the currents as $\dot{N}^{(i)} = \sum_\alpha I_\alpha^{(i)}$

$$\dot{N}^{(1)} = \sum_\alpha \Big[\dot{\epsilon}_d \int \frac{d\epsilon}{4\pi i} \frac{2i\Gamma_\alpha A}{\Gamma} + \dot{\Gamma}_\alpha \int \frac{d\epsilon}{4\pi i} 2i Re G^R \Big] = \dot{\epsilon}_d \int \frac{d\epsilon}{2\pi} A + \dot{\Gamma} \int \frac{d\epsilon}{2\pi} Re G^R. \tag{C.26}$$

Likewise for the heat current

$$I_{H,\alpha} = \int_{-\infty}^{\infty} \frac{dE}{2\pi} \sum_n (E_n - \mu) \sum_\beta |S^F_{\alpha\beta}(E_n, E)|^2 (f(E) - f(E_n)) \tag{C.27}$$

Employing the same reasoning as before, we write the first-order heat exchange as

$$I^{(1)}_{H,\alpha} = \int_{-\infty}^{\infty} \frac{dE}{4\pi i} (E - \mu) \left(\frac{\partial S^*_{\alpha\beta}}{\partial t} S_{\alpha\beta} - S^*_{\alpha\beta} \frac{\partial S_{\alpha\beta}}{\partial t} \right) \tag{C.28}$$

and

$$\mathcal{Q}^{(1)} = \sum_\alpha I^{(1)}_{H,\alpha}. \tag{C.29}$$

The energy current reads

$$I_{E,\alpha} = \int_{-\infty}^{\infty} \frac{dE}{2\pi} E \sum_\beta \sum_n |S^F_{\alpha\beta}(E_n, E)|^2 (f(E) - f(E_n)) \tag{C.30}$$

and at first order

$$\dot{E}^{(1)} = \dot{\epsilon}_d \int_{-\infty}^{\infty} \frac{dE}{2\pi} E(-\partial_\epsilon f) A + \dot{\Gamma} \int_{-\infty}^{\infty} \frac{dE}{2\pi} E(-\partial_\epsilon f) Re G^R \tag{C.31}$$

Finally, let us introduce the entropy current with lead α, which has the following expression [1]

$$I^\Sigma = k_B \int \frac{dE dE'}{(2\pi)^2} e^{i(E-E')t} \Big[\log f(b^\dagger_\alpha(E) b_\alpha(E') + a^\dagger_\alpha(E) a_\alpha(E')) + \log(1-f)(b_\alpha(E) b^\dagger_\alpha(E') + a_\alpha(E) a^\dagger_\alpha(E')) \Big] \tag{C.32}$$

In terms of the Floquet scattering matrix, the latter reads

$$I^\Sigma = \int \frac{dE}{2\pi} \frac{(E-\mu)}{T} \sum_n (E_n - \mu) \sum_\beta |S^F_{\alpha\beta}(E_n, E)|^2 (f(E) - f(E_n)) \tag{C.33}$$

Repeating the analysis of the current, one ends up with this expression

$$\dot{S}^{(1)} = \dot{\epsilon}_d \int_{-\infty}^{\infty} \frac{dE}{2\pi} \frac{(E-\mu)}{T} (-\partial_\epsilon f) A + \dot{\Gamma} \int_{-\infty}^{\infty} \frac{dE}{2\pi} \frac{(E-\mu)}{T} (-\partial_\epsilon f) Re G^R. \tag{C.34}$$

The work rate $\dot{W}$ can be obtained by using the first law of thermodynamics. This analysis can be extended to further orders, and it is concluded that all our results coincide with the gradient expansion method.

C.1 Comparison between the leading order terms of noise in quantum pumps

As pointed out in [66], there are three different regimes in which the different leading order terms of the noise are relevant. One has three relevant terms for our analysis. The first is the first-order thermal noise arising from the thermal excitation of the scatterer, corresponding to Eq. 2.54. It contains an energy scale proportional to $k_B T \frac{\Omega T_0}{\Gamma}$. The second term is the shot noise term (Eq. 2.55), which contains an energy scale of ΩT_0. The third term is the second-order adiabatic shot noise in the high-temperature limit of Eq. C.18 This term is, strictly speaking, singular in the zero-temperature limit and it contains an energy scale of $\frac{\Omega^2 T_0}{k_B T}$.
By examining the ratio of these terms, we will determine the regimes in which each of these terms is relevant. One can conclude that in the low-temperature regime $K_B T \ll \Omega$, the first-order "shot" noise is prevalent. There is an intermediate temperature regime $\Omega \ll k_B T \ll \sqrt{\Omega\Gamma}$ in which the high-temperature "shot" noise is prevalent, while in the high-temperature limit $\sqrt{\Omega\Gamma} \ll k_B T$.

Appendix D

The expansions of the Green functions in presence of a finite bias

In this Section, we will extend the treatment of Section 2.3 to the case of a driven quantum dot, when a bias is present between the source and the drain. As in the previous Chapter, both the energy level and the couplings are time-dependent.

As one can verify, for the retarded and advanced Green functions one has the usual form $G^R(\epsilon,t) = (\epsilon - \epsilon_d(t) + i\frac{\Gamma(t)}{2})^{-1}$ and $G^A(\epsilon,t) = (\epsilon - \epsilon_d(t) - i\frac{\Gamma(t)}{2})^{-1}$ up to first order in the expansion.

Let us recall that the lesser component of the Green function $G^<(t,t') = i\langle c^\dagger(t')c(t)\rangle$ is given by the double convolution

$$G^< = \int dt_1 dt_2 G^R(t,t_1)\Sigma^<(t_1,t_2)G^A(t_2,t'). \tag{D.1}$$

The zero order of the series reads

$$G^{<(0)}(\epsilon,t) = G^R\Sigma^<G^A = iA\bar{f}. \tag{D.2}$$

where we have defined the non-equilibrium stationary distribution $\bar{f} = \sum_{i=L,R}\frac{\Gamma_i f_i}{\Gamma}$ The general expression of the expansion of the lesser Green function is

$$G^<(\epsilon,T) = G^R(\epsilon,T) * \Sigma^<(\epsilon,T) * G^A(\epsilon,T) \tag{D.3}$$

At first order, it reads

$$G^{<(1)}(\epsilon,T) = \frac{i}{2}\Big[\partial_\epsilon G^R\partial_t\Sigma^< - \partial_t G^R\partial_\epsilon\Sigma^<\Big]G^A + \frac{i}{2}\Big[\partial_\epsilon(G^R\Sigma^<)\partial_t G^A - \partial_t(G^R\Sigma^<)\partial_\epsilon G^A\Big] \tag{D.4}$$

The part dependent on $\dot{\epsilon_d}$ yields a contribution $-i\frac{\dot{\epsilon_d}}{2}\partial_\epsilon \bar{f} A^2$. Now, let us work out the different contributions to the part which is dependent on $\dot{\Gamma}_\alpha$

$$\begin{aligned} 1) \qquad & \frac{i}{2}\Big(\partial_\epsilon G^R \partial_t \Sigma^< G^A - G^R \partial_t \Sigma^< \partial_\epsilon G^A\Big) = \sum_\alpha \frac{i}{2}(i\dot{\Gamma}_\alpha f_\alpha)(\partial_\epsilon G^R G^A - G^R \partial_\epsilon G^A) \\ & = -\frac{i}{2}\sum_\alpha \dot{\Gamma}_\alpha f_\alpha \frac{A^2}{\Gamma} \end{aligned} \tag{D.5}$$

$$\begin{aligned} 2) \qquad & \frac{i}{2}\Big(- \partial_t G^R \partial_\epsilon \Sigma^< G^A + G^R \partial_\epsilon \Sigma^< \partial_t G^A\Big) \\ & = \sum_\alpha \frac{i}{2}\dot{\Gamma}(i\Gamma_\alpha \partial_\epsilon f_\alpha)\frac{i}{2}([G^R]^2 G^A + G^R [G^A]^2) = -\frac{i}{2}\dot{\Gamma}\partial_\epsilon \bar{f}\frac{A^2}{\Gamma}(\epsilon - \epsilon_d(t)) \end{aligned} \tag{D.6}$$

$$\begin{aligned} 3) \qquad & \frac{i}{2}\Big(\partial_\epsilon G^R \Sigma^< \partial_t G^A - \partial_t G^R \Sigma^< \partial_\epsilon G^A\Big) \\ & = \frac{i}{2}\dot{\Gamma}(i\Gamma\bar{f})\frac{i}{2}\Big(\partial_\epsilon G^R [G^A]^2 + [G^R]^2 \partial_\epsilon G^A\Big) = \frac{i}{2}\dot{\Gamma}\bar{f}\frac{A^2}{\Gamma} \end{aligned} \tag{D.7}$$

where we used the following relations: $\partial_\epsilon G^R G^A - G^R \partial_\epsilon G^A = i\frac{A^2}{\Gamma}$, $\partial_t G^{R/A} = -\dot{\epsilon_d}\partial_\epsilon G^{R/A} + \dot{\Gamma}(\mp\frac{i}{2})[G^{R/A}]^2$, $Re(G^R) = \frac{\epsilon-\epsilon_d}{\Gamma}A$ and $[G^R]^2[G^A]^2 = (\frac{A}{\Gamma})^2$.
Overall, one obtains

$$G^<(\epsilon,t) = iA\bar{f} - i\frac{\dot{\epsilon_d}}{2}\partial_\epsilon \bar{f} A^2 + i\sum_j \frac{\dot{\Gamma}_j}{2}(\bar{f} - f_j)\frac{A^2}{\Gamma} - i\frac{\dot{\Gamma}}{2}\partial_\epsilon \bar{f}\frac{A^2}{\Gamma}(\epsilon - \epsilon_d). \tag{D.8}$$

As a consequence, one can identify a non-equilibrium distribution function

$$\phi = \bar{f} - \frac{\dot{\epsilon_d}}{2}\partial_\epsilon \bar{f} A - \frac{\dot{\Gamma}}{2}\partial_\epsilon \bar{f}\frac{A}{\Gamma}(\epsilon - \hat{\epsilon}_d) + \sum_j \frac{\dot{\Gamma}_j}{2}(\bar{f} - f_j)\frac{A}{\Gamma}. \tag{D.9}$$

I report here the second order of the expansion, since it will be useful

$$\begin{aligned} G^{<(2)} = & -\frac{1}{8}\Big[\partial_\epsilon^2 G^R \partial_t^2 \Sigma^< - 2\partial_{\epsilon t}^2 G^R \partial_{\epsilon t}^2 \Sigma^< + \partial_t^2 G^R \partial_\epsilon^2 \Sigma^<\Big] G^A - \frac{1}{8}\Big[\partial_\epsilon^2 (G^R\Sigma^<)\partial_t^2 G^A \\ & - 2\partial_{\epsilon t}^2 (G^R\Sigma^<)\partial_{\epsilon t}^2 G^A + \partial_t^2 (G^R\Sigma^<)\partial_\epsilon^2 G^A\Big] - \frac{1}{4}\Big[\partial_\epsilon(\partial_\epsilon G^R \partial_t \Sigma^< - \partial_\epsilon \Sigma^< \partial_t G^R)\partial_t G^A \\ & - \partial_t(\partial_\epsilon G^R \partial_t \Sigma^< - \partial_\epsilon \Sigma^< \partial_t G^R)\partial_\epsilon G^A\Big]. \end{aligned} \tag{D.10}$$

Let us then distinguish all the different contributions

$$\begin{aligned} (1) = & -\frac{1}{8}\partial_t^2 \Sigma^<(\partial_\epsilon^2 G^R G^A + G^R \partial_\epsilon^2 G^A - 2\partial_\epsilon G^R \partial_\epsilon G^A) = \\ & - \frac{i}{4}\sum_\alpha \ddot{\Gamma}_\alpha f_\alpha \frac{A}{\Gamma}[(G^R)^2 + (G^A)^2 - G^R G^A]; \end{aligned} \tag{D.11}$$

$$
\begin{aligned}
(2) &= -\frac{1}{8}\partial_\epsilon^2\Sigma^<(\partial_t^2 G^R G^A + G^R\partial_t^2 G^A - 2\partial_t G^R\partial_t G^A) = \\
&- \frac{i}{8}\Gamma\partial_\epsilon^2\bar{f}\Big[\dot{\epsilon}_d^2\Big(\partial_\epsilon^2 G^R G^A + G^R\partial_\epsilon^2 G^A - 2\partial_\epsilon G^R\partial_\epsilon G^A\Big) + \dot{\Gamma}^2\Big(\partial_\Gamma^2 G^R G^A + G^R\partial_\Gamma^2 G^A \\
&- 2\partial_\Gamma G^R\partial_\Gamma G^A\Big) + \dot{\epsilon}_d\dot{\Gamma}\Big(-2\partial_{\epsilon\Gamma}^2 G^R G^A - 2G^R\partial_{\epsilon\Gamma}^2 G^A + 2\partial_\epsilon G^R\partial_\Gamma G^A + 2\partial_\Gamma G^R\partial_\epsilon G^A\Big) \\
&- \ddot{\epsilon}_d\Big(\partial_\epsilon G^R G^A + G^R\partial_\epsilon G^A\Big) + \ddot{\Gamma}\Big(\partial_\Gamma G^R G^A + G^R\partial_\Gamma G^A\Big)\Big] \\
&= -\frac{i}{8}\Gamma\partial_\epsilon^2\bar{f}\Big[\dot{\epsilon}_d^2\frac{A}{\Gamma}\Big[(G^R)^2 + (G^A)^2 - 2G^R G^A\Big] - \frac{\dot{\Gamma}^2}{4}\frac{A}{\Gamma}\Big((G^R)^2 + (G^A)^2 \\
&+ 2G^R G^A\Big) + i\dot{\epsilon}_d\dot{\Gamma}\frac{A}{\Gamma}\Big((G^R)^2 - (G^A)^2\Big) + 2\ddot{\epsilon}_d\frac{A}{\Gamma}ReG^R - i\frac{A^2}{\Gamma^2}\ddot{\Gamma}\Big];
\end{aligned}
\tag{D.12}
$$

$$
\begin{aligned}
(3) &= \frac{1}{4}\partial_\epsilon\partial_t\Sigma^<(\partial_{\epsilon t}^2 G^R G^A + G^R\partial_{\epsilon t}^2 G^A - \partial_\epsilon G^R\partial_t G^A - \partial_t G^R\partial_\epsilon G^A) = \\
&\frac{i}{4}\sum_\alpha \dot{\Gamma}_\alpha\partial_\epsilon f_\alpha\Big[-\dot{\epsilon}_d\Big(\partial_\epsilon^2 G^R G^A + G^R\partial_\epsilon^2 G^A - 2\partial_\epsilon G^R\partial_\epsilon G^A\Big) + \dot{\Gamma}\Big(\partial_\Gamma\partial_\epsilon G^R G^A \\
&+ G^R\partial_\Gamma\partial_\epsilon G^A - \partial_\Gamma G^R\partial_\epsilon G^A - \partial_\epsilon G^R\partial_\Gamma G^A\Big)\Big] \\
&= \frac{i}{4}\sum_\alpha \dot{\Gamma}_\alpha\partial_\epsilon f_\alpha\Big[-\dot{\epsilon}_d\frac{A}{\Gamma}\Big((G^R)^2 + (G^A)^2 - 2G^R G^A\Big) - \frac{1}{4}\dot{\Gamma}\frac{A}{\Gamma}\Big((G^R)^2 \\
&- (G^A)^2\Big)\Big];
\end{aligned}
\tag{D.13}
$$

$$
\begin{aligned}
(4) &= -\frac{1}{4}\partial_\epsilon\Sigma^<(\partial_\epsilon G^R\partial_t^2 G^A - \partial_t G^R\partial_{\epsilon t}^2 G^A - \partial_{\epsilon t}^2 G^R\partial_t G^A + \partial_t^2 G^R\partial_\epsilon G^A) = \\
&- \frac{i}{4}\Gamma\partial_\epsilon\bar{f}\Big[\dot{\Gamma}^2\Big(-\partial_\Gamma^2 G^R\partial_\epsilon G^A - \partial_\epsilon G^R\partial_\Gamma^2 G^A + \partial_\Gamma\partial_\epsilon G^R\partial_\Gamma G^A + \partial_\Gamma G^R\partial_\Gamma\partial_\epsilon G^A\Big) \\
&+ \dot{\epsilon}_d\dot{\Gamma}\Big(\partial_\epsilon G^R\partial_\epsilon\partial_\Gamma G^A + \partial_\epsilon\partial_\Gamma G^R\partial_\epsilon G^A - \partial_\Gamma G^R\partial_\epsilon^2 G^A - \partial_\epsilon^2 G^R\partial_\Gamma G^A\Big) \\
&- \ddot{\epsilon}_d\Big(\partial_\epsilon G^R\partial_\epsilon G^A + \partial_\epsilon G^R\partial_\epsilon G^A\Big) + \ddot{\Gamma}\Big(\partial_\Gamma G^R\partial_\epsilon G^A + \partial_\epsilon G^R\partial_\Gamma G^A\Big)\Big] \\
&= \frac{i}{4}\Gamma\partial_\epsilon\bar{f}\Big[-\dot{\Gamma}^2\frac{A^2}{\Gamma^2}ReG^R - \dot{\epsilon}_d\dot{\Gamma}2\frac{A^2}{\Gamma^2}ReG^R - \ddot{\epsilon}_d\frac{2A^2}{\Gamma^2}\Big]
\end{aligned}
\tag{D.14}
$$

$$
\begin{aligned}
&(5) = \frac{1}{4}\partial_t\Sigma^<(\partial_\epsilon G^R\partial^2_{t\epsilon}G^A - \partial_t G^R\partial^2_\epsilon G^A - \partial^2_{\epsilon t}G^R\partial_\epsilon G^A + \partial^2_\epsilon G^R\partial_t G^A) = \\
&\frac{i}{4}\dot\Gamma_\alpha f_\alpha\Big[\dot\Gamma\Big(\partial_\epsilon G^R\partial^2_{\epsilon\Gamma}G^A - \partial_\Gamma G^R\partial^2_\epsilon G^A - \partial_\Gamma\partial_\epsilon G^R\partial_\epsilon G^A + \partial^2_\epsilon G^R\partial_\Gamma G^A\Big)\Big] \\
&= \frac{i}{4}\sum_\alpha \dot\Gamma_\alpha f_\alpha\Big[-i\dot\Gamma 2\frac{A^2}{\Gamma^2}ReG^R\Big]
\end{aligned}
\tag{D.15}
$$

$$
\begin{aligned}
&(6) = -\frac{1}{8}\Sigma^<(\partial^2_\epsilon G^R\partial^2_t G^A + \partial^2_t G^R\partial^2_\epsilon G^A - 2\partial^2_{\epsilon t}G^R\partial^2_{\epsilon t}G^A + \partial^2_\epsilon G^R\partial_t G^A) = \\
&-\frac{i}{8}\Gamma\bar f\Big[\dot\Gamma^2\Big(\partial^2_\epsilon G^R\partial^2_\Gamma G^A + \partial^2_\Gamma G^R\partial^2_\epsilon G^A - 2\partial_\Gamma\partial_\epsilon G^R\partial_\epsilon\partial_\Gamma G^A\Big) - \ddot\epsilon_d\Big(\partial_\epsilon G^R\partial^2_\epsilon G^A \\
&+ \partial^2_\epsilon G^R\partial_\epsilon G^A\Big) + \ddot\Gamma\Big(\partial^2_\epsilon G^R\partial_\Gamma G^A + \partial_\Gamma G^R\partial^2_\epsilon G^A\Big)\Big] \\
&= -\frac{i}{8}\Gamma\bar f\Big[-\dot\Gamma^2\frac{A^2}{\Gamma^2} + \ddot\epsilon_d\frac{A^2}{\Gamma^2}2ReG^R\Big].
\end{aligned}
\tag{D.16}
$$

All these six terms have to be combined

$$
\begin{aligned}
&G^{<(2)} = -\frac{i}{4}\sum_\alpha\ddot\Gamma_\alpha f_\alpha\frac{A}{\Gamma}[(G^R)^2 + (G^A)^2 - G^RG^A] - \frac{1}{8}\frac{A^2}{\Gamma}\partial^2_\epsilon\bar f - \dot\epsilon_d\Big[\frac{i}{4}\Gamma\bar f\frac{A^2}{\Gamma^2}ReG^R \\
&+ \frac{i}{4}\Gamma\partial_\epsilon\bar f\frac{2A^2}{\Gamma^2} + \frac{i}{4}\Gamma\partial^2_\epsilon\bar f\frac{A}{\Gamma}ReG^R\Big] + \dot\epsilon_d^2\Big[-\frac{i}{8}\Gamma\partial^2_\epsilon\bar f\frac{A}{\Gamma}\Big((G^R)^2 + (G^A)^2 - 2G^RG^A\Big)\Big] \\
&+ \dot\epsilon_d\dot\Gamma\Big[-\frac{i}{4}\partial^2_\epsilon\bar f A^2ReG^R - \frac{i}{2}\partial_\epsilon\bar f\frac{A^2}{\Gamma}ReG^R\Big] + \frac{i}{4}\sum_\alpha\dot\Gamma_\alpha\dot\epsilon_d\partial_\epsilon f_\alpha\Big[-\frac{A}{\Gamma}\Big((G^R)^2 + (G^A)^2 \\
&- 2G^RG^A\Big)\Big] + \dot\Gamma^2\Big[+\frac{i}{32}\partial^2_\epsilon\bar f A\Big((G^R)^2 + (G^A)^2 + 2G^RG^A\Big) - \frac{i}{4}\partial_\epsilon\bar f\frac{A^2}{\Gamma}ReG^R \\
&- \frac{i}{8}\bar f\frac{A^2}{\Gamma}\Big] + \frac{i}{8}\sum_\alpha\dot\Gamma_\alpha\partial_\epsilon f_\alpha\frac{A^2}{\Gamma}ReG^R + \frac{i}{4}\sum_\alpha\dot\Gamma_\alpha f_\alpha\Big[-i\dot\Gamma 2\frac{A^2}{\Gamma^2}ReG^R\Big].
\end{aligned}
\tag{D.17}
$$

Similarly, the expansion for the greater Green's function up to first order is the following:

$$
G^>(\epsilon,t) = -iA(1-\bar f) - i\frac{\dot\epsilon_d}{2}\partial_\epsilon\bar f A^2 + i\sum_j\frac{\dot\Gamma_j}{2}(\bar f - f_j)\frac{A^2}{\Gamma} - i\frac{\dot\Gamma}{2}\partial_\epsilon\bar f\frac{A^2}{\Gamma}(\epsilon-\epsilon_d), \tag{D.18}
$$

satisfying the relation $G^>(\epsilon,T) = -iA(1-\phi)$. The expression of $G^{>(2)}$ is the same as $G^{<(2)}$.

$G^<_{d,ki} = i\langle a^\dagger_{ki}(t')c(t)\rangle$, for which the property $G^<_{d,ki}(t,t) = -\big(G^<_{ki,d}(t,t)\big)^*$ holds. Now, the

equation of motion for the mixed Green function at equal times reads

$$\begin{aligned} V_i(t)G^<_{d,ki}(t,t) &= V_i(t)\sum_k \left(\int dt' [G^R(t,t')g^<_{ki}(t',t) + G^<(t,t')g^A_{ki}(t',t)] \right) \\ &= \left(\int dt' [G^R(t,t')\Sigma^<_i(t',t) + G^<(t,t')\Sigma^A_i(t',t)] \right). \end{aligned} \tag{D.19}$$

Moving to the Wigner transform

$$\sum_k V_i(t)G^<_{d,ki}(t,t) = \left(\int \frac{d\epsilon}{2\pi} [G^R(\epsilon,t) * \Sigma^<_i(\epsilon,t) + G^<(\epsilon,t) * \Sigma^A_i(\epsilon,t)] \right). \tag{D.20}$$

Up to first order

$$\begin{aligned} \sum_k V_\alpha(t)G^<_{d,ki}(t,t) &= \int \frac{d\epsilon}{2\pi} \left[G^R(\epsilon,t) i f_j(\epsilon)\Gamma_j - \frac{i}{2}\partial_t G^R(\epsilon,t) i\partial_\epsilon f_i \Gamma_i + \frac{i}{2}\partial_\epsilon G^R(\epsilon,t) i f_i(\epsilon)\dot{\Gamma}_i \right] \\ &+ \int \frac{d\epsilon}{2\pi} \left[-\frac{A}{2}\bar{f}\Gamma_i - \frac{i}{2}\partial_\epsilon(A\bar{f})\frac{\dot{\Gamma}_i}{2} \right] + \int \frac{d\epsilon}{2\pi} \left[G^{<(1)}(\epsilon,T)\frac{i}{2}\Gamma \right]. \end{aligned} \tag{D.21}$$

The expression for the Green function of the bath, renormalized by the interaction with the dot stems from the Dyson equation represented on the Keldysh contour. In terms of the lesser/greater Green functions one has

$$G^{<(0)}_{\substack{k\alpha \\ \alpha' k'}} = G^{0,<}_{k\alpha}\delta_{\substack{k\alpha \\ \alpha' k'}} + G^{0,<}_{k\alpha}\Sigma^A_{\substack{\alpha \\ \alpha'}}G^{0,A}_{k'\alpha'} + G^{0,R}_{k\alpha}\Sigma^<_{\substack{\alpha \\ \alpha'}}G^{0,A}_{k'\alpha'} + G^{0,R}_{k\alpha}\Sigma^R_{\substack{\alpha \\ \alpha'}}G^{0,<}_{k'\alpha'}. \tag{D.22}$$

And similarly for the greater component. One has

$$\Sigma^{</>/R/A}_{\substack{\alpha \\ \alpha'}} = T_\alpha T_{\alpha'} G^{</>/R/A}. \tag{D.23}$$

Substituting the expression of the Green functions

$$\begin{aligned} &= \sum_{kk'} T_\alpha T_{\alpha'} \left[2\pi i f_\alpha(\epsilon)\delta(\epsilon - \epsilon_{k\alpha})\delta_{\substack{k\alpha \\ \alpha' k'}} + 2\pi i f_\alpha(\epsilon)\delta(\epsilon - \epsilon_{k\alpha})\frac{T_\alpha T_{\alpha'}}{\epsilon - \epsilon_d - i\frac{\Gamma}{2}}\frac{1}{\epsilon - \epsilon_{k'\alpha'} - i\eta^+} \right. \\ &+ \frac{1}{\epsilon - \epsilon_{k\alpha} + i\eta^+}\frac{T_\alpha T_{\alpha'}}{\epsilon - \hat{\epsilon}_d + i\frac{\Gamma}{2}} 2\pi i\delta(\epsilon - \epsilon_{k'\alpha'}) f_{\alpha'}(\epsilon) + \frac{1}{\epsilon - \epsilon_{k\alpha} + i\eta^+} T_\alpha T_{\alpha'} i A\bar{f} \\ &\left. \frac{1}{\epsilon - \epsilon_{k\alpha} - i\eta^+} \right]. \end{aligned} \tag{D.24}$$

By plugging in the expression for the decay rates and $\frac{1}{\epsilon - \epsilon_{k\alpha} \pm \eta^+} = \mp i\pi\delta(\epsilon - \epsilon_{k\alpha})$, we obtain

$$\sum_{kk'} T_\alpha T_{\alpha'} G^{<(0)}_{\substack{k\alpha \\ \alpha' k'}} = \left[i\Gamma_\alpha f_\alpha(\epsilon)\delta_{\alpha\alpha'} - \Gamma_\alpha f_\alpha G^A \frac{\Gamma_{\alpha'}}{2} + \frac{\Gamma_\alpha}{2} G^R \Gamma_{\alpha'} f_{\alpha'} + iA\bar{f}\frac{\Gamma_\alpha \Gamma_{\alpha'}}{4} \right]. \tag{D.25}$$

Similarly for the greater Green function

$$\sum_{kk'} T_\alpha T_{\alpha'} G^{>(0)}_{\substack{k\alpha \\ \alpha' k'}} = \Big[-i\Gamma_\alpha(1-f_\alpha(\epsilon))\delta_{\alpha\alpha'} + \Gamma_\alpha(1-f_\alpha) G^A \frac{\Gamma_{\alpha'}}{2} - \frac{\Gamma_\alpha}{2} G^R \Gamma_{\alpha'}(1-f_{\alpha'}) - iA(1-\bar{f})\frac{\Gamma_\alpha \Gamma_{\alpha'}}{4}\Big]. \tag{D.26}$$

The general expression of this quantity in the gradient expansion is

$$\sum_{kk'} T_\alpha T_{\alpha'} G^{<}_{\substack{k\alpha \\ \alpha' k'}} = i\Gamma_\alpha f_\alpha(\epsilon)\delta_{\alpha\alpha'} + \sum_{kk'} [G^{0,<}_{k\alpha} * T_\alpha \Sigma^A_{\substack{\alpha \\ \alpha'}} T_{\alpha'} * G^{0,A}_{k'\alpha'} + G^{0,R}_{k\alpha} * T_\alpha \Sigma^<_{\substack{\alpha \\ \alpha'}} T_{\alpha'} * G^{0,A}_{k'\alpha'} + G^{0,R}_{k\alpha} * T_\alpha \Sigma^R_{\substack{\alpha \\ \alpha'}} T_{\alpha'} * G^{0,<}_{k'\alpha'}]. \tag{D.27}$$

At first order, one has four contributions

$$(1) = \frac{i}{2}\Big[\partial_\epsilon(i\Gamma_\alpha f_\alpha)\partial_t G_A - \partial_t(i\Gamma_\alpha f_\alpha)\partial_\epsilon G_A\Big]\frac{i}{2}\Gamma_{\alpha'} + \frac{i}{2}\Big[\partial_\epsilon(i\Gamma_\alpha f_\alpha G^A)\partial_t(\frac{i}{2}\Gamma_{\alpha'}) - \partial_t(i\Gamma_\alpha f_\alpha G^A)\partial_\epsilon(\frac{i}{2}\Gamma_{\alpha'})\Big] = -\frac{i}{4}\dot{\Gamma}_\alpha f_\alpha \Gamma_{\alpha'}\partial_\epsilon G^A + \frac{i}{4}\Gamma_\alpha \partial_\epsilon f_\alpha \partial_t G^A \Gamma_{\alpha'}, \tag{D.28}$$

$$(2) = \frac{i}{2}\Big[\partial_\epsilon(-\frac{i}{2}\Gamma_\alpha)\partial_t G_R - \partial_t(-\frac{i}{2}\Gamma_\alpha)\partial_\epsilon G_R\Big] i\Gamma_{\alpha'} f_{\alpha'} + \frac{i}{2}\Big[\partial_\epsilon(-\frac{i}{2}\Gamma_\alpha G^R)\partial_t(i\Gamma_{\alpha'} f_{\alpha'}) - \partial_t(-\frac{i}{2}\Gamma_{\alpha'} G^R)\partial_\epsilon(i\Gamma_{\alpha'} f_{\alpha'})\Big] = \frac{i}{4}\dot{\Gamma}_{\alpha'} f_{\alpha'}\Gamma_\alpha \partial_\epsilon G^R - \frac{i}{4}\Gamma_{\alpha'}\partial_\epsilon f_{\alpha'}\partial_t G^R \Gamma_\alpha, \tag{D.29}$$

$$(3) = \frac{i}{2}\Big[\partial_t(-\frac{i}{2}\Gamma_\alpha)\partial_\epsilon(iA\bar{f}) - \partial_\epsilon(-\frac{i}{2}\Gamma_\alpha)\partial_t(iA\bar{f})\Big](\frac{i}{2}\Gamma_{\alpha'}) + \frac{i}{2}\Big[\partial_t(-\frac{i}{2}\Gamma_\alpha iA\bar{f})\partial_\epsilon(\frac{i}{2}\Gamma_{\alpha'}) - \partial_\epsilon(-\frac{i}{2}\Gamma_{\alpha'} iA\bar{f})\partial_t(\frac{i}{2}\Gamma_{\alpha'})\Big] = 0, \tag{D.30}$$

$$(4) = \sum_{kk'} T_\alpha T_{\alpha'} G^{R,0}\Sigma^{<(1)}_{\alpha\alpha'} G^{A,0} = \frac{T_\alpha T_{\alpha'}}{\epsilon - \epsilon_{k\alpha} + i\eta^+} G^{<(1)} \frac{1}{\epsilon - \epsilon_{k'\alpha'} - i\eta^+} = \frac{\Gamma_\alpha \Gamma'_\alpha}{4} \tag{D.31}$$

$G^{<(1)}(\epsilon, T)$.

In total:

$$\sum_{kk'} T_\alpha T_{\alpha'} G^{<(1)}_{\substack{k\alpha \\ \alpha' k'}} = -\frac{i}{4}\dot{\Gamma}_\alpha f_\alpha \Gamma_{\alpha'}\partial_\epsilon A + \frac{i}{4}\Gamma_\alpha \partial_\epsilon f_\alpha \partial_t A \Gamma_{\alpha'} + \frac{\Gamma_\alpha \Gamma_{\alpha'}}{4} G^{<(1)}(\epsilon, T). \tag{D.32}$$

Similarly for $G^{>(1)}_{\substack{k\alpha \\ \alpha' k'}}$

$$\sum_{kk'} T_\alpha T_{\alpha'} G^{>(1)}_{\substack{k\alpha \\ \alpha' k'}} = \frac{i}{4}\dot{\Gamma}_\alpha (1-f_\alpha)\Gamma_{\alpha'}\partial_\epsilon A + \frac{i}{4}\Gamma_\alpha \partial_\epsilon f_\alpha \partial_t A \Gamma_{\alpha'} + \frac{\Gamma_\alpha \Gamma_{\alpha'}}{4} G^{>(1)}(\epsilon, T). \tag{D.33}$$

Appendix E

The expectation value of the coupling term of the Hamiltonian

The expression of $\langle H_V \rangle$ reads

$$\langle H_V \rangle = \sum_\alpha V_\alpha(t) \sum_k \Big[\langle c^\dagger a_{k\alpha} \rangle + \langle a^\dagger_{k\alpha} c \rangle \Big] = \sum_\alpha \langle H_V^\alpha \rangle. \tag{E.1}$$

Where we define $H_V^\alpha = V_\alpha(t) \sum_k \Big[c^\dagger a_{k\alpha} + a^\dagger_{k\alpha} c \Big]$.

Now, let us derive the expression of $\langle H_V \rangle$ up to the first order from the expansion of the mixed Green function. Up to the first order in the velocity, the gradient expansion yields:

$$\langle H_V \rangle = 2 \sum_\alpha Im \Big(\int \frac{d\epsilon}{2\pi} \Big[G^R(\epsilon, t) i f_\alpha(\epsilon) \Gamma_\alpha - \frac{i}{2} \partial_t G^R(\epsilon, t) i \partial_\epsilon f_\alpha \Gamma_\alpha + \frac{i}{2} \partial_\epsilon G^R(\epsilon, t) i f_\alpha(\epsilon) \dot{\Gamma}_\alpha \Big] \Big) \tag{E.2}$$

One can rewrite this expression as

$$\langle H_V \rangle = 2 \sum_\alpha \int \frac{d\epsilon}{2\pi} \Big[Re G^R(\epsilon) \Gamma_\alpha f_\alpha - \frac{i}{2} \partial_t G^R(\epsilon, t) i \partial_\epsilon f \Gamma_\alpha + \frac{i}{2} \partial_\epsilon G^R(\epsilon, t) i f(\epsilon) \dot{\Gamma}_i \Big] \tag{E.3}$$

The components which come from the second term of D.20 are vanishing as they are real or they get integrated out at the boundaries.

Appendix F

The energy rate at zero order in the charge shuttle

The zero order of the internal energy has this expression

$$\dot{E}^{(0)} = \epsilon_d \langle \frac{d}{dt} c^\dagger c \rangle^{(0)} + \frac{1}{2} \sum_{k\alpha} \left(T_\alpha \langle \frac{d}{dt} c^\dagger a_{k\alpha} \rangle^{(0)} + h.c. \right). \tag{F.1}$$

The first derivative reads

$$\begin{aligned} \langle \frac{d}{dt} c^\dagger c \rangle^{(0)} &= i \langle [H, c^\dagger c] \rangle^{(0)} = i \sum_{k\alpha} (T_\alpha \langle a_{k\alpha}^\dagger c \rangle^{(0)} - T_\alpha \langle c^\dagger a_{k\alpha} \rangle^{(0)}) = \\ &= I_L^{(0)} + I_R^{(0)} = 0 \end{aligned} \tag{F.2}$$

for charge conservation (the latter equality is demonstrated in Sec. 3.4.1).

$$\langle \frac{d}{dt} c^\dagger a_{k\alpha} \rangle = i \langle [H, c^\dagger a_{k\alpha}] \rangle = i \sum_{k\alpha} (\epsilon_d - \epsilon_{k\alpha}) \langle c^\dagger a_{k\alpha} \rangle + i \sum_{k\alpha} T_\alpha (\langle a_{k\alpha}^\dagger a_{k\alpha} - c^\dagger c \rangle) \tag{F.3}$$

and likewise

$$\langle \frac{d}{dt} a_{k\alpha}^\dagger c \rangle = -i \sum_{k\alpha} (\epsilon_d - \epsilon_{k\alpha}) \langle a_{k\alpha}^\dagger c \rangle - i \sum_{k\alpha} T_\alpha (\langle a_{k\alpha}^\dagger a_{k\alpha} - c^\dagger c \rangle) \tag{F.4}$$

Therefore one has (see Appendix D)

$$\frac{i}{2} \sum_{k\alpha} (\epsilon_{k\alpha} - \epsilon_d)(T_\alpha \langle c^\dagger a_{k\alpha} \rangle - T_\alpha \langle a_{k\alpha}^\dagger c \rangle) = \sum_{k\alpha} (\epsilon_{k\alpha} - \epsilon_d) Re[T_\alpha(t) G_{d,k\alpha}^<(t)]. \tag{F.5}$$

In terms of the mixed Green function $G_{d,ki}^<(t',t) = i \langle a_{ki}^\dagger(t) c(t') \rangle$. Substituting the expression of this Green function (see Appendix D) yields

$$= \sum_{k\alpha} (\epsilon_{k\alpha} - \epsilon_d) Re \left[\int dt' G^R(t,t') \Sigma_\alpha^<(t',t) + G^<(t,t') \Sigma^A(t',t) \right]. \tag{F.6}$$

At zero order this expression reads

$$= \sum_{\alpha} Re\Big[\int \frac{d\epsilon}{2\pi}(\epsilon - \epsilon_d)\Big(G^R i\Gamma_\alpha f_\alpha + iA\bar{f}\frac{i}{2}\Gamma_\alpha \Big)\Big] = 0, \tag{F.7}$$

where we substituted the definition of $\bar{f} = \sum_\alpha \frac{\Gamma_\alpha f_\alpha}{\Gamma}$.

Appendix G

The adiabaticity conditions in the electronic shuttle

In this Chapter, we will check the validity of the adiabatic expansion we have employed in the main article. To do so, we compare the current calculated at different orders. In particular, the condition for the adiabatic approximation to be valid, the leading-order contribution of the current should be larger than the subsequent orders of the expansion. This condition reads

$$Q_\alpha^{(0)} \gg Q_\alpha^{(1)}, Q_\alpha^{(2)}. \tag{G.1}$$

Since the first order of the expansion of the current over a period of the stationary solution is trivially null, we concentrate on the second order.
Following the calculations of Sec. 3.4.1, we extend the treatment of the current to subsequent orders.
At first order, we obtain

$$Q_L^{(1)} = \frac{1}{T_0}\int_0^{T_0} dT \langle I_L\rangle^{(1)} = \frac{1}{T_0}\int_0^{T_0} dT \int \frac{d\epsilon}{4\pi i} 2Re\Big[\partial_T G^R(\epsilon,T)\partial_\epsilon f_L \Gamma_L - \partial_\epsilon G^R(\epsilon,T) f_L \dot{\Gamma}_L$$
$$- \partial_\epsilon G^<(\epsilon,T)\frac{i}{2}\dot{\Gamma}_L\Big] + \frac{1}{T_0}\int_0^{T_0} dt \int \frac{d\epsilon}{2\pi} 2Re\Big[G^{<(1)}(\epsilon,T)\frac{i}{2}\Gamma\Big]. \tag{G.2}$$

As pointed out, this expression vanishes as all the first-order quantities. Now, let us turn our attention towards the second order of the current. Its expression reads

$$Q_L^{(2)} = \frac{1}{T_0}\int_0^{T_0} dT \langle I_L\rangle^{(2)} = \frac{1}{T_0}\int_0^{T_0} dT \int \frac{d\epsilon}{-16\pi} 2Re\Big[\partial_T^2 G^R i\partial_\epsilon^2 f_L \Gamma_L + \partial_\epsilon^2 G^R i f_L \ddot{\Gamma}_L$$
$$- 2\partial_\epsilon\partial_T G^R i\partial_\epsilon f_L \dot{\Gamma}_L\Big] + \frac{1}{T_0}\int_0^{T_0} dT \int \frac{d\epsilon}{4\pi i} 2Re\Big[\partial_\epsilon G^{<(1)}(\epsilon,T)\frac{i}{2}\dot{\Gamma}_L\Big]$$
$$+ \frac{1}{T_0}\int_0^{T_0} dT \int \frac{d\epsilon}{2\pi} 2Re\Big[G^{<(2)}(\epsilon,T)\frac{i}{2}\Gamma_L\Big] + \frac{1}{T_0}\int_0^{T_0} dT \int \frac{d\epsilon}{-16\pi} 2Re\Big[\partial_\epsilon^2(iA\bar{f})\frac{i}{2}\ddot{\Gamma}_L\Big]. \tag{G.3}$$

The last term vanishes if the integration over the ϵ variable is performed.
Once one calculates all these integrals, one is able to calculate the second order of the current over a cycle. The final expression in the zero temperature limit is reported below

$$Q_L^{(2)} = \lambda^{-2}\frac{1}{T_0}\int_0^{T_0} dT \Gamma_L\Gamma_R\Big(W_0(x,\epsilon_0,\chi,\lambda,eV,\Gamma_0) + W_1(x,\epsilon_0,\chi,\lambda,eV,\Gamma_0)\Big), \tag{G.4}$$

where the two functions are defined as

$$W_0(x,\epsilon_0,\chi,\lambda,eV,\Gamma_0) = \frac{1}{4\pi}\Big(- \Gamma_L^2\frac{A(eV/2)^2}{\Gamma^2}(G^R(eV/2)+G^A(eV/2))$$
$$+ 2i\Gamma_L\frac{A(eV/2)}{\Gamma}[(G^R(eV/2))^2 - (G^A(eV/2))^2]\Big), \tag{G.5}$$

$$W_1(x,\epsilon_0,\chi,\lambda,eV,\Gamma_0) = \frac{1}{4\pi}\Big[- 1/2\frac{A(-eV/2)}{\Gamma}(G^R(-eV/2) - G^A(-eV/2)) - \Gamma_L\Gamma_R$$
$$\frac{A^2(-eV/2)}{\Gamma^2}(G^R(-eV/2)+G^A(-eV/2)) + iA(-eV/2)[(G^R(-eV/2))^2 - (G^A(-eV/2))^2]\Big]. \tag{G.6}$$

We plot the ratio between the second order of the current and the leading order contribution in Figg. G.1 and G.2. This analysis points out that the adiabatic expansion is valid close to the transition for small values of the limit cycle. Then, the corrections to the leading term become prevalent.

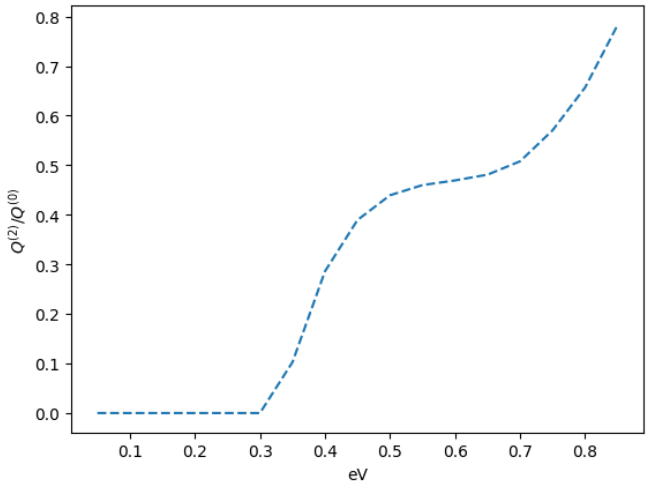

Figure G.1: This is the ratio between the current $Q^{(2)}$ and the leading order $Q^{(0)}$ plotted for different values of eV and the same choice of parameters of Fig. 3.2. The results indicate that the adiabatic approximation ceases to be appropriate for large values of eV.

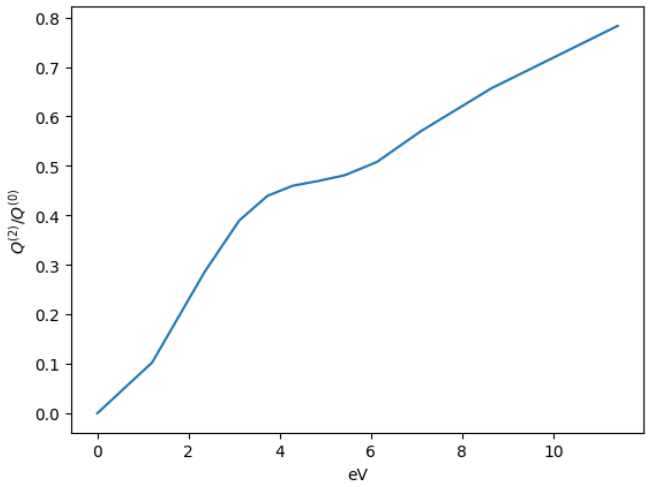

Figure G.2: This is the ratio between the current $Q_L^{(2)}$ and the leading order $Q_L^{(0)}$ plotted for different values of eV and the same choice of parameters of Fig. 3.2. The results indicate that the adiabatic approximation ceases to be valid for large values of A^C.

Appendix H

The calculation of the correlation function of the force fluctuations

The correlation function of the force reads

$$\langle \delta F(t)\delta F(t')\rangle = \langle F(t)F(t')\rangle - \langle F(t)\rangle\langle F(t')\rangle. \tag{H.1}$$

The expression of the force is in eq. 3.14. Plugging it into the correlation, one obtains

$$\langle \delta F(t)\delta F(t')\rangle = \langle\Bigg(dc^\dagger c - \sum_{k\alpha}\lambda^{-1}(-1)^\alpha(T_\alpha a^\dagger_{k\alpha}c + h.c.)\Bigg)(t)\Bigg(dc^\dagger c - \sum_{\alpha' k'}\lambda^{-1}(-1)^\alpha(T_{\alpha'}a^\dagger_{\alpha' k'}c + h.c.)\Bigg)(t')\rangle - \langle\Bigg(dc^\dagger c - \sum_{k\alpha}\lambda^{-1}(-1)^\alpha(T_\alpha a^\dagger_{k\alpha}c + h.c.)\Bigg)\rangle(t)\langle\Bigg(dc^\dagger c - \sum_{\alpha' k'}\lambda^{-1}(-1)^\alpha (T_\alpha a^\dagger_{k\alpha}c + h.c.)\Bigg)\rangle(t') \tag{H.2}$$

Now, we have to calculate each of these terms separately, up to the first order of the expansion. From the expression of the correlation written above, one can distinguish three different contributions. Each one of them is calculated separately in the adiabatic limit. The first one reads

$$(1) = d^2\Bigg(\langle c^\dagger c(t)c^\dagger c(t')\rangle - \langle c^\dagger c\rangle(t)\langle c^\dagger c\rangle(t')\Bigg) \tag{H.3}$$

In order to evaluate the first expectation value, since we are dealing with a quadratic model, one can use the Wick theorem for the full Green function on the Keldysh contour:

$$\langle T_c[c^\dagger c(t)c^\dagger c(t')]\rangle = \langle T_c[cc^\dagger]\rangle(t)\langle T_c[cc^\dagger]\rangle(t') - \langle T_c[c(t)c^\dagger(t')]\rangle\langle T_c[c(t')c^\dagger(t)]\rangle \tag{H.4}$$

In terms of the contour-ordered Green functions [46] eq.(H.4) reads

$$= iG^c(t,t_+)iG^c(t',t'_+) - iG^c(t,t')iG^c(t',t) \tag{H.5}$$

Using Langreth rules (Chapter 2) one rewrites the expression as

$$= iG^{<}(t,t)iG^{<}(t',t') - iG^{<}(t,t')iG^{>}(t',t) \tag{H.6}$$

The first term of Eq.(H.4) cancels the second term in eq.(H.3). As a consequence of that

$$(1) = d^2 G^{<}(t,t')G^{>}(t',t). \tag{H.7}$$

At zero order it reads

$$(1) = d^2\Big(\int \frac{d\epsilon}{2\pi} e^{i\epsilon\tau} G^{<(0)}(\epsilon,T)\Big)\Big(\int \frac{d\epsilon\,'}{2\pi}\, e^{-i\epsilon'\tau} G^{>(0)}(\epsilon,T)\Big), \tag{H.8}$$

which amounts to

$$(1) = d^2\Big(\int \frac{d\epsilon}{2\pi} e^{i\epsilon\tau} A\bar{f}\Big)\Big(\int \frac{d\epsilon\,'}{2\pi}\, e^{-i\epsilon'\tau} A(1-\bar{f})\Big). \tag{H.9}$$

In the first order, this correlator reads

$$\begin{aligned} &- d^2\Big(\int \frac{d\epsilon}{2\pi} e^{i\epsilon\tau} G^{<(1)}(\epsilon,T)\Big)\Big(\int \frac{d\epsilon\,'}{2\pi}\, e^{-i\epsilon'\tau} G^{>(0)}(\epsilon',T))\Big) - d^2\Big(\int \frac{d\epsilon}{2\pi} e^{i\epsilon\tau} G^{<(0)}(\epsilon,T) \\ &\Big)\Big(\int \frac{d\epsilon\,'}{2\pi}\, e^{-i\epsilon'\tau} G^{>(1)}(\epsilon',T))\Big). \end{aligned} \tag{H.10}$$

One can evaluate this expression

$$\begin{aligned} &- d^2\Big(\int \frac{d\epsilon}{2\pi} e^{i\epsilon\tau}[-\frac{\dot{\epsilon}_d}{2}\partial_\epsilon \bar{f}A^2 + \sum_j \frac{\dot{\Gamma}_j}{2}(\bar{f}-f_j)\frac{A^2}{\Gamma} - \frac{\dot{\Gamma}}{2}\partial_\epsilon\bar{f}\frac{A^2}{\Gamma}(\epsilon-\epsilon_d)]\Big)\Big(\int \frac{d\epsilon'}{2\pi} e^{-i\epsilon'\tau} A(1-\bar{f})\Big) \\ &- d^2\Big(\int \frac{d\epsilon}{2\pi} e^{i\epsilon\tau} A\bar{f}\Big)\Big(\int \frac{d\epsilon'}{2\pi} e^{-i\epsilon'\tau}[\frac{\dot{\epsilon}_d}{2}\partial_\epsilon \bar{f}A^2 - \sum_j \frac{\dot{\Gamma}_j}{2}(\bar{f}-f_j)\frac{A^2}{\Gamma} + \frac{\dot{\Gamma}}{2}\partial_\epsilon\bar{f}\frac{A^2}{\Gamma}(\epsilon-\epsilon_d)]\Big). \end{aligned} \tag{H.11}$$

All these Fourier transforms have been computed numerically in the zero-temperature limit.

Similarly, for the second term of eq.(H.1) one can write

$$\begin{aligned} (2) = -d/\lambda \sum_{k\alpha} (-1)^\alpha (T_\alpha(t)T_\alpha(t')\langle [a^\dagger_{k\alpha}c + c^\dagger a_{k\alpha}](t)[c^\dagger c](t') + [c^\dagger c](t)[a^\dagger_{k\alpha}c + c^\dagger a_{k\alpha}](t') \\ \rangle - T_\alpha(t)\langle [a^\dagger_{k\alpha}c + c^\dagger a_{k\alpha}](t)\rangle\langle c^\dagger c(t')\rangle + \langle c^\dagger c(t)\rangle\langle [a^\dagger_{k\alpha}c + c^\dagger a_{k\alpha}](t')\rangle T_\alpha(t')). \end{aligned} \tag{H.12}$$

In terms of the Green's functions

$$\begin{aligned} &= -d\lambda^{-1}\sum_{k\alpha}(-1)^{\alpha}T_{\alpha}(t)\Big(G^{<}_{k\alpha,d}(t,t')G^{>}(t',t)+G^{<}(t,t')G^{>}_{k\alpha,d}(t',t)\Big)\\ &- d\lambda^{-1}\sum_{k\alpha}(-1)^{\alpha}T_{\alpha}(t')\Big(G^{<}(t,t')G^{>}_{d,k\alpha}(t',t)+G^{<}_{d,k\alpha}(t,t')G^{>}(t',t)\Big)\end{aligned} \tag{H.13}$$

Let us rewrite this quantity as

$$\begin{aligned} &= -d\lambda^{-1}\sum_{k\alpha}(-1)^{\alpha}G^{<}(t,t')\Big(T_{\alpha}(t)G^{>}_{k\alpha,d}(t',t)+T_{\alpha}(t')G^{>}_{d,k\alpha}(t',t)\Big)\\ &- d\lambda^{-1}\sum_{k\alpha}(-1)^{\alpha}G^{>}(t',t)\Big(T_{\alpha}(t)G^{<}_{k\alpha,d}(t,t')+T_{\alpha}(t')G^{<}_{d,k\alpha}(t,t')\Big).\end{aligned} \tag{H.14}$$

The gradient expansion can be performed in the same way as before

$$-d\lambda^{-1}\sum_{k\alpha}(-1)^{\alpha}\Big(\int\frac{d\epsilon}{2\pi}e^{i\epsilon\tau}G^{<(0)}\Big)\Big(\int\frac{d\epsilon'}{2\pi}e^{-i\epsilon'\tau}[T_{\alpha}G^{<,(0)}_{d,k\alpha}+h.c.]\Big) \tag{H.15}$$

at zero order. The first order reads

$$\begin{aligned} &d\lambda^{-1}\sum_{k\alpha}(-1)^{\alpha}\Big(\int\frac{d\epsilon}{2\pi}e^{i\epsilon\tau}G^{<(1)}\Big)\Big(\int\frac{d\epsilon'}{2\pi}e^{-i\epsilon'\tau}[T_{\alpha}G^{<,(0)}_{d,k\alpha}+h.c.]\Big)+d\lambda^{-1}\sum_{k\alpha}(-1)^{\alpha}\\ &\Big(\int\frac{d\epsilon}{2\pi}e^{i\epsilon\tau}G^{<(0)}\Big)\Big(\int\frac{d\epsilon'}{2\pi}e^{-i\epsilon'\tau}[T_{\alpha}G^{<,(1)}_{d,k\alpha}+h.c.]\Big)\end{aligned} \tag{H.16}$$

Now, the third term of the correlation (H.1) reads

$$\begin{aligned} (3) = \lambda^{-2}\sum_{\substack{k\alpha\\ \alpha'k'}}(-1)^{\alpha\alpha'}T_{\alpha}(t)T_{\alpha'}(t')\Big[&\langle[a^{\dagger}_{k\alpha}c+c^{\dagger}a_{k\alpha}](t)[a^{\dagger}_{k\alpha}c+c^{\dagger}a_{k\alpha}](t')\rangle\\ &-\langle[a^{\dagger}_{k\alpha}c+c^{\dagger}a_{k\alpha}](t)[a^{\dagger}_{k\alpha}c+c^{\dagger}a_{k\alpha}](t')\rangle\Big].\end{aligned} \tag{H.17}$$

Then rewriting the 4-order correlation in terms of Green's functions

$$\begin{aligned} (3) = \lambda^{-2}\sum_{\substack{k\alpha\\ \alpha'k'}}(-1)^{\alpha\alpha'}T_{\alpha}(t)T_{\alpha'}(t')\Big\{&G^{<}_{k\alpha,d}(t,t')G^{>}_{\alpha'k',d}(t',t)\\ &+G^{<}_{d,k\alpha}(t,t')G^{>}_{d,k'\alpha'}(t',t)+G^{<}(t,t')G^{>}_{\substack{\alpha'k'\\ k\alpha}}(t',t)\\ &+G^{<}_{\substack{k\alpha\\ \alpha'k'}}(t,t')G^{>}(t',t)\Big\}.\end{aligned} \tag{H.18}$$

There are two components

$$(3.1) = \lambda^{-2}\sum_{\substack{\alpha\alpha'\\kk'}}(-1)^{\alpha+\alpha'}\Big\{\int\frac{d\epsilon}{2\pi}e^{i\epsilon\tau}[T_\alpha G^{<(0)}_{d,k\alpha}]\int\frac{d\epsilon'}{2\pi}e^{-i\epsilon'\tau}[T_{\alpha'}G^{>(0)}_{d,\alpha'k}]+\int\frac{d\epsilon}{2\pi}e^{-i\epsilon\tau}$$
$$[T_\alpha G^{<(0)}_{d,k\alpha}]^*\int\frac{d\epsilon'}{2\pi}e^{i\epsilon'\tau}[T_{\alpha'}G^{>(0)}_{d,\alpha'k}]^*+\int\frac{d\epsilon}{2\pi}e^{i\epsilon\tau}[T_\alpha G^{<(0)}_{d,k\alpha}]\int\frac{d\epsilon'}{2\pi}e^{-i\epsilon'\tau}[T_{\alpha'}G^{>(1)}_{d,\alpha'k}] \tag{H.19}$$
$$+\int\frac{d\epsilon}{2\pi}e^{i\epsilon\tau}[T_\alpha G^{<(0)}_{d,k\alpha}]\int\frac{d\epsilon'}{2\pi}e^{-i\epsilon'\tau}[T_{\alpha'}G^{>(1)}_{d,\alpha'k}]+\int\frac{d\epsilon}{2\pi}e^{-i\epsilon\tau}[T_\alpha G^{<(1)}_{d,k\alpha}]^*$$
$$\int\frac{d\epsilon'}{2\pi}e^{i\epsilon'\tau}[T_{\alpha'}G^{>(0)}_{d,\alpha'k}]^*+\int\frac{d\epsilon}{2\pi}e^{-i\epsilon\tau}[T_\alpha G^{<(0)}_{d,k\alpha}]^*\int\frac{d\epsilon'}{2\pi}e^{i\epsilon'\tau}[T_{\alpha'}G^{>(1)}_{d,\alpha'k}]^*\Big\}$$

and

$$(3.2) = \lambda^{-2}\sum_{\substack{\alpha\alpha'\\kk'}}(-1)^{\alpha+\alpha'}\Big\{\int\frac{d\epsilon}{2\pi}e^{i\epsilon\tau}G^{<(0)}\int\frac{d\epsilon'}{2\pi}e^{-i\epsilon'\tau}[T_\alpha T_{\alpha'}G^{>(0)}_{\substack{\alpha'k'\\k\alpha}}]+\int\frac{d\epsilon}{2\pi}e^{i\epsilon\tau}$$
$$[T_\alpha T_{\alpha'}G^{<(0)}_{\substack{k\alpha\\\alpha'k'}}]\int\frac{d\epsilon'}{2\pi}e^{-i\epsilon'\tau}G^{>(0)}+\int\frac{d\epsilon}{2\pi}e^{i\epsilon\tau}G^{<(1)}\int\frac{d\epsilon'}{2\pi}e^{-i\epsilon'\tau}[T_\alpha T_{\alpha'}G^{>(0)}_{\substack{\alpha'k'\\k\alpha}}] \tag{H.20}$$
$$\int\frac{d\epsilon}{2\pi}e^{i\epsilon\tau}G^{<(0)}(\epsilon,T)\int\frac{d\epsilon'}{2\pi}e^{-i\epsilon'\tau}[T_\alpha T_{\alpha'}G^{>(1)}_{\substack{\alpha'k'\\k\alpha}}]+\int\frac{d\epsilon}{2\pi}e^{i\epsilon\tau}[T_\alpha T_{\alpha'}G^{<(1)}_{\substack{k\alpha\\\alpha'k'}}]$$
$$\int\frac{d\epsilon'}{2\pi}e^{-i\epsilon'\tau}G^{>(0)}+\int\frac{d\epsilon}{2\pi}e^{i\epsilon\tau}[T_\alpha T_{\alpha'}G^{<(0)}_{\substack{k\alpha\\\alpha'k'}}]\int\frac{d\epsilon'}{2\pi}e^{-i\epsilon'\tau}G^{>(1)}\Big\}$$

Adding all these different contributions allows one to arrive at the final form of the force fluctuations

$$\langle\delta F(t)\delta F(t')\rangle = (1)+(2)+(3). \tag{H.21}$$

Now, let us plot the leading order of the correlation with respect to the time $\tau = t - t'$ (Fig. H.1). One can see that it is well approximated by a delta function. This justifies assuming a noise which satisfies

$$\langle\xi(t)\rangle = 0 \tag{H.22}$$

and

$$\langle\xi(t)\xi(t')\rangle = D(x,p)\delta(t-t') \tag{H.23}$$

The diffusion coefficient has the subsequent expansion

$$D(x,p) \simeq D^{(0)}(x) + D^{(1)}(x)p + O[(\Omega/\Gamma_{i,av})^2] \tag{H.24}$$

The coefficients $D_i(x)$ are calculated on the basis of the expansion of the force fluctuations up to the first order.

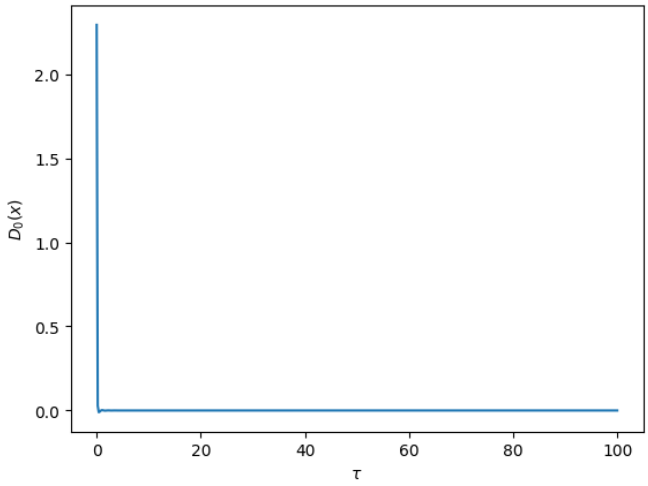

Figure H.1: This is the zero order of the expansion of the correlation function in the time domain, plotted versus $\tau = t - t'$. The parameters chosen are x=3, eV=0.5 and the selection of figure 3.2. This image shows that the equal times component at $\tau = 0$ is indeed prevalent and the white noise approximation is relevant.

Appendix I

The imaginary part of the response function

In this Chapter, we will define on general terms the steady-state imaginary part of the response function. Suppose one starts from a Hamiltonian depending on the initial parameter of the quench λ_i, $H(\lambda_i)$ and the system is prepared in the initial state $|\psi_0\rangle$. Then, the parameter is quenched to λ_f and subject to an external time-dependent perturbation $V(t) = h(t)B$. For any generic observable A, the expectation value in the linear response regime reads

$$\langle A\rangle(t) = \langle A\rangle(0) + \int_0^t dt' \chi_{AB}(t,t')h(t') \tag{I.1}$$

where

$$\chi_{AB}(t,t') = -i\theta(t-t')\langle\psi_0|[A(t),B(t')]|\psi_0\rangle. \tag{I.2}$$

Let us rewrite the latter in terms of the time variables $T = \frac{t+t'}{2}$ and $\tau = t - t'$ and average over the centre-of-mass time variable

$$\bar{\chi}_{A,B}(\tau) = -i\theta(\tau)\lim_{T\to\infty}\frac{1}{T}\int_0^T dt' Tr\Big\{\rho(0)\Big[A(T+\tau/2),B(T-\tau/2)\Big]\Big\} \tag{I.3}$$

where the initial density matrix is $\rho(0) = |\psi_0\rangle\langle\psi_0|$. The expression inside the parenthesis can be rewritten as $e^{-iH_fT}[A(\tau/2),B(-\tau/2)]e^{iH_fT}$. After averaging, the trace over $\rho(0)$ can be performed under the diagonal ensemble, representing the stationary state $\rho_{st} = \sum_{ki} p_k^i|\psi_{n,i}\rangle\langle\psi_{n,i}|$, where p_k^i is the overlap with the initial state and i a degeneracy index. At the end, one obtains

$$\bar{\chi}_{A,B}(\tau) = -i\theta(\tau)\sum_n p_n\langle\psi_n|[A(\tau/2),B(-\tau/2)]|\psi_n\rangle. \tag{I.4}$$

In this case, $\bar{\chi}(\omega)$ represents the Fourier transform of $\bar{\chi}_{A,B}(\tau)$ and $\bar{\chi}''(\omega) = -Im\bar{\chi}(\omega)$.